NASA CR-72280
PWA FR-3960

FINAL REPORT

ADVANCED BEARING STUDY
PART II, BEARING TESTS

by

C. R. Comolli, R. Newton and R. E. Dotson

PRATT & WHITNEY AIRCRAFT
FLORIDA RESEARCH AND DEVELOPMENT CENTER

Prepared for

NATIONAL AERONAUTICS AND SPACE ADMINISTRATION

Contract NAS3 7943

NASA Lewis Research Center
Cleveland, Ohio
Werner R. Britsch,
Liquid Rocket Technology Branch

Requests for copies of this report should be referred to:

National Aeronautics and Space Administration
Scientific and Technical Information Facility
P.O. Box 33
College Park, Md. 20740

NASA CR-72280
PWA FR-3960

FINAL REPORT

ADVANCED BEARING STUDY
PART II, BEARING TESTS

by

C. R. Comolli, R. Newton and R. E. Dotson

PRATT & WHITNEY AIRCRAFT
FLORIDA RESEARCH AND DEVELOPMENT CENTER

Prepared for

NATIONAL AERONAUTICS AND SPACE ADMINISTRATION

8 SEPTEMBER 1971

NASA Lewis Research Center
CONTRACT NAS3-7943

37

FOREWORD

This report was prepared by the Pratt & Whitney Aircraft Division of United Aircraft Corporation, under Contract NAS3-7943, for Lewis Research Center of National Aeronautics and Space Administration. The work was administered under the technical direction of the Lewis Research Center's Chemical Rocket Division. Mr. Werner R. Britsch was the NASA Project Manager, and Mr. Herbert W. Scibbe of the Fluid Systems Components Division was the NASA Research Advisor.

This is Part II of the final report, prepared at the conclusion of the bearing test phase. The Part I study of the Materials Evaluation Phase was submitted as NASA CR-72279.

CONTENTS

ILLUSTRATION LIST

ILLUSTRATION LIST (Continued)

TABLE LIST

LIST OF SYMBOLS

B	Total curvature ($f_i + f_o - 1$)		
DN	Bearing bore x inner race speed	mm x rpm	
d	Ball diameter	inches	cm
E_B	Bearing pitch diameter	inches	cm
f_i	Inner race curvature fraction of ball diameter		
f_o	Outer race curvature fraction of ball diameter		
HP	Spin power or heat generation	horsepower	watts
N	Rotation speed	rpm	rad/s
N_R	Ball roll speed with respect to inner race	rpm	rad/s
N_S	Ball spin speed with respect to inner race	rpm	rad/s
n	Number of balls in bearing		
P_d	Internal clearance	inches	cm
ΔP_d	Change in internal clearances	inches	cm
S_m	Mean compressive stress (Hertz stress)	psi	N/cm^2
S_{max}	Maximum compressive stress	psi	N/cm^2
S_s	Maximum subsurface shear stress	psi	N/cm^2
V	Velocity	ft/sec	cm/sec
V_c	Cage rub velocity	fps	cm/sec
V_s	Maximum tangential velocity in contact area	fps	cm/sec
Z	Depth of S_s	inches	cm
β_o	Free contact angle	degrees	radians
β^*	Calculated static contact angle with clearances corrected for thermal changes, centrifugal growth, and press fit	degrees	radians

LIST OF SYMBOLS (Continued)

μ	Sliding coefficient of friction

SUBSCRIPTS

B	Ball
b	Bearing
c	Cage
i	Inner race
o	Outer race
r	Roll component
s	Spin component

ABSTRACT

Twenty 110-mm ball bearing tests in liquid hydrogen were conducted with bearings constructed of material combinations selected from the materials evaluation portion (Part I) of this program. In thirteen of these tests the bearings consisted of AISI 440C(1) races and balls with Chemloy 719(2) cages supplying the lubricant. A successful 15 min test at a rotational speed of 12,000 rpm (1256 rad/s) and an axial load of 9,000 lb (40,034 N) was completed with this configuration. Five tests were made with bearings consisting of AISI 440C races, Stellite Star J(3) balls, and Salox M(4) for the cage material. A successful 33 min test at a rotational speed of 13,000 rpm (1361 rad/s) and an axial load of 7,200 lb (32,027 N) was completed with this combination. The remaining two tests were made with bearings consisting of AISI 440C races and balls and a Salox-M cage. A total of 35.1 min at 13,000 rpm (1361 rad/s) and a 7,200-lb (32,027 N) load was accumulated with this material combination.

Star J ball failures that occurred in two tests were attributed to poor ball material grain structures. Failures experienced with the AISI 440C races and balls were associated with failure of the cages due to wear and/or fractures.

---

(1) High chromium hardenable steel

(2) Glass-fiber, MoS_2, Teflon mixture manufactured by Crane Packing Co., Morton Grove, Illinois

(3) Complex alloy of cobalt, produced by Haynes Stellite Division, Union Carbide Corporation

(4) Mixture of bronze and Teflon manufactured by Alleghany Plastics, Inc., Corropolis, Pennsylvania.

SECTION I
INTRODUCTION

Turbopumps for advanced high pressure liquid hydrogen fueled rocket engines require fuel cooled bearings capable of consistent operation at speed and thrust load conditions beyond the current state-of-the-art. These operating goals have been achieved in some instances, but bearing performance has not been consistent, and demonstrated reliability is below desirable levels. The advanced bearing technology required to improve bearing life at increased loads and speeds must consider improved materials and material combinations as well as optimization of the bearing internal geometry to reduce heat generation. In order to achieve the operating goals required for advanced bearing technology the Lewis Research Center of the National Aeronautics and Space Administration sponsored this technical effort under Contract NAS3-7943.

The program under this contract was directed toward the evaluation of materials suitable for use as balls, races, and cages for bearings operating in a liquid hydrogen environment. In the first phase of the Advanced Bearing Study (reported in NASA CR-72279), several material combinations were evaluated in liquid hydrogen by endurance tests in a ball and plate rig. From this portion of the program, a single race material was selected to be used with two ball materials and two lubricant cage materials in a 110-mm ball bearing.

The second phase, as reported herein, provided for the fabrication and evaluation in liquid hydrogen of ball bearings consisting of material combinations selected in Phase I. All of the bearings were 110-mm diameter bore. They were of the counterbore type, and all were of like geometry, using AISI 440C races. Three ball and cage material combinations were evaluated with the AISI 440C races. These included AISI 440C balls with both Chemloy 719 and Salox-M cages, and Stellite Star J balls with Salox-M cages.

A test rig designed to minimize radial loads and provide control of bearing thrust loads up to 20,000 lb (88,964 N) was used for the bearing testing. A 150-hp (112-kw) variable drive system capable of rotating speeds up to 24,150 rpm (2529 rad/s) was used. Bearing cooling was achieved by flowing liquid hydrogen through each bearing from separate supply lines. The test rig and procedures used during the program are defined in Section II.

The design of the 110-mm counterbore ball bearing and inner land riding cage is described in Section III. Sections IV and V of this report are devoted to a detailed discussion of each of the tests, and a discussion of the results.

SECTION II
TEST APPARATUS AND PROCEDURE

A. APPARATUS

1. Test Stand

The bearing program was conducted on B-14 stand located in Pratt & Whitney Aircraft's FRDC liquid hydrogen component test facility. The stand is equipped with a variable speed drive system, liquid hydrogen and ancillary gas supply systems, and data recording facilities. The principal components and critical instrumentation locations are depicted in figure 1.

The variable speed drive system includes a 150-hp (1190-kw) electric motor driving a 7:1 gearbox through a variable slip electric clutch. This drive provides speed control over a range of 0 to 24,150 rpm (2529 rad/s), and has a digital readout accurate to ±15 rpm (1.57 rad/s).

A schematic of the liquid hydrogen and ancillary gaseous helium system is shown in figure 2. The liquid hydrogen flows through vacuum-jacketed lines, and control is maintained by dewar pressurization and variable area cryogenic valving. Hydrogen discharge from the rig is ducted to a burn stack for disposal. The high pressure gaseous helium is passed through pressure regulators that provide preset pressure levels for the bearing rig axial load piston and the rig shaft seals.

Instrumentation compatible with the environmental operating conditions is used to measure the following parameters: (1) front and rear bearing outer race temperatures at two locations each; (2) front and rear bearing, radial and axial vibrations; (3) shaft speed; (4) drive torque; (5) thrust load bellows pressure; (6) coolant flowrate to each bearing; (7) coolant inlet pressure; and (8) coolant inlet and discharge temperature. Vibration data are recorded on magnetic tape, and all other data are recorded on conventional two-channel strip charts.

2. Test Rig

The 110-mm bearing rig shown schematically in figure 3 was designed to provide high thrust load test conditions at little or no radial loading. A lightweight hollow shaft was dynamically balanced to minimize both static and dynamic radial loads. The test rig consisted of a rigid cylindrical housing, a bellows-actuated piston, a hollow drive shaft, the two test bearings, the endplates and seals. Special consideration was given to simplifying the assembly for easy access to the test bearings. The test rig materials were chosen for LH_2 compatibility. Detail parts are shown in figure 4; the rotating components are represented by the lower grouping of parts.

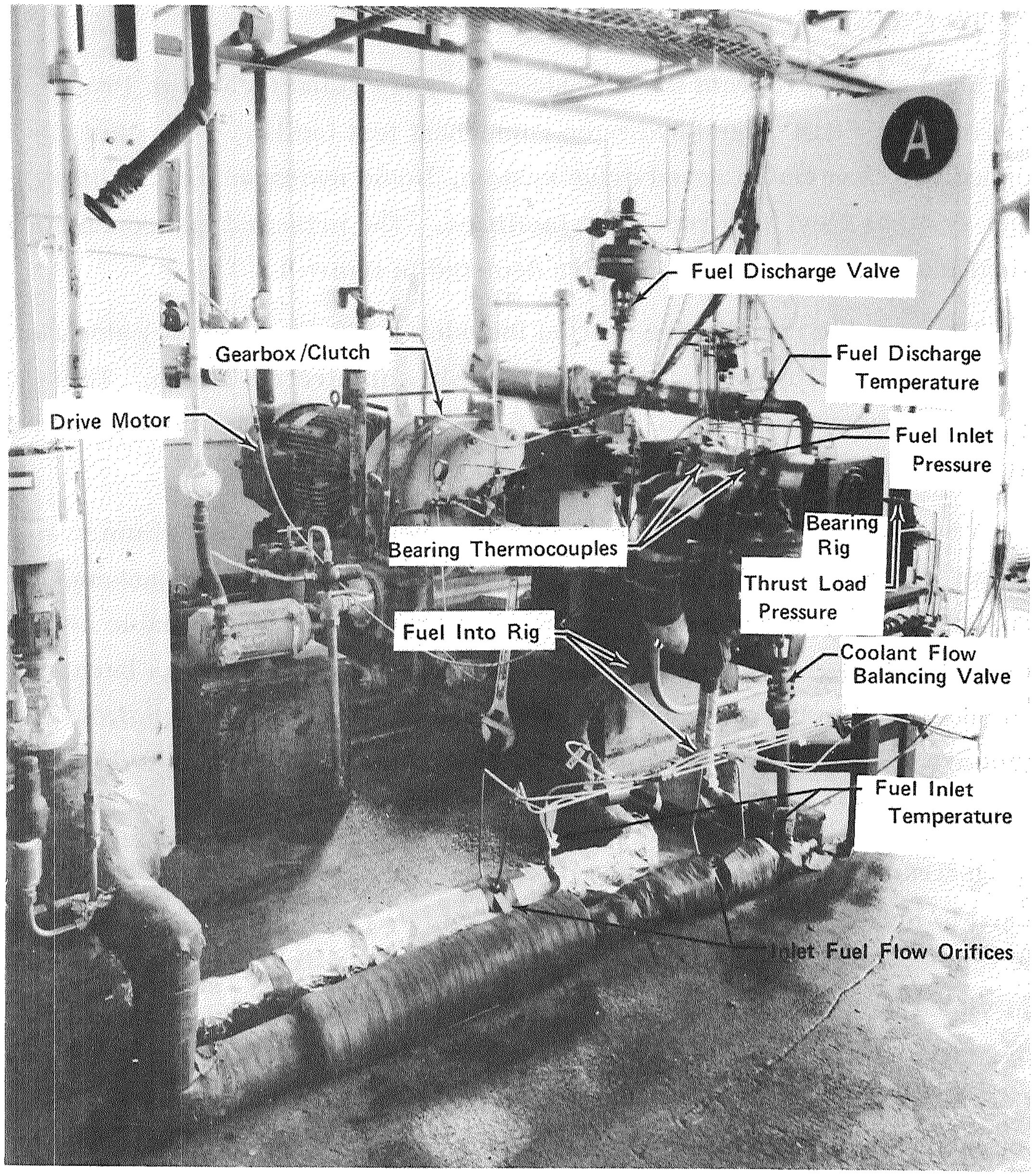

Figure 1. 110-mm Bearing Rig Installed in B-14 Test Cell Showing Major Equipment and Instrumentation FD 42563

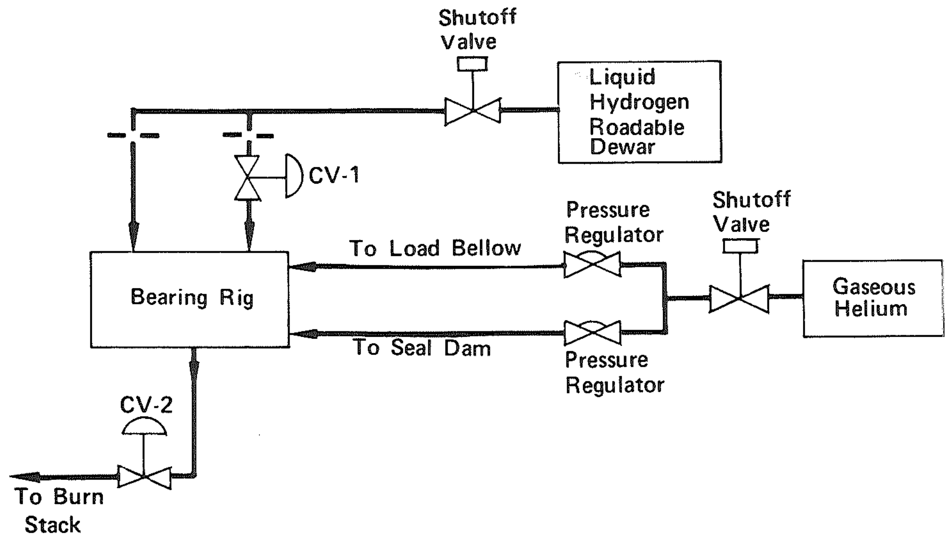

Figure 2. Schematic of the Liquid Hydrogen and Ancillary Gaseous Helium System FD 43863

The test bearings were mounted onto the shaft from each end and retaining nuts secured them to the shaft. The first critical speed for the shaft was computed to be 49,000 rpm (5130 rad/s), well above the maximum test speed of 13,500 rpm (1413 rad/s). The shaft seal consisted of a 1.5 in. dia (3.81 cm) bellows assembly with a carbon face running on a chromium rub face. A helium seal dam was used to prevent hydrogen leakage through the shaft seal and into the test cell. The seal dam was composed of a small chamber around the shaft, which was pressurized with helium gas to 1 psi (0.69 N/cm^2) above rig internal pressure. The helium gas leakage from this chamber was minimized by a stack of Teflon wafers with tightly fitting knife edge shaft seals. Static sealing was accomplished with two Teflon-coated, metal O-rings under the bolted endplates.

The bearing rig was mounted on external trunnion bearings to adapt it for measuring bearing torque using a reaction arm and load cell arrangement. This approach encountered data repeatability problems at cryogenic test temperatures due to unpredictable thermal effects on external plumbing and trunnion bearings. The problem was solved by changing to a torque measuring system based on drive shaft torque input. A water brake calibration of the drive system was completed at ambient operating temperatures to obtain torque data as a function of the excitation current of the electric clutch over the expected operating range of the bearing rig. The motor and clutch, as shown in figure 1, are well outside the cold affected zone of the rig, thereby providing ambient operating conditions regardless of test conditions, and good repeatability of torque data.

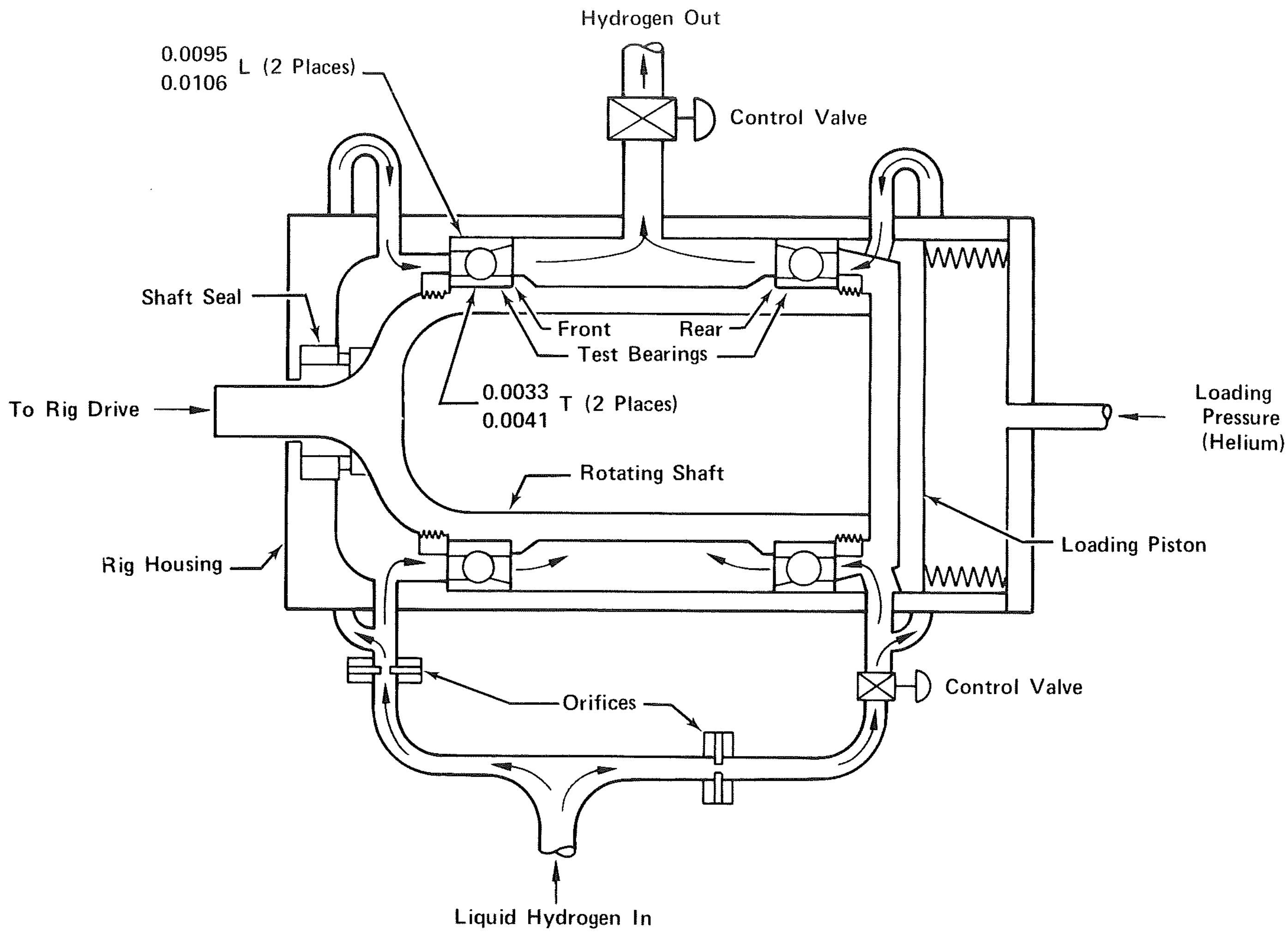

Figure 3. Bearing Test Rig Schematic Showing Coolant Flowpath

FD 42556

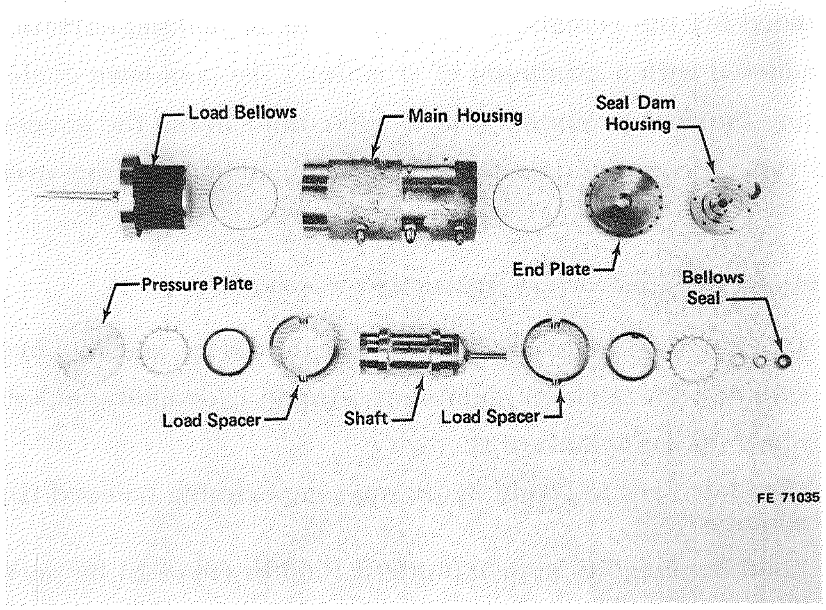

Figure 4. Bearing Test Rig Components FD 49349

The thrust loads were applied to the rear bearing outer race by pressurizing the bellows-actuated piston with helium gas. The load was transferred to the front bearing through the inner race and shaft. This arrangement is shown in figure 3.

B. PROCEDURE

The test procedure consisted of cooling the test rig to LH_2 temperature, applying a partial thrust load to prevent skidding of the balls while accelerating the rig to 4000 rpm (419 rad/s), gradually applying the remainder of the thrust load and accelerating to test speed. Bearing outer-race temperatures and vibrations were monitored continuously for indications of a failure and shutdown was initiated at any sign of distress. Bearing distress was always exhibited as an increase in race temperature that could not be controlled by increasing the coolant flow (referred to as overheating), or as an increase in rig vibration. Other parameters such as axial load, shaft speed, coolant flows-pressures-temperatures and bearing torque were also monitored, and adjusted when necessary to satisfy test conditions.

Test rig cooldown data were recorded during tests No. 2 through 10, but delays imposed by last minute adjustments to instrumentation and stand equipment resulted in variations in cooldown time. Recording of the cooldown data was discontinued for the remaining tests in favor of making certain that the test would be conducted with a minimum of trouble. The cooldown cycle was used to correct for any thermal problems that would compromise the success of the subsequent test run. From the data that were taken, cooldown time varied from 22 to 31 min.

The following detailed test procedure was used:

1. Purge rig with gaseous nitrogen followed by gaseous hydrogen
2. Cooldown test stand plumbing to liquid hydrogen temperature
3. Start instrumentation recorder
4. Cooldown rig to liquid hydrogen temperature (record time and flow required)
5. Load bearings to approximately 1000 lb (4448 N) by pressurizing loading bellows
6. Slowly accelerate rig to 4000 rpm (419 rad/s)
7. Increase load to that required for test
8. Accelerate to full test speed
9. Run steady-state test
10. Decrease speed to 4000 rpm (419 rad/s)
11. Decrease bearing load to 1000 lb (4448 N)
12. Shut down rig and release bearing load
13. Purge rig with gaseous hydrogen followed by gaseous nitrogen

SECTION III
DESIGN OF TEST BEARINGS

A. GENERAL

Within the general constraints of bearing size and number of balls, as specified by the contract, P&WA completed a design of the 110-mm bearings. Previous successful designs of 35-mm and 40-mm bearings for the RL10 rocket engines, 55-mm bearings for a high pressure hydrogen pump, and experimental 80-mm bearings provided basic data on race and cage configurations.

As in selecting the geometry for most bearing designs, various load and speed conditions were input into a computer to solve iteratively for Hertzian deflection, contact angle, Hertz stress, and internal velocity relationships. In this case the computer was programed with a P&WA bearing program written for ball bearings under pure thrust load, a condition which was closely approximated in the test rig. This bearing program was the same as that used for all preceeding bearing designs for cryogenic application including a 4×10^6 DN test bearing, RL10 engine bearings, 50K engine pump bearings and 350K engine pump bearings. This program is generally equivalent to the more recent computer program, presently used by P&WA, which was written by A. B. Jones.(1) The program had not been developed at the time of the 110-mm bearing design. This newer program affords a more detailed analysis of bearing internal kinetics such as ball excursions and the effect of ball diameter deviation.

If the test bearings used in this program were to be redesigned with the newer computer deck, the increased awareness of internal kinetics would probably result in smaller contact angles, with some sacrifice in expected life, as well as reduced race curvature and larger ball size. The current state-of-the-art indicates that these changes in conjunction with more stringent control of the raceway waviness, ball diameter deviation, and surface finish of all contact area would considerably enhance the capability of the bearing to operate in the load/speed range of this test program.

---

(1) The A. B. Jones bearing design computer program is based on bearing design theories as expressed in Mechanical Design and Systems Handbook, Rothbart, H. A., Mac Graw Hill, 1964. (Section XIII, "The Mathematical Theory of Rolling Element Bearings," A. B. Jones.)

B. RACE DESIGN

1. Inner Race Curvature

One of the most important items that must be determined in a bearing design is that of race curvatures, as this affects both life and heat generation. If other factors remain constant an increase in the inner race curvature decreases the heat generation. Lower heat generation will allow the bearing clearances to remain essentially constant, but at the same time the fatigue life is decreased. This interaction effect requires a tradeoff to be made between heat generation and fatigue life to optimize a bearing design.

Figure 5 is a curve illustrating the reduced relative life with increasing inner race curvature expressed as a percentage of ball diameter. (Relative life compared to that of 52% outer race curvature - 53% inner race curvature was used as a base for computation.) Figure 6 is a curve showing the heat generations vs inner race curvature at an outer race curvature of 52%. (The figure 52% is representative of most bearings and was selected only for convenience of comparison in this study.)

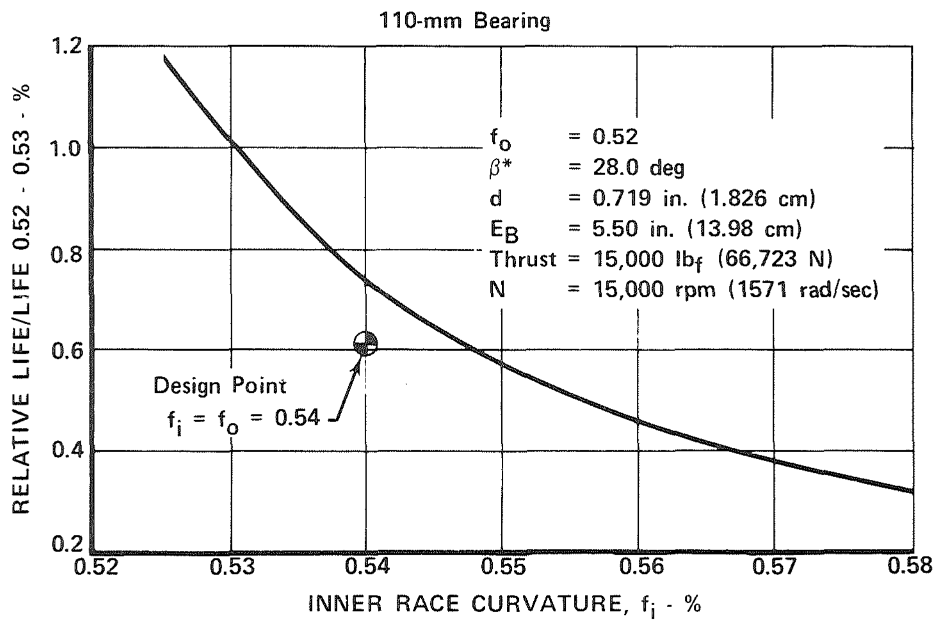

Figure 5. Life vs Inner Race Curvature FD 42560

As a result of the tradeoff study between fatigue life and heat generation, the inner race curvature of 54% was selected as optimum for this design. This point is plotted on both figures 5 and 6.

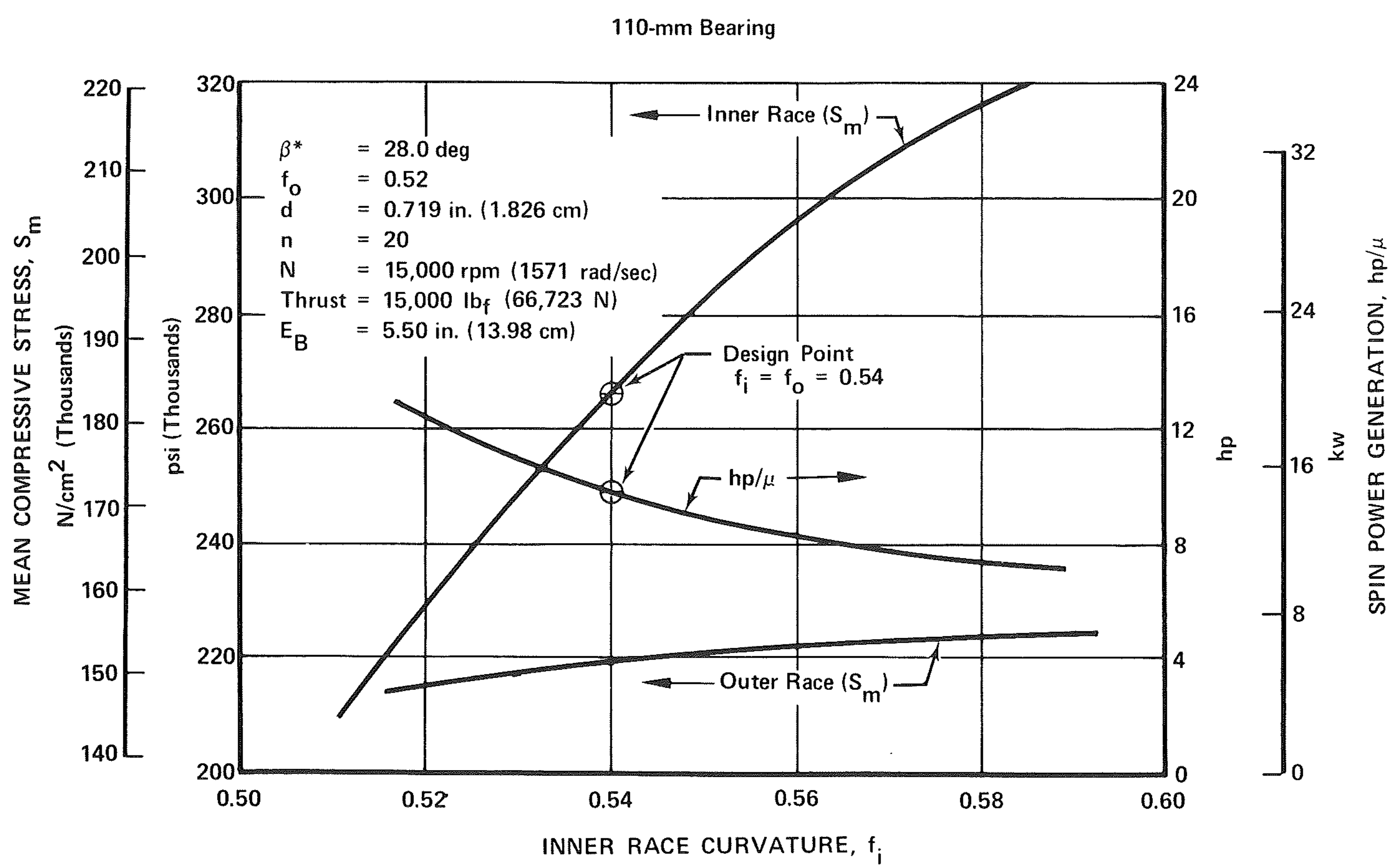

Figure 6. Mean Hertz Stress, Spin Power vs Inner Race Curvature

FD 42558

2. Total Race Curvature

Total curvature has a significant effect on the sensitivity of bearing contact angle to internal clearance changes. Figure 7 is a plot of free contact angle vs internal clearance for various values of total curvature ($B = f_i + f_o - 1$). Where: f_i = inner race curvature, and f_o = outer race curvature. The slope of each curve represents the sensitivity of the free contact angle (β_o) to changes in internal clearance. The internal clearance (P_d) is defined as the difference between outer raceway diameter and the sum of twice the ball diameter plus the inner raceway diameter.

The predicted change of internal clearances for the 110-mm bearing is 0.0054 in. (0.0137 cm), nominal at the maximum DN of 2.5×10^6. This decrease is based on centrifugal growth, thermal changes, and mechanical fits. (See inset of figure 7 for clearance change vs speed.)

For specific values of internal clearance, decreasing values of total curvature result in increasing contact angles and higher heat generation. Likewise, increasing values of total curvature decreases the contact areas in the bearing with resulting higher Hertz stresses and decreased life. Therefore, the selection of an optimum total curvature value is based on the curve that provides the lowest sensitivity of contact angle to change in internal clearance, but still provides adequate life.

A minimum total curvature of 0.08 was selected for the 110-mm bearing design. This value was chosen because the contact angle sensitivity to change in internal clearance allows the bearing to operate in the desired range of contact angle and remain within the predicted range of internal clearance. In a previous study, the equation for contact angle as a function of internal clearance was differentiated with respect to clearance and was plotted for various initial angles. This study substantiated the fact that the slight decrease in sensitivity for values of total curvature greater than 0.08, although desirable, was not worth the resulting decrease in bearing life.

3. Outer Race Curvature

The curvature of the outer race has little effect on heat generation if the ball has pure rolling on the outer race (outer race control) and likewise an increase in outer race curvature does not reduce fatigue life appreciably since the inner race is much more susceptible to fatigue failure due to higher Hertz stress. Therefore, the value of 0.54 was also selected for the outer race curvature to obtain the desired total curvature.

With race curvatures of 0.54, the transition from inner raceway control to outer raceway control, at thrust loads of 20,000 lb (88964-N) or less, occurs at or below a DN of 0.25×10^6. This transition point was well outside of the test condition envelope of this program.

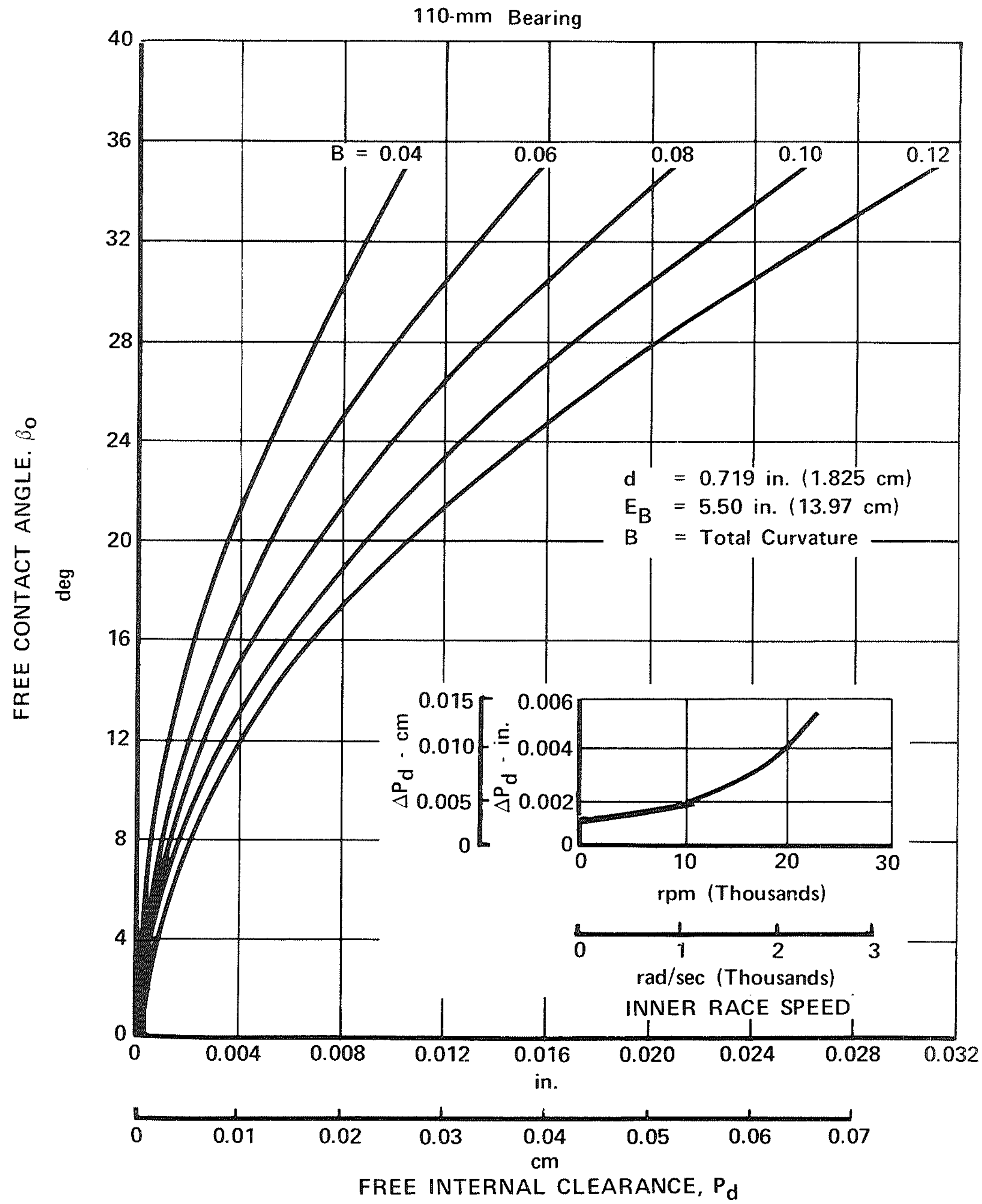

Figure 7. Free Contact Angle vs Internal Clearance

FD 42711

4. Race Control

Race control is defined as the race on which essentially pure rolling occurs. Due to the centrifugal loads of the balls, a divergence in contact angles occurs. Therefore, pure rolling on both races is not possible. The ball will spin at the race having the smaller moment in the contact ellipse.

It is possible to design for either inner or outer race control. The selection of the controlling race is a function of the required load and speed conditions. Relatively constant conditions of high load at low speed dictate use of inner race control, while widely varying load and speed conditions, such as the 110-mm bearing, dictate selection of outer race control. The transition from inner raceway control to outer raceway control is a function of friction and therefore is not precisely controlled. While the transition is occurring, it is theoretically possible to have skidding damage occur on both races. This was minimized in this program by designing the bearing to pass through the transition zone before achieving steady-state test conditions. Examples of this design approach used to prevent raceway control change in the steady-state operating range are the successful low load-high speed bearings for the RL10 LH_2 pump and the LH_2 pump for Contract NAS3-11714. For reference purposes, the internal geometry of these two bearings and one other is included in table I.

5. Contact Angle

Low contact angles, like open curvatures, can decrease heat generation, but also decrease fatigue life. The contact angle (β^*) discussed here is defined as the calculated static contact angle in the bearing corrected for changes in internal clearance due to centrifugal forces on rotating rings, thermals, press fits, Poisson's effect, etc. These must be included as part of the input to the computer program because the program considers only the effects of applied loads, centrifugal forces on the balls, and misalignments on the contact angle.

For the 110-mm bearing, a contact angle of 28 deg (0.148 rad) was selected at the design point of 15,000 rpm (1571 rad/s) and 15,000 lb (66,723 N). Figure 8 shows that the heat generation for this bearing does not change with contact angle. This is a result of a changing heat generation due to a changing normal load being offset by a changing heat generation due to a ball spin speed change with changing contact angle. Both Hertz stress and life are adversely affected by decreasing contact angle, as shown in figures 9 and 10, respectively. Higher contact angles would appear to provide better conditions; however, the gyroscopic torque on the balls increased to a point where, under transient conditions, this can result in ball-to-race skidding damage.

Table I. Comparison of Parameters for Several Bearings for Use in Liquid Hydrogen

Parameters	110-mm Bearing for NAS3-7943	55-mm Bearing for NAS8-11714	35-mm Bearing for RL10	110-mm Bearings with Armalon Cages Furnished by NASA
d, in. (cm)	0.719 (1.82)	0.3437 (0.87)	0.3125 (0.79)	0.719 (1.82)
E_B, in. (cm)	5.5 (13.97)	2.85 (7.24)	1.91 (4.85)	-
n	20	18	13	20
f_o	0.54	0.52	0.52	0.52
f_i	0.54	0.54	0.58	0.53
β_o	30.5	22.5	20	30
β^*	28	20	18	-
rpm, (rad/s)	15,000 (1571) nominal	40,000 (4188)	30,000 (3141)	13,000 (1393) nominal
	22,750 (2382) maximum			15,000 (1571) maximum
Thrust, lb (N)	15,000 (66,723) nominal	500 (2224)	450 (2002)	14,000 (62,275) nominal
	20,000 (88,964) maximum			20,000 (88,964) maximum

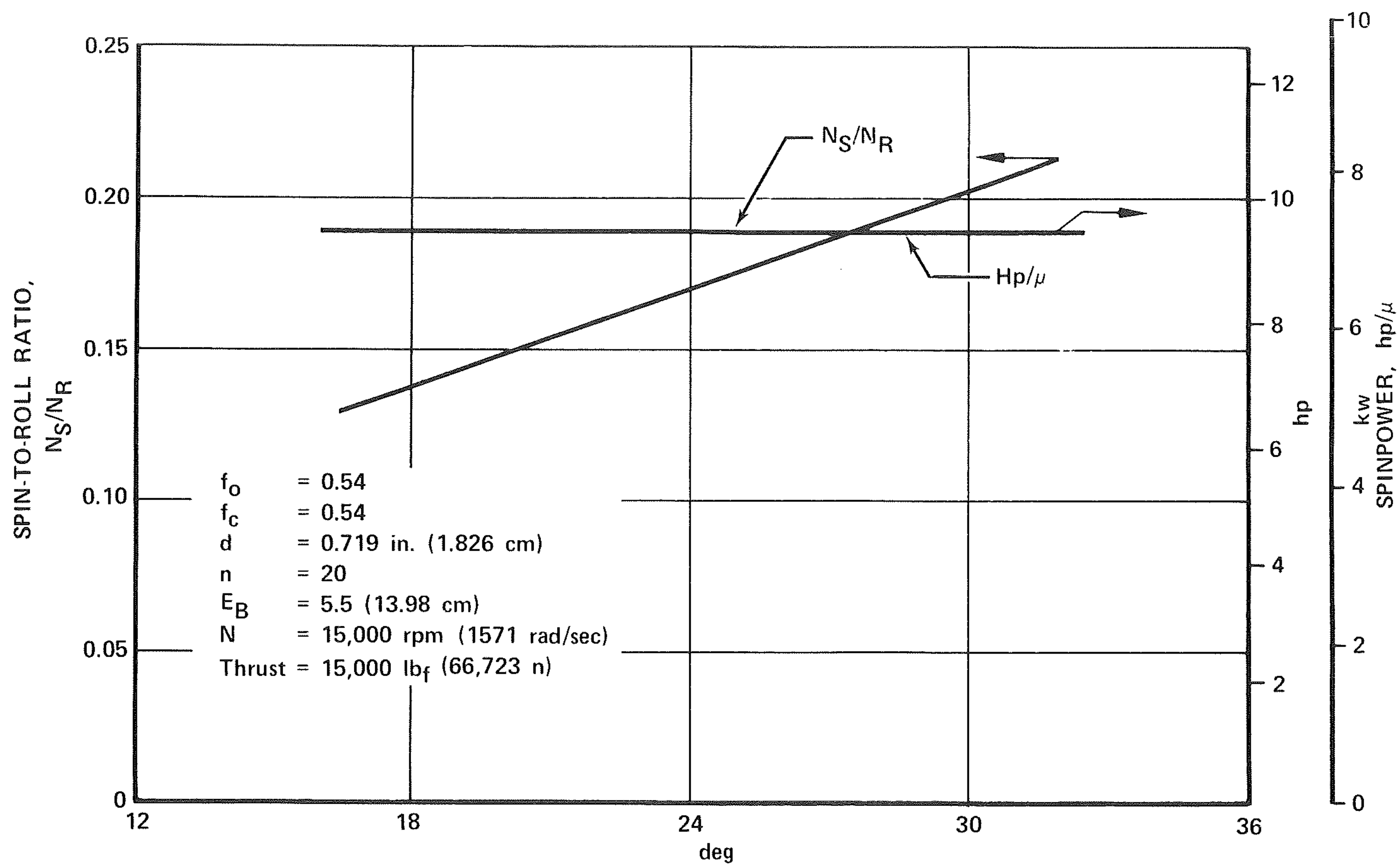

Figure 8. 110-mm Ball Bearing Spin-to-Roll Ratio and Spin Power Generation vs Contact Angle, β^*

FD 42557

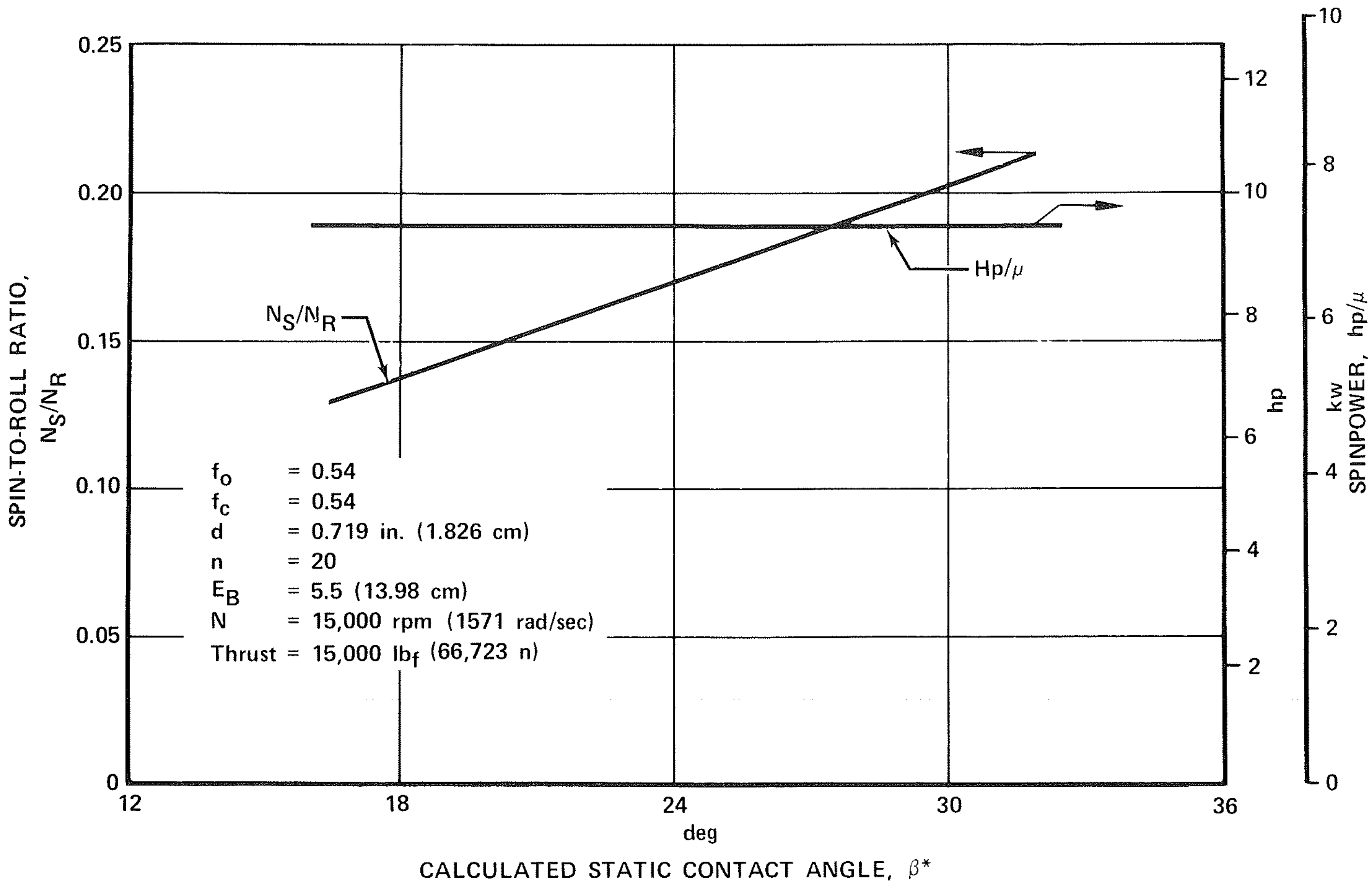

Figure 9. 110-mm Ball Bearing Mean Hertz Stress vs β^* FD 42710

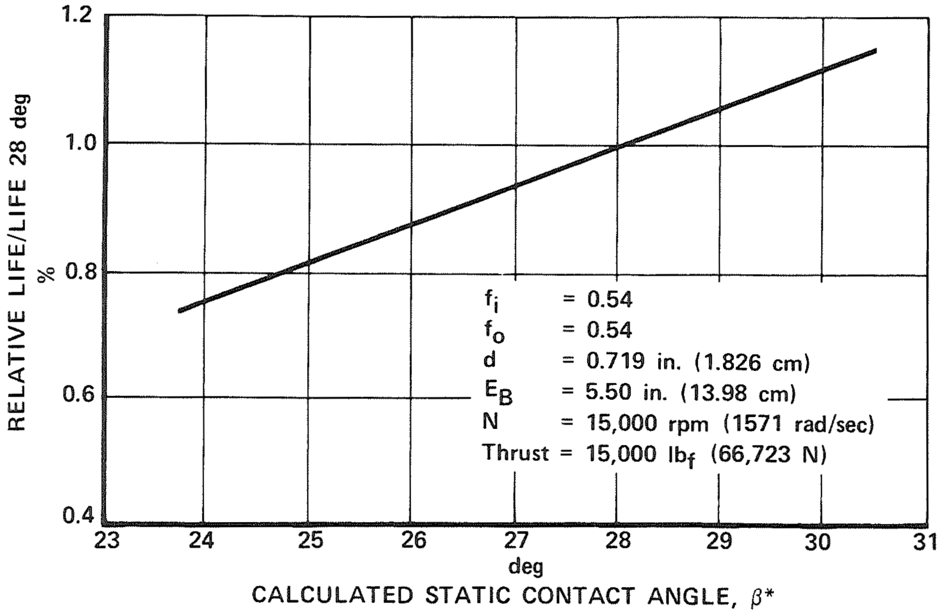

Figure 10. Life vs Contact Angle, 110-mm Bearing FD 42561

C. MATERIAL EFFECTS

After definition of the bearing geometry, the effect of the materials to be tested was studied. This portion of the design study considered the Hertz stress, subsurface shear stress, depth to maximum subsurface stress, spin to roll ratios, maximum spin velocity, and spin power (heat generation) for the full scale bearing.

Comparison of figure 11 and 12 shows that the 440C bearing would have lower spin-to-roll ratios, and lower spin-power generation than the equivalent Star J bearing. This is primarily due to the greater divergence in contact angle between the inner and outer race for the Star J bearing because of its greater density and resultant greater centrifugal loading.

Comparison of figures 13 and 14 shows that little difference is apparent in the mean compressive stress value (2/3 of maximum compressive stress) between the Star J bearing and the AISI 440C bearing, but the AISI 440C bearing would experience slightly lower shear stresses and these would occur at greater depth than in the Star J bearing because of the greater modules of elasticity (36×10^6 vs 32×10^6 lb/in^2, 24.82×10^6 vs 22.06×10^6 N/cm^2) of the Star J material. This would tend to show a greater resistance to subsurface fatigue for the AISI 440C bearing as compared to the Star J bearing.

D. BEARING TYPE

A counterbored bearing with the counterbore on the outer race was selected. This allowed relatively simple disassembly by heating the outer race and cooling the inner race, and provided better assurance of retaining the ball identity. This type of bearing design also permitted the use of an inner land riding cage, the type with which P&WA has the most successful experience. Figure 15 shows the principal features of the final design.

E. CAGE DESIGN

Based on the successful cage design used in the RL10 engine bearings, the original 110-mm bearing cage design as shown in figure 16 utilized a core of the Salox M or Chemloy 719 lubricant reinforced by an aluminum shroud. The cage was riveted together by steel rivets between each ball pocket. This design exposes the lubricant at the inside diameter so that it may freely contact the inner race piloting surfaces. To allow assembly into the aluminum shroud the cage body of the lubricant material was split into two pieces.

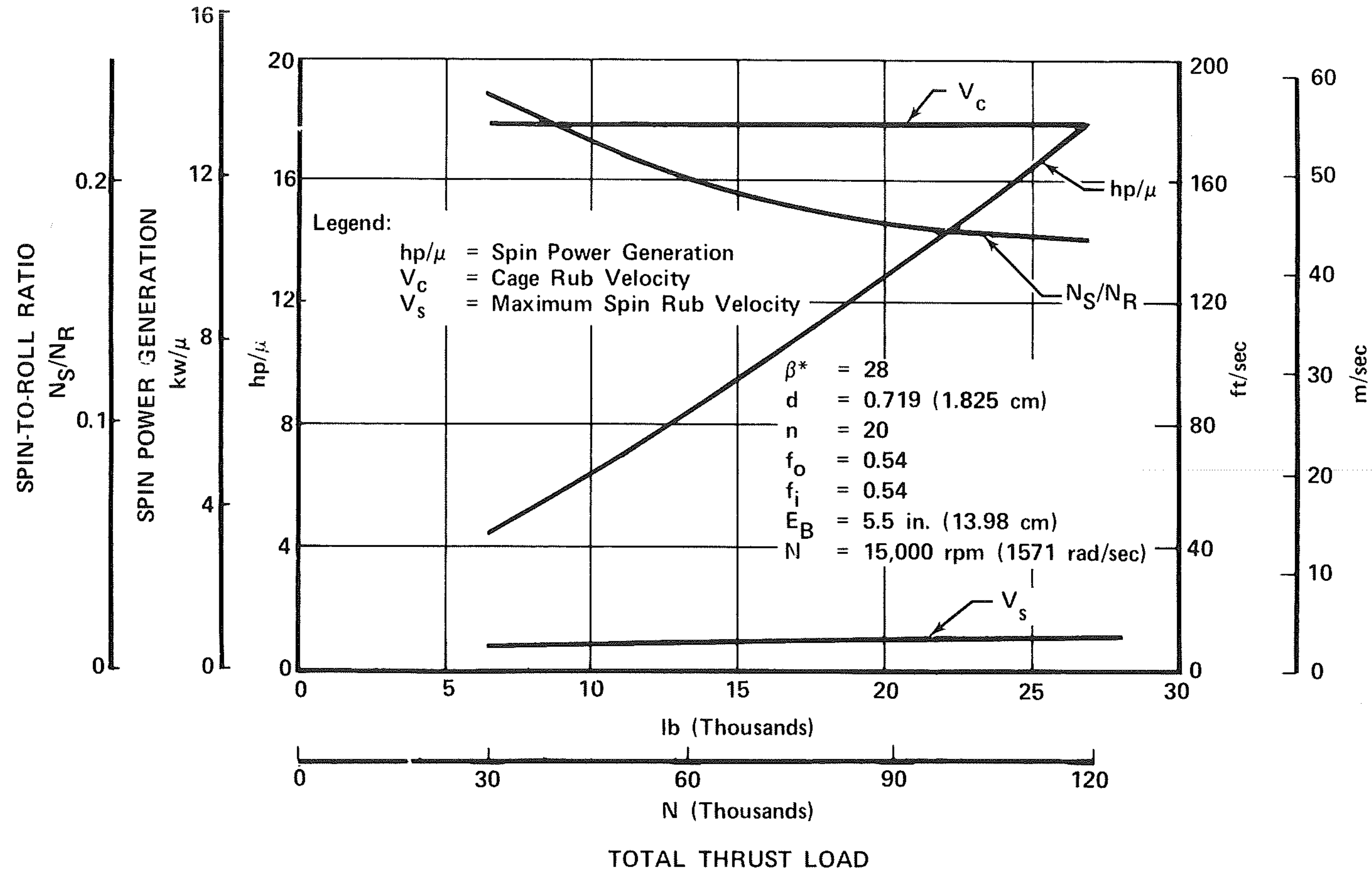

Figure 11. 110-mm Ball Bearing Star J Design Speed

FD 42712

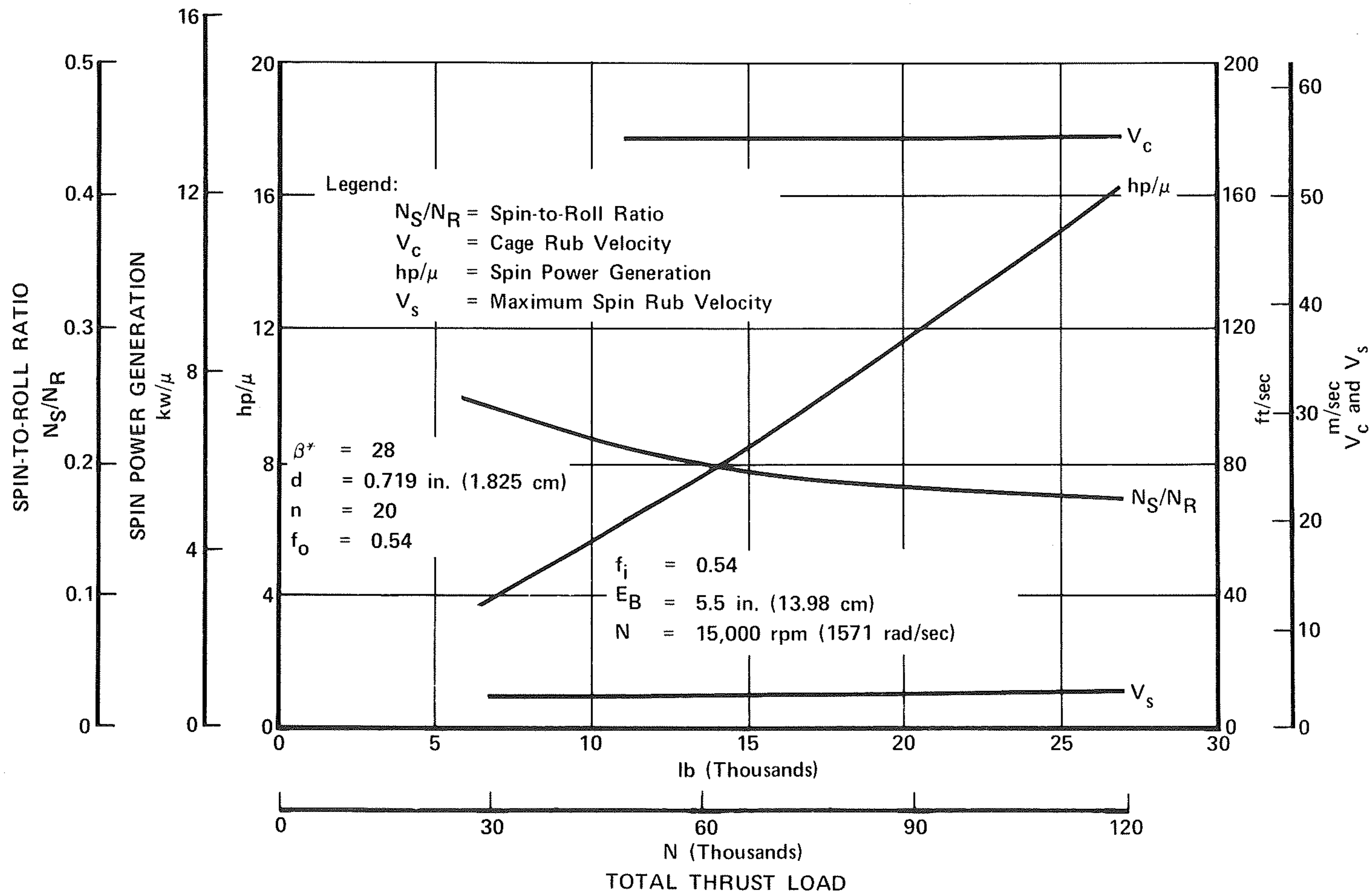

Figure 12. 110-mm Ball Bearing 440C Design Speed

FD 42714

22

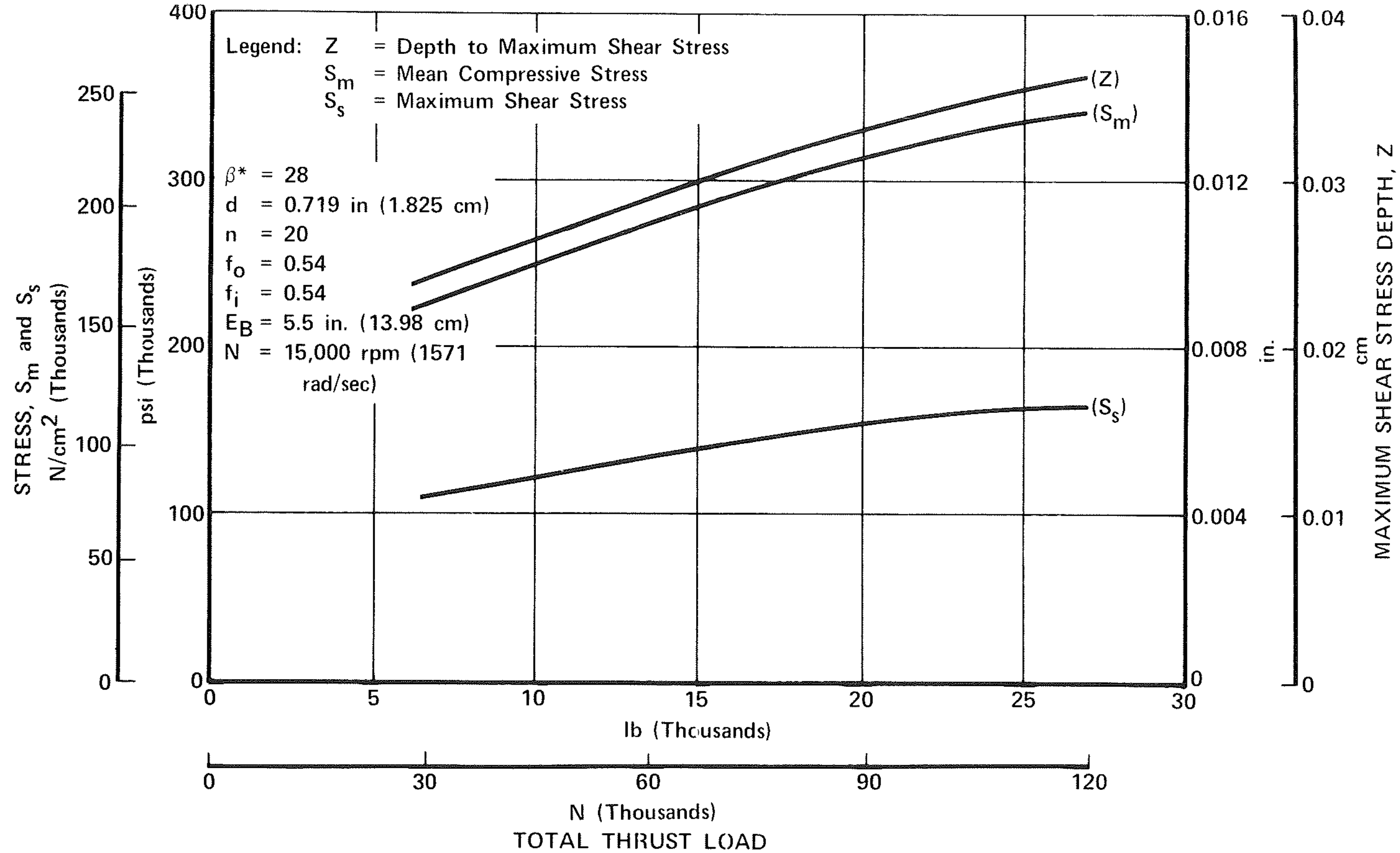

Figure 13. 110-mm Ball Bearing 440C Design Speed

FD 42693

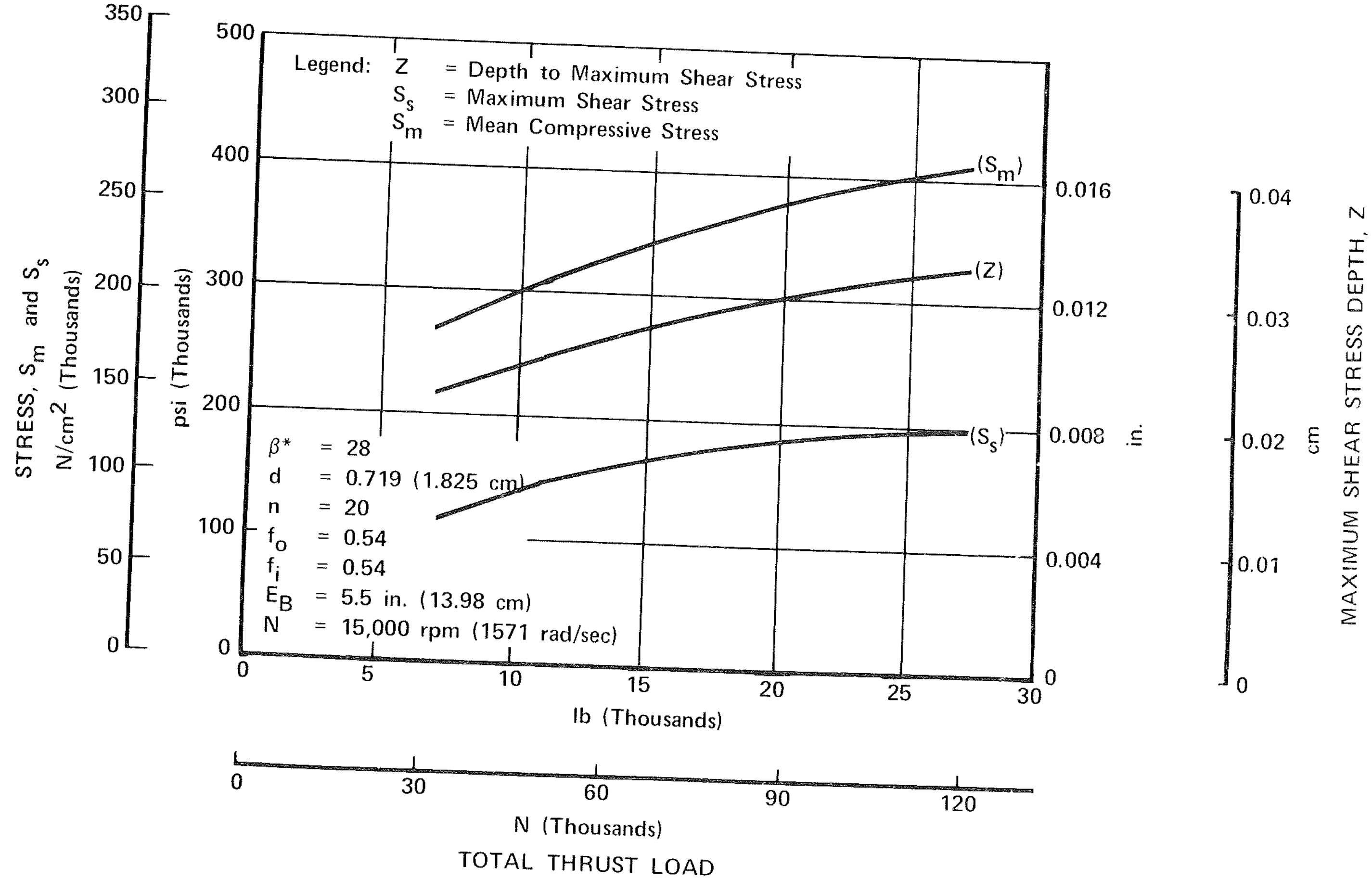

Figure 14. 110-mm Ball Bearing Star J Design Speed

FD 42713

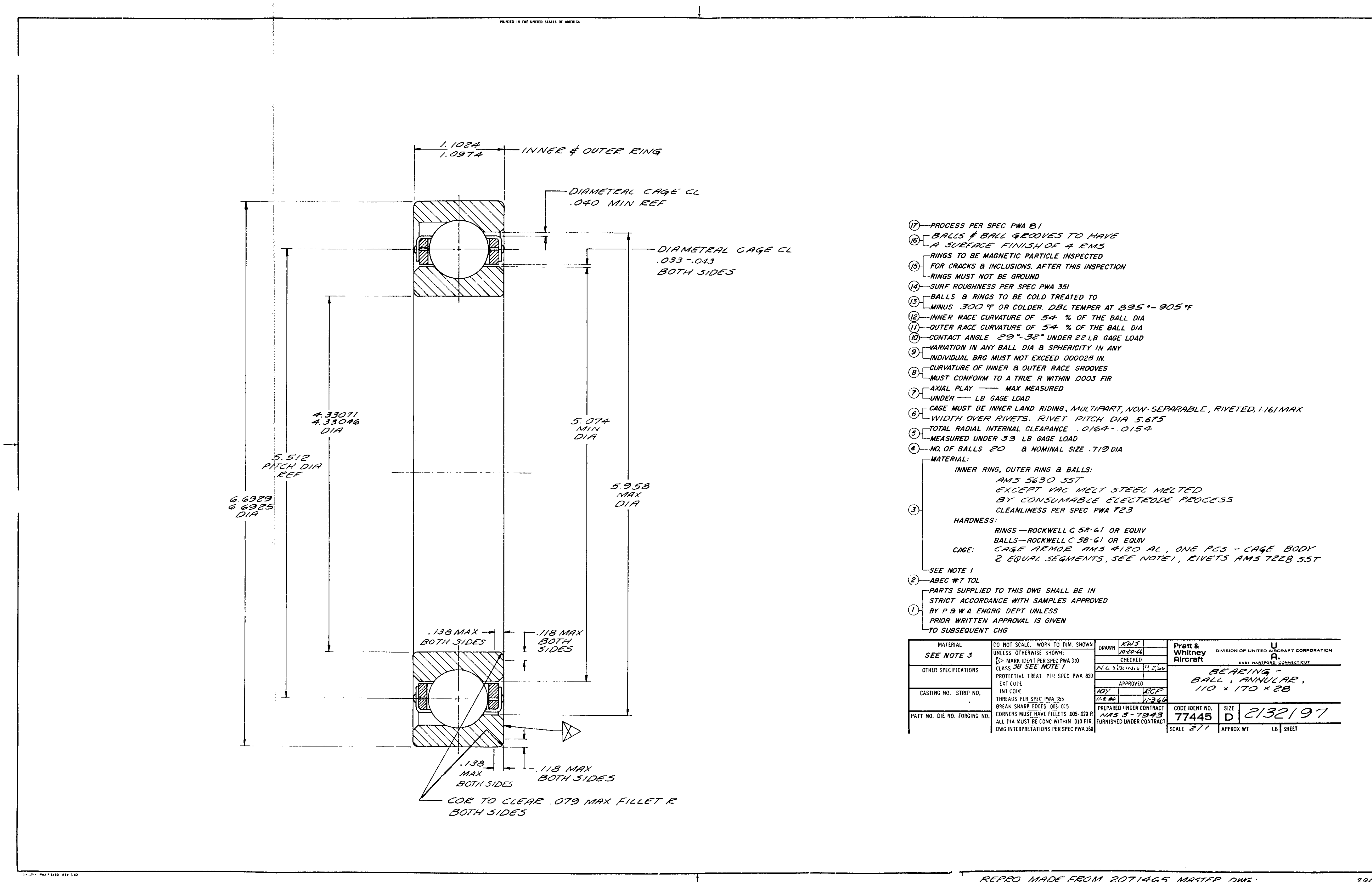

Figure 15. Annular Ball Bearing, 110 x 170 x 28 mm

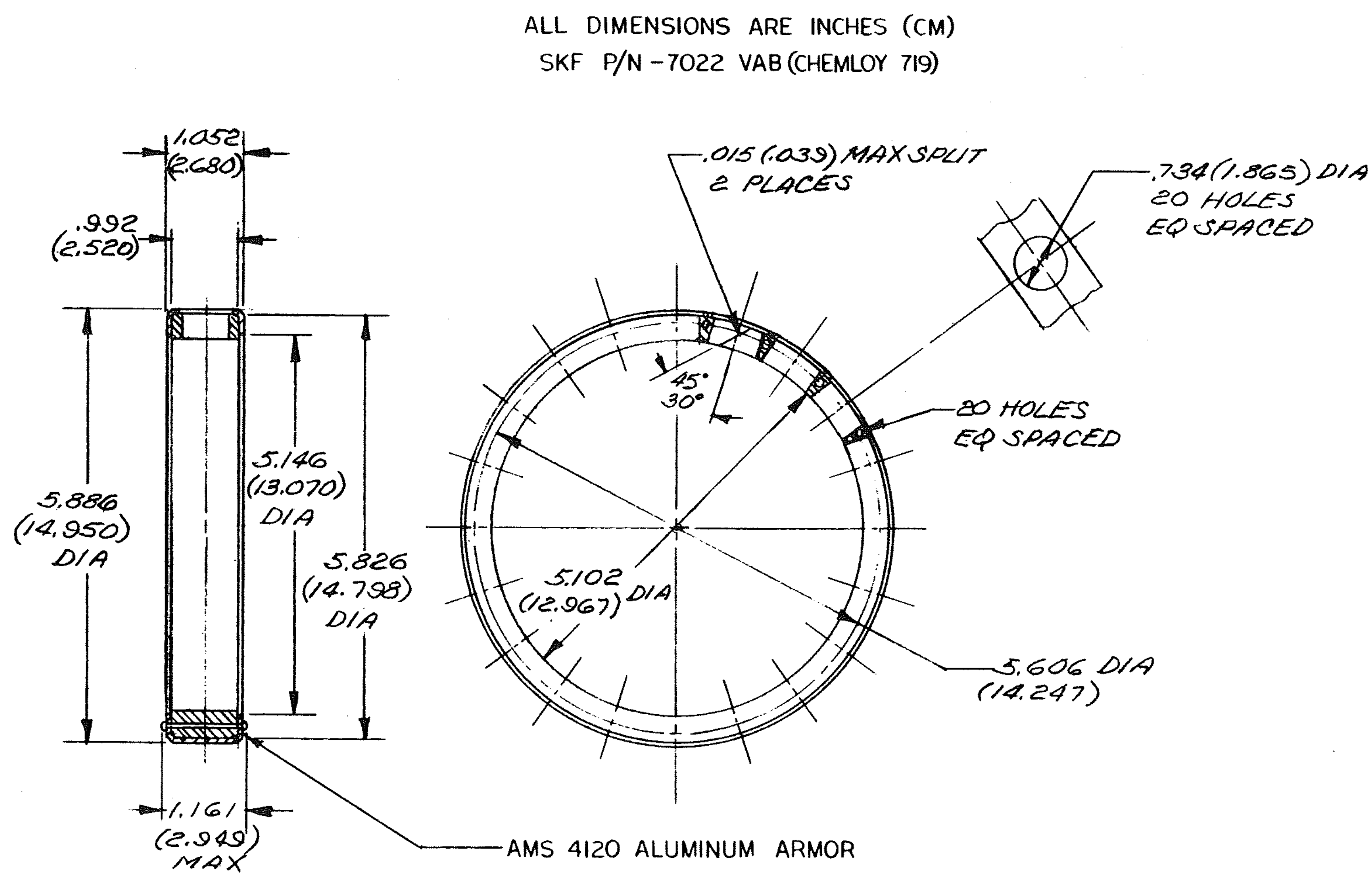

Figure 16. Original 20-Ball Cage Configuration

A detailed stress and deflection analysis of the cage was performed using the best available data on the materials such as expansion coefficients, density, etc. This showed the design to be satisfactory in both strength and rigidity based on expected forces on the cage.

SECTION IV
TEST PROGRAM

The test program on the 110-mm ball bearings included a preliminary functional test of the facility, test rig, and instrumentation. This was accomplished using existing 110-mm ball bearings furnished by NASA instead of the 110-mm test bearings designed and fabricated under the contract. The NASA bearings were used during this preliminary test to minimize exposure of any of the limited number of test bearings to a premature stand and/or rig malfunction, thereby providing some assurance that useful data would be obtained on all bearing samples.

The NASA ball bearings were of the split inner race type using an outer land riding Armalon cage. A pair of these bearings was operated at load/speed conditions ranging to 7000 lb (33,362-N) and 10,000 rpm (1047 rad/s), respectively. Testing was terminated by a sudden bearing temperature rise above established steady-state values. The test verified the adequate functional characteristics of the rig and instrumentation over the range of values tested.

Following the functional test, the 110-mm test bearings designed in this program were tested. Details of each test are discussed in the following paragraphs and a summary is presented in table II.

A. TEST NO. 1, BEARING SET NO. 1

The initial test of the 110-mm counterbore ball bearings designed and procured for this program was conducted with bearings consisting of AISI 440C balls and races with Chemloy 719 cages (S/N 225 front and 226 rear). Figure 17 shows the components of bearing S/N 226, including the two-piece Chemloy 719 cage and its riveted aluminum armor. Design details for this bearing are shown in figure 15, with cage details depicted in figure 16.

The rig was mounted in test stand B-14, and an attempt was made to run the 12,000-rpm (1256-rad/s) and 9000-lb (40,034-N) thrust load condition as specified in the test plan. Cooldown of the rig and bearings was completed at zero rotation and load conditions. Subsequent to cooldown, an operational point of 500-rpm (52-rad/s) and 150-lb (667-N) thrust load was established. At this point the data indicated excessive power requirements for the drive motor, which was attributed to the binding of Teflon shaft seals.

Table II. Test Summary

Test No.	Bearing Set No.	Bearing Serial No. Front	Bearing Serial No. Rear	Rotation Time, min	Scheduled Load, lb (N)	Scheduled Speed, rpm (rad/s)	Maximum Load, lb (N)	Sustained Speed, rpm (rad/s)	Time at Sustained Load/Speed, min	New Cage	Test Date	Bearing** Part No.	Cage Modification	Cause for Test Termination	Damage to Components
1	1	225	226	15	9,000 (40,034)	12,000 (1,256)	150 (667)	500 (52)	15	X	11-29-67	2132197		Excessive drive torque.	Surface scuffing of balls and races in both bearings due to ball skidding. Slight pocket wear in both cages.
2	2	248	249	15	9,000 (40,034)	12,000 (1,256)	9,000 (40,034)	12,200 (1,277)	15	X	12-26-67	2132197	CKJ 7153	Successful completion.	None
3	2	248	249	11.5	9,000 (40,034)	13,000 (1,361)	9,000 (40,034)	12,000 (1,256)	1.25		4-16-68	2132197	CKJ 7153	Uncontrolled temperature rise in rear bearing.	Severe rear cage pocket wear.
4	3	L5	L6	5.75	12,000 (53,379)	12,000 (1,256)	12,000 (53,379)	12,000 (1,256)	2.4	X	4-18-68	2132197	CKJ 7153	Uncontrolled temperature rise in front bearing.	None - Light cage pocket wear.
5	4	L4	L5	10.5	9,000 (40,034)	12,000 (1,256)	6,200 (27,579)	9,500 (995)	0.5	X	5-15-68	2137774	CKJ 8836	Uncontrolled temperature rise in rear bearing.	High rear cage pocket wear.
6	5	L1	L3	5.75		12,000 (1,256)	5,800 (25,800)	11,800 (1,235)	0.5	X	5-22-68	2137774	CKJ 8836	Uncontrolled temperature rise in both bearings.	Ball failure in both bearings, surface roughened on races, and cages fractured.
7*	2	248	249	6.5	9,000 (40,034)	13,500 (1,413)	5,500 (24,465)	13,000 (1,361)	0.67	X	5-31-68	2132197	CKJ 7153	Uncontrolled temperature rise in both bearings.	Severe pocket wear in both cages - surfaces of races and balls showed minute pitting.
8*	3	L5	L6	5.5	12,000 (53,379)	12,000 (1,256)	5,800 (25,800)	8,000 (838)	1.5		6-04-68	2132197	CKJ 7153	Uncontrolled temperature rise in rear bearing and excessive drive torque.	Severe rear cage pocket wear.
9*	2	248	249	4	9,000 (40,034)	13,500 (1,413)	2,500 (11,120)	12,000 (1,256)	2	X	7-01-68	2132197	CKJ 9256	Load bellows pressure fluctuations, and uncontrolled temperature rise in rear bearing.	Moderate rear cage pocket wear. Increase in minute pitting on ball surface as compared to test 7.
10A*	3	L5	L6	4.75	12,000 (53,379)	12,000 (1,256)	11,000 (48,930)	12,000 (1,256)	0.33	X	7-09-68	2132197	CKJ 9256	Uncontrolled temperature rise in front bearing.	None.
10B*	3	L5	L6	3.5	2,900 (12,900)	12,000 (1,256)	2,900 (12,900)	12,000 (1,256)	1.5		7-09-68	2132197	CKJ 9256	Uncontrolled temperature rise in front bearing.	Severe pocket wear in front cage.
11*	2	248	249	15.25	9,000 (40,034)	13,000 (1,361)	6,000 (26,689)	13,000 (1361)	2	X	1-21-70	2132197	DKJ 1015	Uncontrolled temperature rise in front bearing.	Moderate pocket wear in front cage.
12*	2	249	248	15.0	9,000 (40,034)	13,000 (1,361)	6,500 (28,913)	13,000 (1,361)	4		1-28-70	2132197	DKJ 1015	Uncontrolled temperature rise in rear bearing.	Severe pocket wear in rear cage.
13A*	3	L5	L6	36.0	-	-	7,200 (32,027)	13,000 (1,361)	4	X	2-19-70	2132197	DKJ 1015	Depletion of liquid hydrogen coolant supply.	None.
13B*	3	L5	L6	15.0	7,200 (32,027)	13,000 (1,361)	2,500 (11,120)	13,000 (1,361)	6.25		2-20-70	2132197	DKJ 1015	Uncontrolled temperature rise in rear bearing.	Both cages fractured with failed rivets in front cage. Moderate wear in ball pockets.
14A	6	L9	L10	41.1	7,200 (32,027)	13,000 (1,361)	7,500 (33,362)	13,000 (1,361)	23.66	X	3-19-70	2137774	DKJ 6202	Depletion of liquid hydrogen coolant supply.	None.
14B	6	L9	L10	25.67	7,200 (32,027)	13,000 (1,361)	7,200 (32,027)	13,000 (1,361)	9.33		3-19-70	2137774	DKJ 6202	Uncontrolled temperature rise in rear bearing.	Damage confined to a fractured ball in rear bearing and immediate cage pocket area.
15	7	L7	L8	8.08	7,200 (32,027)	13,000 (1,361)	2,900 (12,900)	12,000 (1,256)	4	X	4-17-70	2137774	DKJ 6202	High vibration in both bearings.	Both cages sustained web cracks with light wear in pockets - no ball or race damage.
16A	8	L2	L6	43.61	7,200 (32,027)	13,000 (1,361)	7,500 (33,362)	13,000 (1,361)	32.0	X	4-27-70	DKJ 7743	DKJ 6202	Depletion of liquid hydrogen coolant supply.	None.
16B	8	L2	L6	10.2	7,200 (32,027)	13,000 (1,361)	2,600 (11,565)	13,000 (1,361)	3.1		4-22-70	DKJ 7743	DKJ 6202	Uncontrolled temperature rise in front bearing.	Severe wear in two pockets of front cage. Fractures in two pockets in both cages.

* One or both bearings had overheated in a previous test.

** 2132197 - AISI 440C balls and races with Chemloy 719 cage
2137774 - AISI 440C Races, Star J Balls, and Salox-M cage
DJK 7743 - AISI 440C balls and races with Salox-M cage

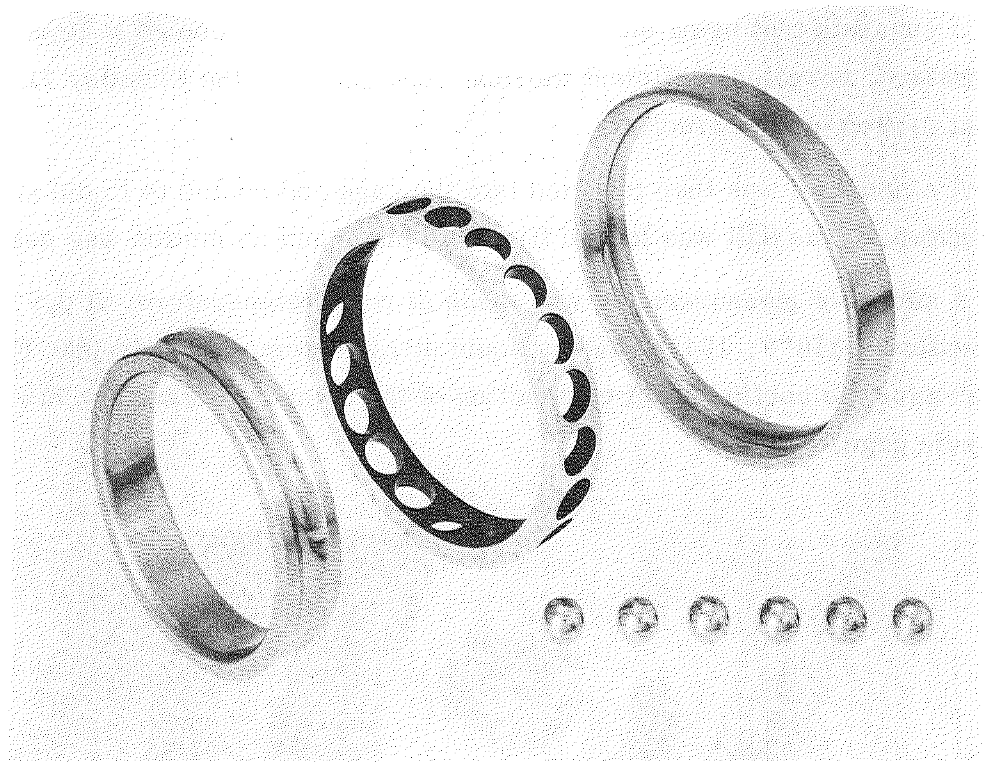

Figure 17. 110-mm Bearing, S/N 226 With AISI 440 Races and Balls; Chemloy 719 20-Pocket Cage FE 71034

To relieve this condition, the rig was allowed to warm to a temperature of -130°F (183°K) at which point shaft torque was within normal operating limits. A short seal wear-in run of 3 min was made at the 500-rpm (52-rad/s) and 150-lb (667-N) thrust condition, then another cooldown to -420°F (22°K) was attempted. Again excessive drive motor power requirements were experienced, and the test was terminated. Total rotating time was 15 min.

A post-test examination revealed that the balls and races of both bearings were damaged by ball skidding. Some of the surface damage (figure 18) shows metal deposited on the ball track of the outer race. The cages showed wear on the ID piloting surfaces and in the ball pockets (figure 19). Close examination of the various pockets revealed heavy wear in the area of the cage split, but only slight scuffing in the other pockets.

To determine the cause of the nonuniform pocket wear, one unmounted bearing was cooled in liquid nitrogen. At liquid nitrogen temperature the bearing components would not rotate, but retained axial play, indicating sufficient ball-to-race radial clearance.

A separate test using only the cage and inner race, cooled to liquid nitrogen temperature, revealed sufficient thermal contraction of the Chemloy 719 cage to prevent motion in any direction.

A single ball was then inserted into the cage and cooled to liquid nitrogen temperature. The ball was locked firmly in place and no motion was possible.

A series of measurements was made at room temperature, at dry ice temperature (-110°F, 194°K) and at liquid nitrogen temperature (-320°F, 77°K) to determine the coefficient of contraction of the composite Chemloy 719 and aluminum cage.

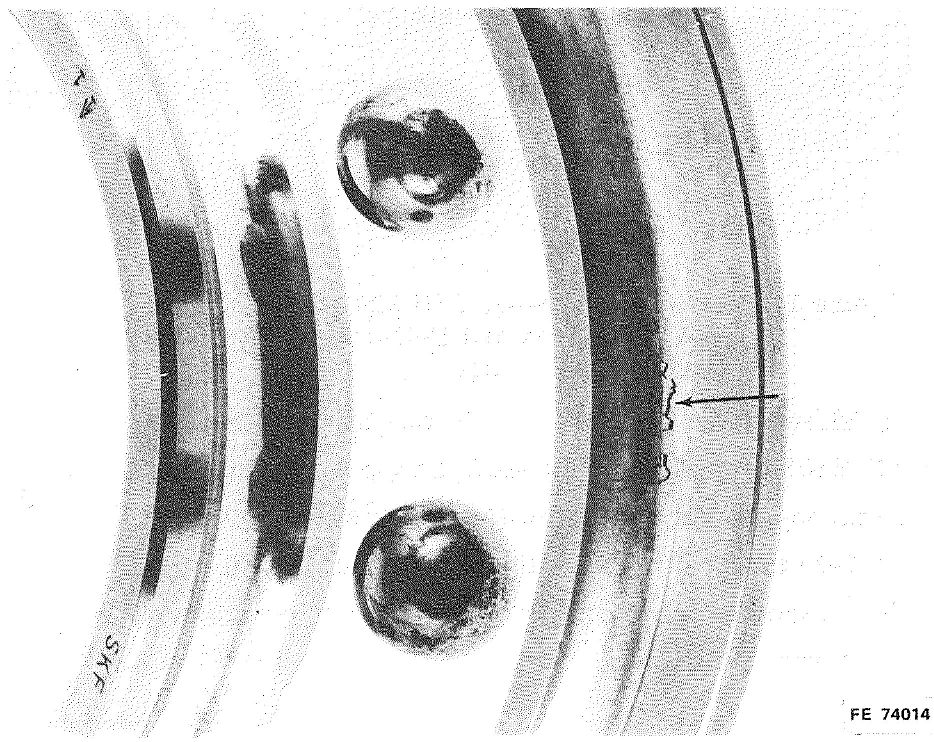

Figure 18. Front bearing S/N 225 From Test No. 1 Showing Ball Scuffing and Race Damage From Skidding

FD 49331

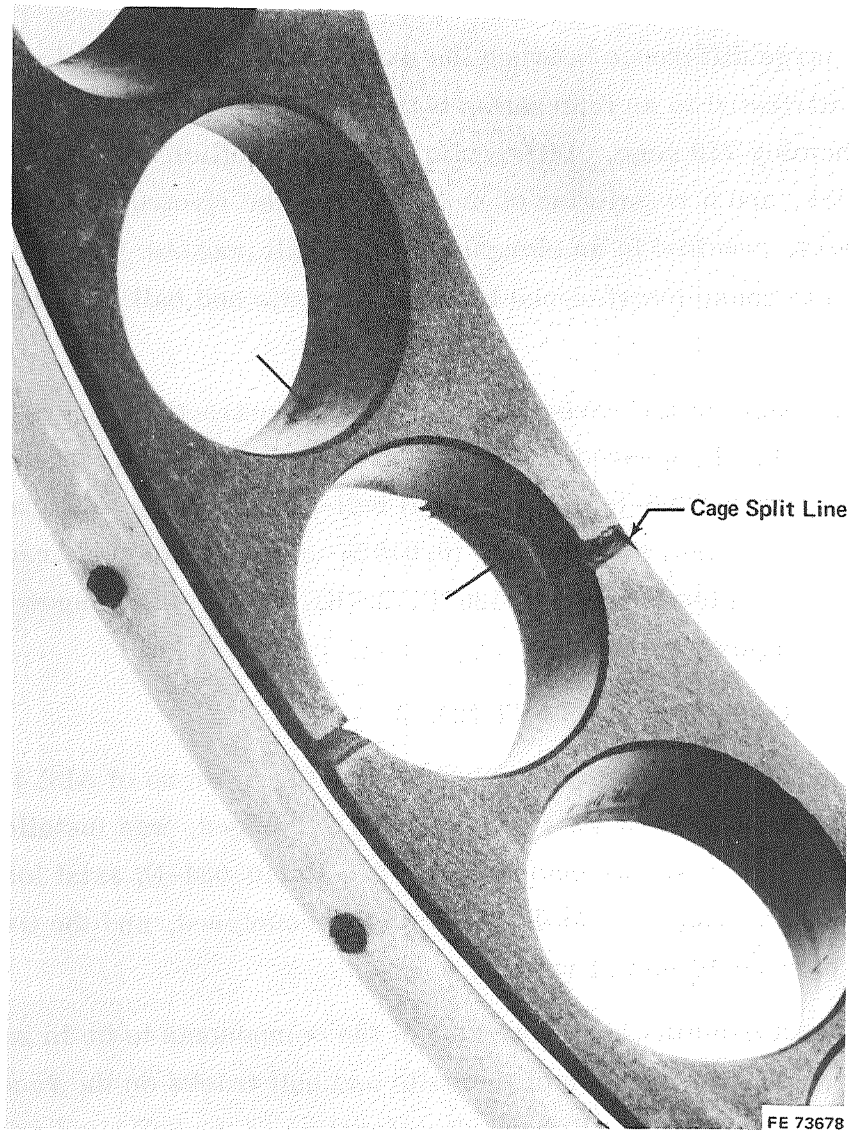

Figure 19. Chemloy 719 Cage From Front Bearing S/N 225 Showing Pocket Wear Patterns FD 49332

Because of the interaction between the aluminum cage supports, the steel rivets, and the Teflon-based Chemloy 719, three different thermal coefficients for the composite structure were obtained. By extrapolation from liquid nitrogen to liquid hydrogen temperature these are:

Cage ID	14.8×10^{-6} in./in./°F (8.23×10^{-6} cm/cm/°C)
Ball Pocket	
Axial	6.8×10^{-5} in./in./°F (3.78×10^{-5} cm/cm/°C)
Circumferential	2.2×10^{-5} in./in./°F (1.22×10^{-5} cm/cm/°C)

The large difference between the axial and circumferential contraction values is attributed to an interaction between the riveted aluminum cage armor and the Chemloy 719 cage. Differential thermal coefficients between aluminum and Chemloy, and a restriction of motion due to the riveted construction between the two parts, resulted in an elongation of the ball pockets. The deformation was enough to cause interference between the balls and ball pockets in the axial direction.

On the basis of the revised coefficients of contraction, new cage clearances were computed and approved by the NASA program manager. The new cage dimensions gave 0.0325-in. (0.0825-cm) ball-to-cage pocket clearance, and 0.004-in. (0.0103-cm) to 0.006-in. (0.01525-cm) cage-to-inner race clearance at liquid hydrogen temperature (-420°F, 22°K). The cage changes (CKJ 7153) are shown in figure 20.

B. TEST NO. 2, BEARING SET NO. 2

A second set of bearings (S/N 248 and 249), made up of AISI 440C balls and races with modified (CKJ 7153) Chemloy 719 cages, was installed in the bearing rig. This test was made with a 9000-lb (40,034-N) axial load at 12,200 rpm (1277 rad/s). No difficulty was encountered, and the test completed the planned 15 min of running.

Post-test examination showed all of the components to be in good condition except for some discoloration of the balls and ball tracks on the races from a material coating. Figure 21 shows discoloration of the balls and races from the black Chemloy cage material. Some slight, rusty yellow discoloration was also evident in the ball tracks, and a spectrographic examination was conducted to determine the composition of the material. The black material was confirmed to be Chemloy 719 and the yellow to be iron oxide. Presumably, the iron oxide originated in the hydrogen supply piping because the bearings are fabricated of a corrosion resistant type steel and did not show signs of rust on any surface prior to test.

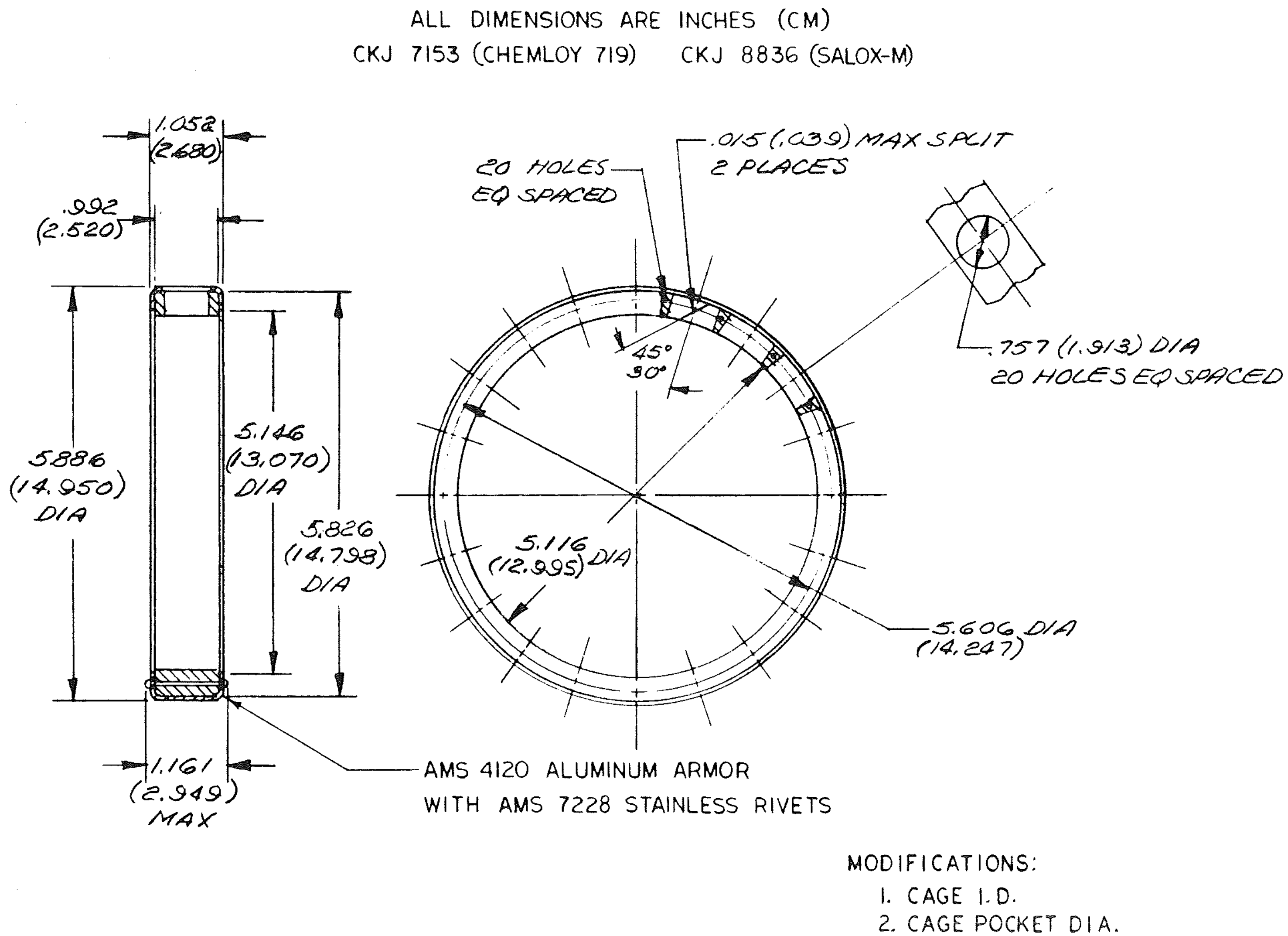

Figure 20. First 20-Ball Cage Modification

FD 49333

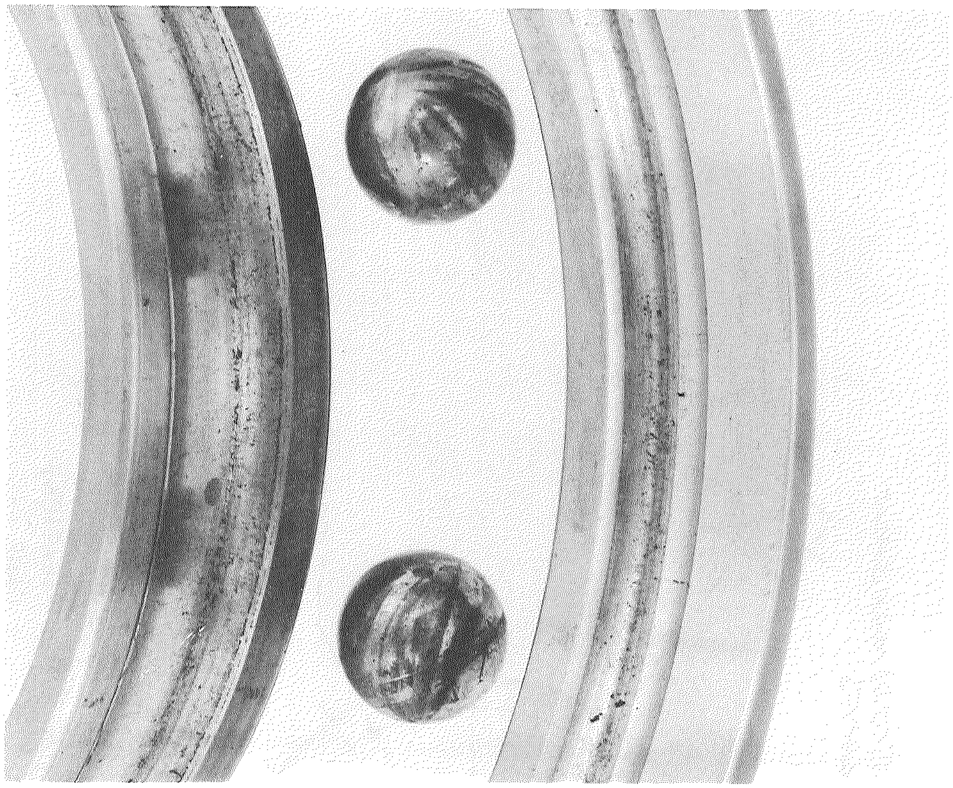

Figure 21. Ball Bearing From Test No. 2 Showing Ball and Race Discoloration From Deposits of Chemloy 719 and Iron Oxide FE 73969

C. TEST NO. 3, BEARING SET NO. 2

After careful measurement and examination of the bearing components following test No. 2, the bearings (S/N 248 front and 249 rear) were reinstalled in the test rig for additional testing. The accumulated deposits of Chemloy 719 on the bearing elements were left in place to provide as much lubrication of the surfaces as possible. All balls and cages were assembled in the same relative positions as in the previous test.

The intended test conditions were 9000-lb (40,034-N) axial load and 13,500 rpm (1413 rad/s). The test started with a normal cooldown and initial rotation with a partial load at 12,000 rpm (1256 rad/s). While the load was being adjusted near 9000-lb (40,034 N) the temperature of the rear bearing rose sharply and rotation was stopped.

As the temperatures had not reached levels that would damage the balls or races, a second attempt to run was made with a higher coolant flowrate. As before, the bearing temperatures rose sharply, so the test was terminated. Total time at 12,000 rpm (1256 rad/s) and 9000-lb (40,034-N) load was 1.25 min.

Post-test examination of the bearings showed severe wear on the cage of the rear bearing (S/N 249). Six cage pockets were worn through the Chemloy 719 and the balls were rubbing directly on the steel rivets. Figure 22 shows the typical wear pattern in the pockets of this bearing cage. The front bearing (S/N 248) was undamaged and in a condition suitable for further tests.

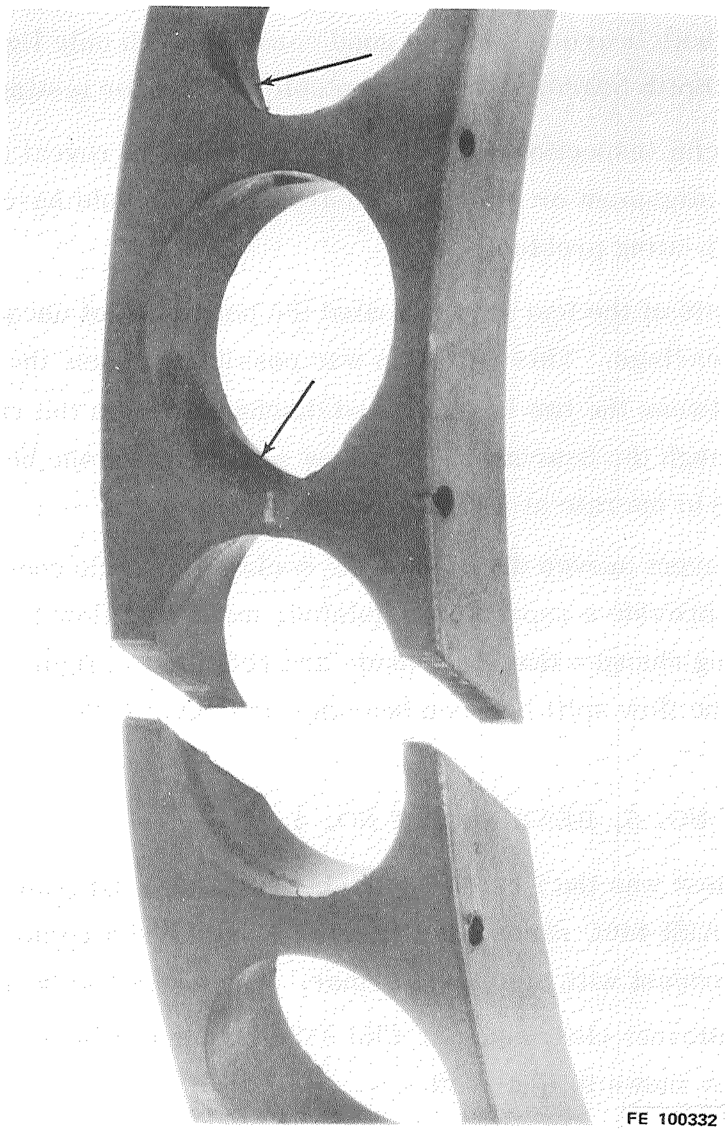

FE 100332

Figure 22. Rear Ball Bearing, S/N 249 Cage Showing Heavy Ball Pocket Wear Patterns During Test No. 3 FD 49334

D. TEST NO. 4, BEARING SET NO. 3

This test was conducted using a new set of AISI 440C bearings (S/N L5 front and L6 rear) with Chemloy 719 cages modified in the same manner as bearing cages S/N 248 and 249 (CKJ 7153). The intended test point was 12,000 lb (53,379 N) axial load at 12,000 rpm (1256 rad/s). After 2.5 min at the test condition, the drive-end (front) bearing overheated and the test was terminated.

Post-test inspection of the bearings failed to show the cause of the overheating, as both bearings were in good condition with only light wear marks on the cages. Bolth bearings were acceptable for further testing.

A careful inspection of the bearing rig failed to reveal any abnormalities, such as misalignment or improper clearances that could have contributed to the bearing heating problem.

Analysis of the test data revealed the possiblity of unequal flow of coolant to the two bearings. This condition was possible because the coolant was introduced between the two bearings and discharged from the rig case after passing through the bearings. High flow resistance in one bearing could cause that bearing to operate at a higher temperature.

To prevent uneven division of the coolant flow, the coolant system was modified to provide a separate, regulated, measured flow to each bearing. The plumbing changes that were made are reflected in figure 2. Valve CV-1 controlled the flow split between bearings and valve CV-2 controlled the total flowrate.

E. TEST NO. 5, BEARING SET NO. 4

This test was the first using the bearings (S/N L4 front and L5 rear) made up of AISI 440C races, Stellite Star J balls and a composite cage using Salox-M lubricant with aluminum armor. The cages had been modified for additional internal clearance per CKJ 8836 (same as CKJ 7153) except for materials as shown in figure 20.

The test was intended to be made at 9000-lb (40,034-N) axial load and 12,000 rpm (1256 rad/s), but before test conditions could be set, the rear bearing overheated. After cooling the rig and setting a higher flowrate, a second attempt was made. Again the rear bearing overheated, and the test was terminated.

Post-test examination showed that the front bearing (S/N L4) was in good condition and showed only slight wear marks. The rear bearing cage (S/N L5) had abnormally high wear in three ball pockets and moderate wear in the remaining pockets.

The wear marks in the badly worn pockets were on the rear face, which indicated that these balls were dragging, at a lower ball speed. This can be explained by oversized balls (Appendix B-5, P. 103), which operate at a lower contact angle and lower peripheral speed, thereby acting as a brake on the cage. The braking action can result in the wear experienced.

To investigate this theory, a comparison was made of the pretest and post-test ball diameters. A total ball size variation in the ball set was found to be 0.000160 in. (0.000406 cm). The blueprint called for a class 25 ball that allows ±0.000025-in. (0.000063-cm) variation from nominal size. The badly worn pockets were matched to the three largest balls. These data are not conclusive, however, as the bearing that operated normally also had a poorly matched set of balls [0.000130 in. (0.00033 cm) variation], and no excess wear occurred in the ball pockets.

F. TEST NO. 6, BEARING SET NO. 5

Bearing set No. 5 (S/N L1 front and L3 rear), consisting of AISI 440C races with Star J balls and Salox-M cages, was tested at 12,000 rpm (1256 rad/s). Ball failures occurred in both bearings as the load was being applied [about 6000 lb (26,689 N) load at failure].

Inspection of the bearings showed that four balls in the front bearing L1 and one ball in the rear bearing L3 had failed. Size variation of the ball set in the front bearing was 0.000160 in. (0.000406 cm), again well above the specifications, whereas the variation in size of the rear set was only 0.000020 in. (0.000051 cm). The bearings were returned to the vendor for failure analysis and the findings were that the balls failed due to internal voids formed during the casting process. Figure 23 shows photomicrographs of voids found in one of the failed balls from bearing L1. Figure 24 shows the surface condition of the races and one of the failed balls from bearing L3. Figure 25 shows the damaged cage after test from bearing L3. One pocket that contained a failed ball is fractured; the other pocket shows light wear patterns.

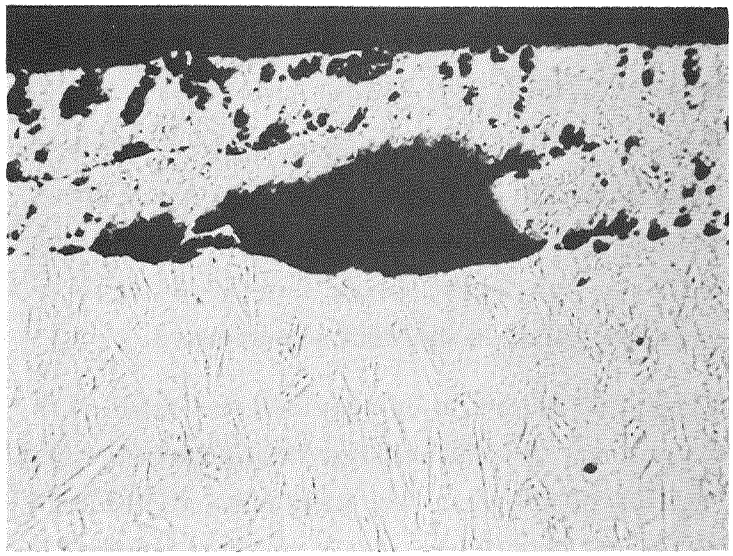

100X

Figure 23a. Photomicrograph Shows Various Sized Voids at Surface of No. 4 Ball From L1 Bearing — FE 99110

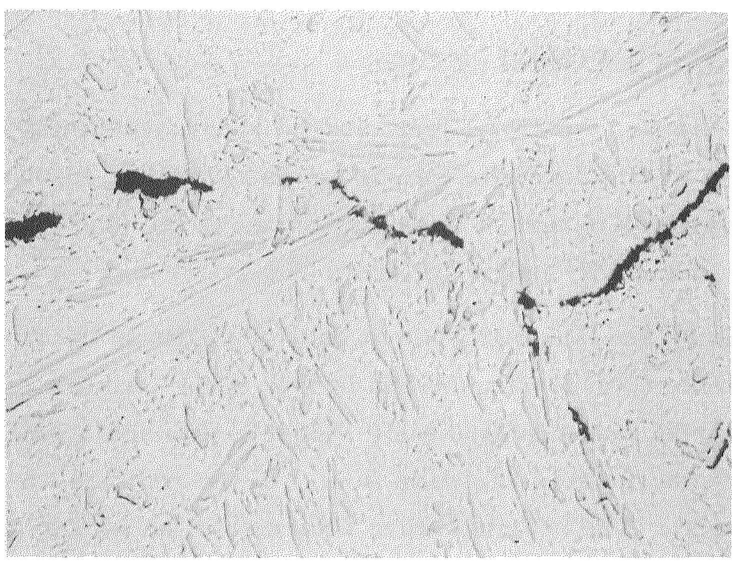

100X

Figure 23b. Crack Through Voids Located at 0.035-in. to 0.040-in. Beneath Ball Surface. — FE 99110

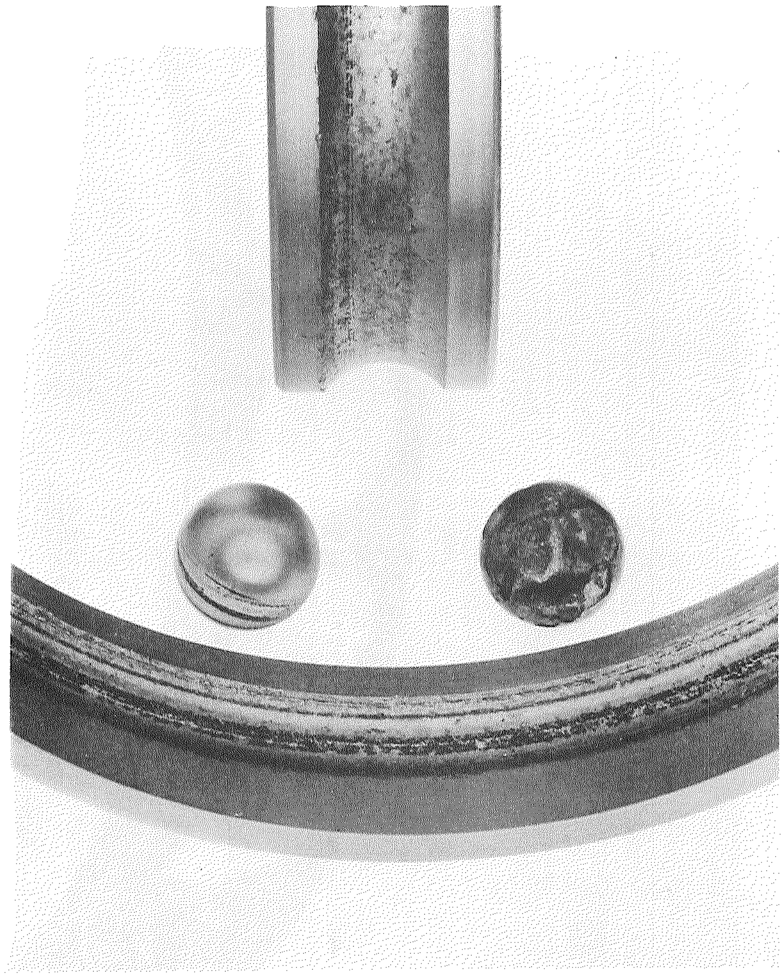

Figure 24. Balls and Races After Test No. 6 (Bearing S/N L3) FE 77811

G. TEST NO. 7, BEARING SET NO. 2

The bearings (S/N 248 front and 249 rear) used for test No. 2 were reinstalled in the test rig after replacement of the Chemloy 719 cage in bearing S/N 249. While the load was being adjusted from 5500 lb (24,465 N) at 13,000 rpm (1361 rad/s), both bearing temperatures rose sharply and the test was terminated.

Post-test examination disclosed heavy circumferential wear in two ball pockets and wear in the axial direction on several other pockets (figure 26). Thermal contraction problems, as well as cage dynamic problems due to the split cage, were suspect. Balls and races appeared to be in good condition, with some minute surface pitting noted on the balls.

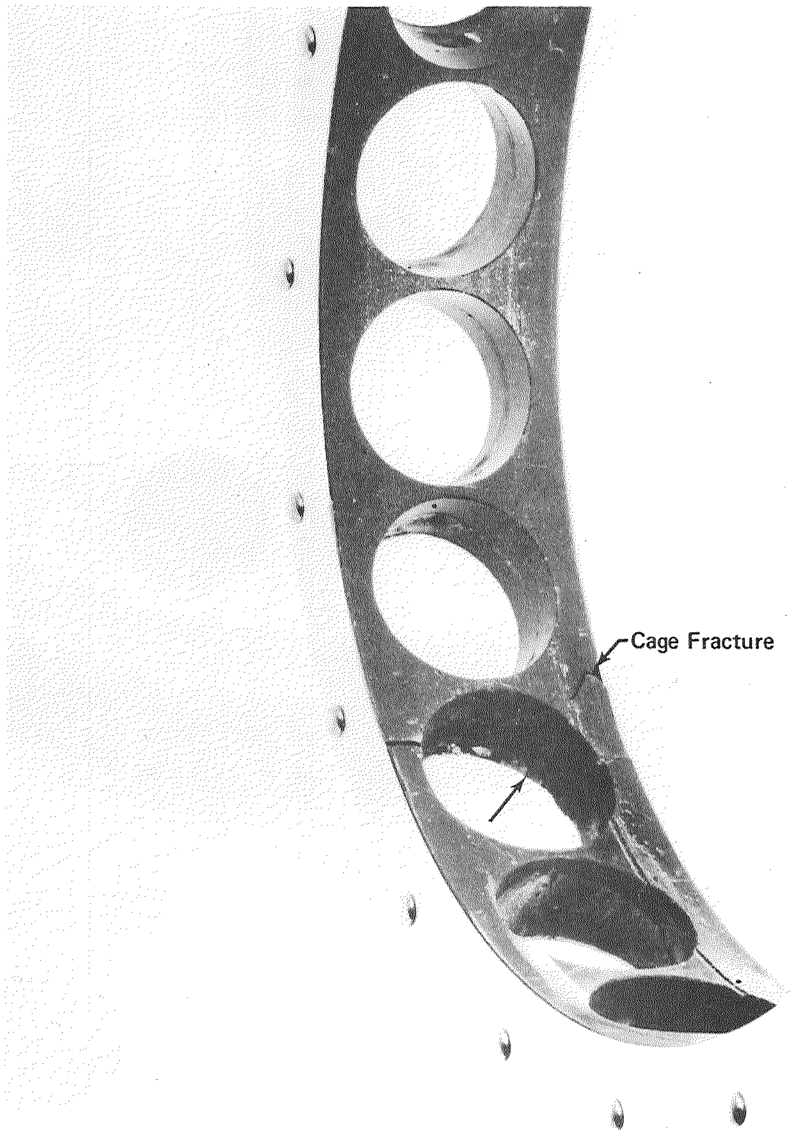

FE 77810

Figure 25. Wear Pattern on Cage After Test No. 6, Showing Typical Wear and Damage To Pocket in Which Star J Ball Failed (Bearing S/N L3) FD 49335

H. TEST NO. 8, BEARING SET NO. 3

The bearing set (S/N L5 front and L6 rear) used in test No. 4 was reinstalled in the test rig. Intended test conditions were 12,000 lb (53,500-N) load and 12,000 rpm (1256 rad/s). Operation was normal until the load was increased over 5800 lb (25,800 N). As the load reached its maximum point, the drive torque and the rear bearing temperature increased and the rig speed decreased.

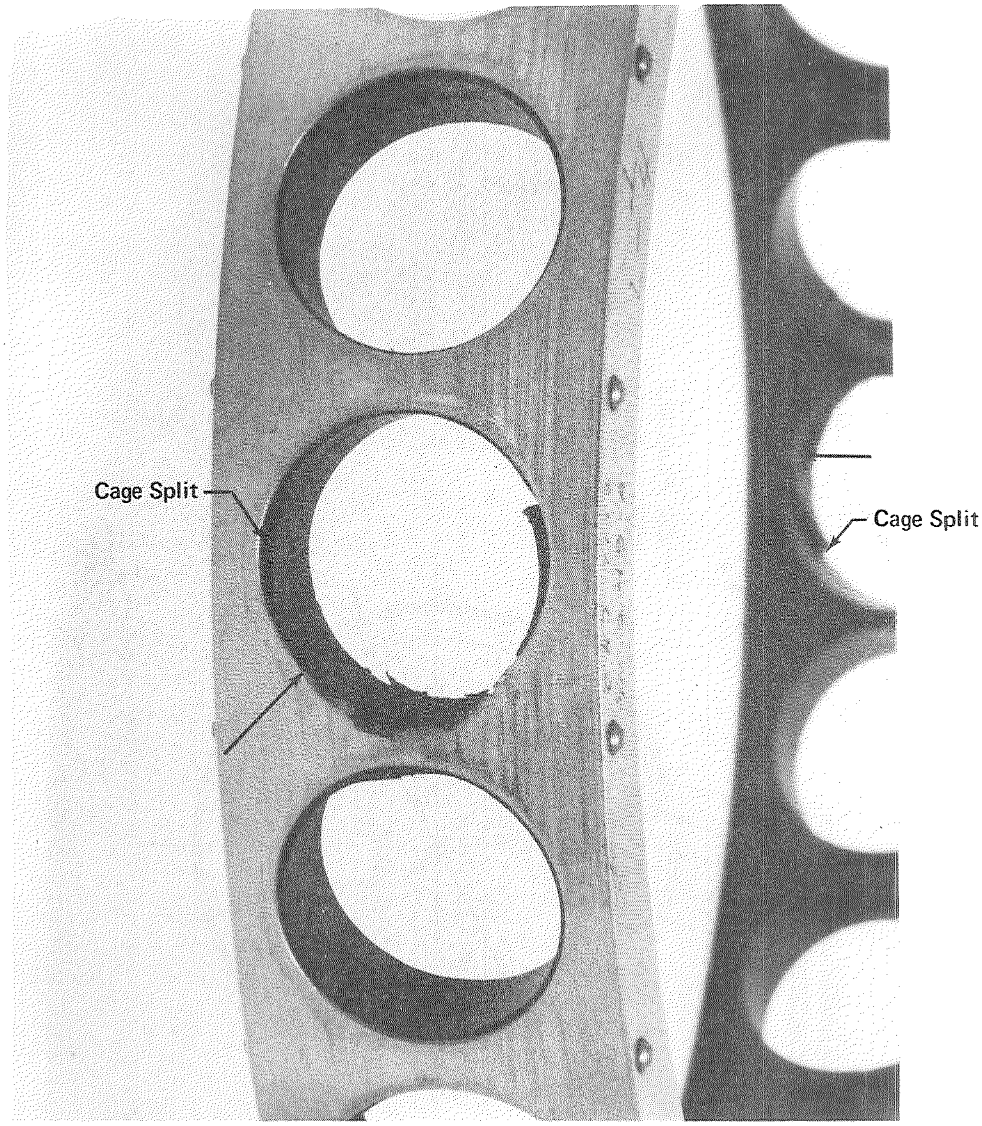

Figure 26. Bearing Cage S/N 249 Showing Damaged Pockets at Cage Split Lines During Test No. 7

FD 49336

Post-test examination showed the front bearing (S/N L5) to be in excellent condition, while the rear bearing (S/N L6) showed heavy wear in four pockets.

I. TEST NO. 9, BEARING SET NO. 2

Bearing set No. 2, (S/N 248 front and 249 rear), previously used in tests No. 2, 3, and 7, was installed in the test rig with new cages, modified for increased ball clearance (figure 27). The intended test condition was 9000 lb (40,034 N) load at 13,500 rpm (1413 rad/s). After test speed was attained, the

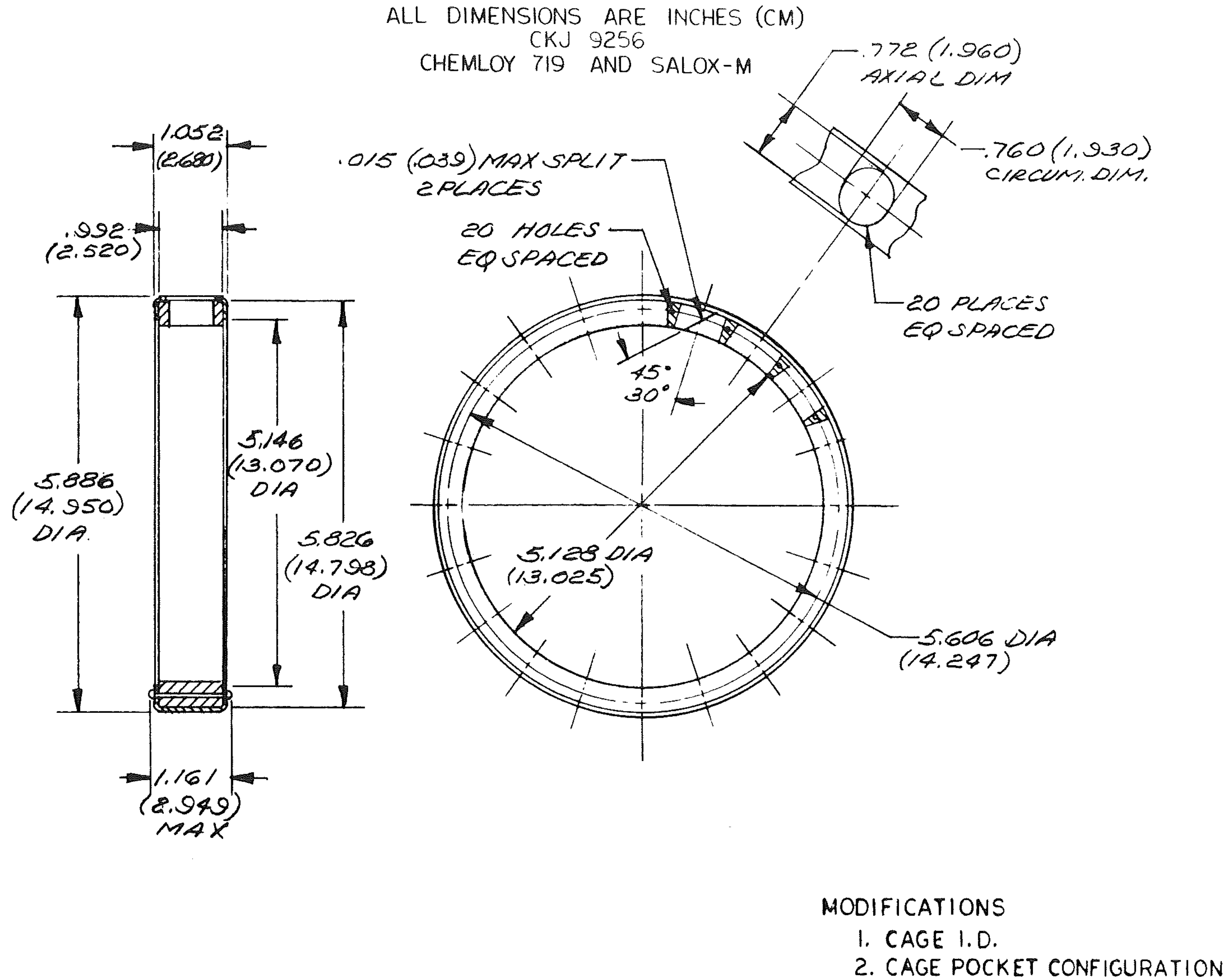

Figure 27. Second 20-Ball Cage Modification

load was brought from 2500 lb (11,120 N) to the test condition of 9000 lb (40,034 N), at which time the load bellows pressure fluctuated widely and the rear bearing temperature rose sharply. The test was terminated.

Post-test examination of the rig revealed that the load bellows had ruptured and allowed high pressure, ambient temperature, gaseous helium to flow through the rear bearing, resulting in the temperature rise.

The rear bearing (S/N 249) had moderate wear in the cage pockets; the front bearing (S/N 248) was in excellent condition.

A visual comparison of the ball surfaces before and after the test revealed that the number of minute pits had increased. The surfaces of the races did not show a visual change.

J. TEST NO. 10A, BEARING SET NO. 3

This set of bearings (S/N L5 front and L6 rear) was equipped with a new set of Chemloy 719 cages and reinstalled for further testing. The bearings operated at 11,000 lb (48,930 N) load and 12,000 rpm (1256 rad/s) for 20 sec, before the front bearing (L5) overheated from -154°F (161°K) to -170°F (170°K) and a shutdown was made.

K. TEST NO 10B, BEARING SET NO. 3

This test was a rerun of bearing set No. 3 (S/N L5 front and L6 rear) for evaluation at a lower load condition of 2900 lb (12,900 N). After running at 12,000 rpm (1256 rad/s) for 1.5 min, the front bearing overheated again. Post-test examination showed the rear bearing (S/N L6) to be in excellent condition, but the front bearing (S/N L5) showed severe cage pocket wear. There was little or no wear on the ID cage piloting surface. Figure 28 shows the severe wear in the cage pockets from bearing S/N L6.

L. CAGE REDESIGN

Following this test, the program was reviewed to determine if major bearing design modifications were required to improve bearing performance. Problem areas involved dimensional control of the bearing components and quality control of the Stellite Star J material. It was mutually agreed upon with the NASA Project Manager that the bearing cage design should be changed; however, other component changes, although desirable, were not feasible within the scope of this program.

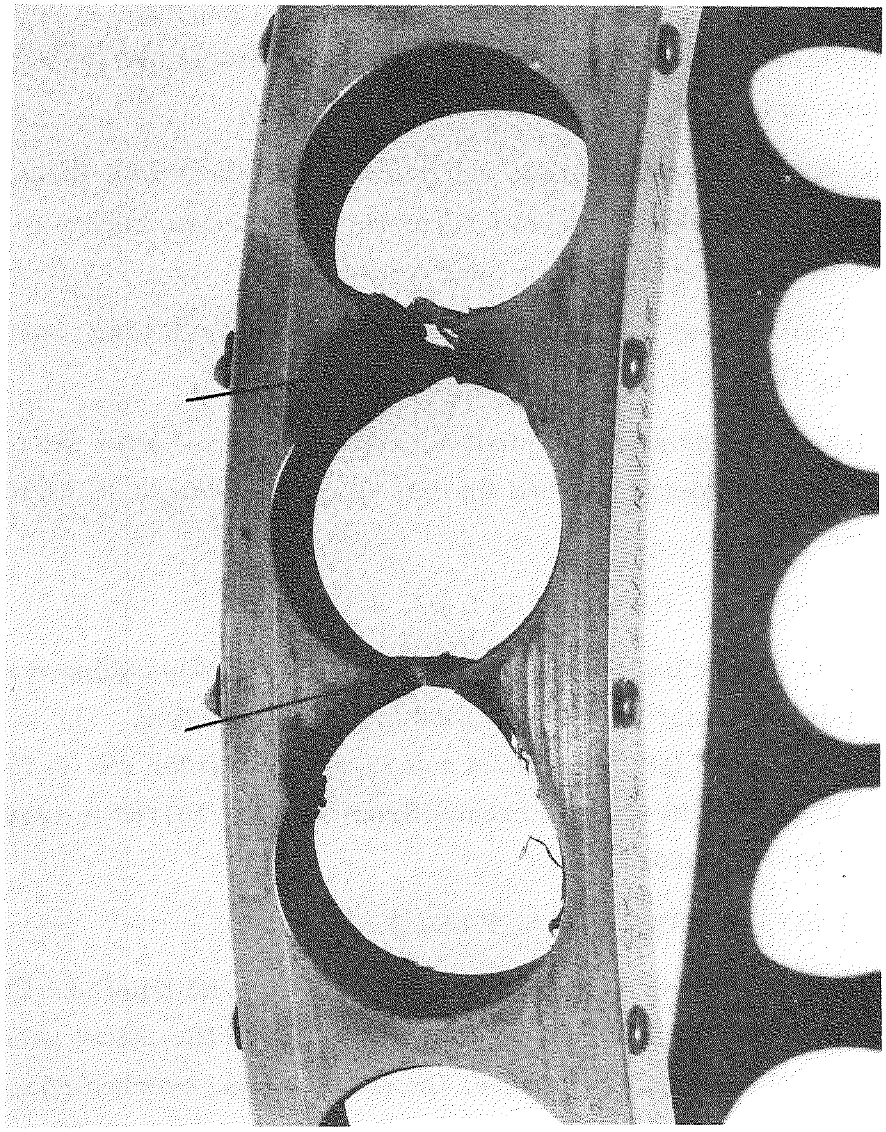

FE 100333
FD 49338

Figure 28. Bearing Cage S/N L5 Showing Pocket Wear Through the Web in Two Places During Test No. 10B

The 20-ball pocket cages had 0.029 in. (0.073 cm) of material between the ball lubricating surface and the cage rivet. The cage was redesigned for a complement of 19 balls to provide for a greater web thickness to increase life. The cage web thickness was increased from 0.028 in. (0.073 cm) to 0.054 in. (0.137 cm). Another change was the use of one-piece cage bodies to provide a more uniform stress distribution and to minimize the tendency to fail in the manufacturing split area. The two-piece cage was necessary in the 20-ball cage to permit assembly of the cage body into the wraparound armor. The 19-ball cage featured split-rail armor to allow assembly with one-piece cage bodies; the cage was also scalloped at the ID between each ball pocket to improve cooling. The 19-ball cage design is presented in figure 29.

M. REVISION OF BEARING TEST PARAMETERS

During the period of inactivity while the cage was redesigned, the contract tasks were modified, reducing the number of bearings to be tested from 32 to 16. Under this realignment of the test program, the goal of the next test was to determine a safe level of operation of the bearings. This was to be accomplished by testing one pair of bearings for 5-min periods at increasing levels of load and speed until a failure occurred. The maximum level at which successful running was achieved was to be used as the test condition for extended duration testing (3 hr or failure) of the remainder of the available bearings.

To obtain a better idea of the change in surface finish and ball track wear, one set of each bearing (AISI 440C balls and races, and AISI 440C races and Star J balls) was inspected at NASA LeRC and profilometer traces were made prior to testing. These bearings were inspected after testing to complete the comparison.

N. TEST NO. 11, BEARING SET NO. 2

This bearing set (S/N 248 front and 249 rear), frequently tested before, was modified with the new 19-ball cages (figure 29) and prepared for a test to determine usable test levels. The test rig was accelerated to 13,000 rpm (1361 rad/s) with a 2500 lb (11,120 N) load. When the load was increased, the front bearing (S/N 248) temperature increased rapidly to -240°F (122°K), necessitating a shutdown because experience had shown that a rapid rise to that temperature level indicated bearing distress.

Visual examination after the test failed to show any cause for the overheating, and only light to moderate wear was evident at the rear of the cage.

O. TEST NO. 12, BEARING SET NO. 2

Test No. 12 was identical to Test No. 11, except that the positions of the bearings were reversed to assure that the overheating was not due to the bearing location in the rig. During application of the load 7000 lb (31,138 N), the rear bearing (S/N 248) temperature gradually increased to about -260°F (111°K). Increasing the coolant flowrate did not control the temperature increase, so the test was stopped.

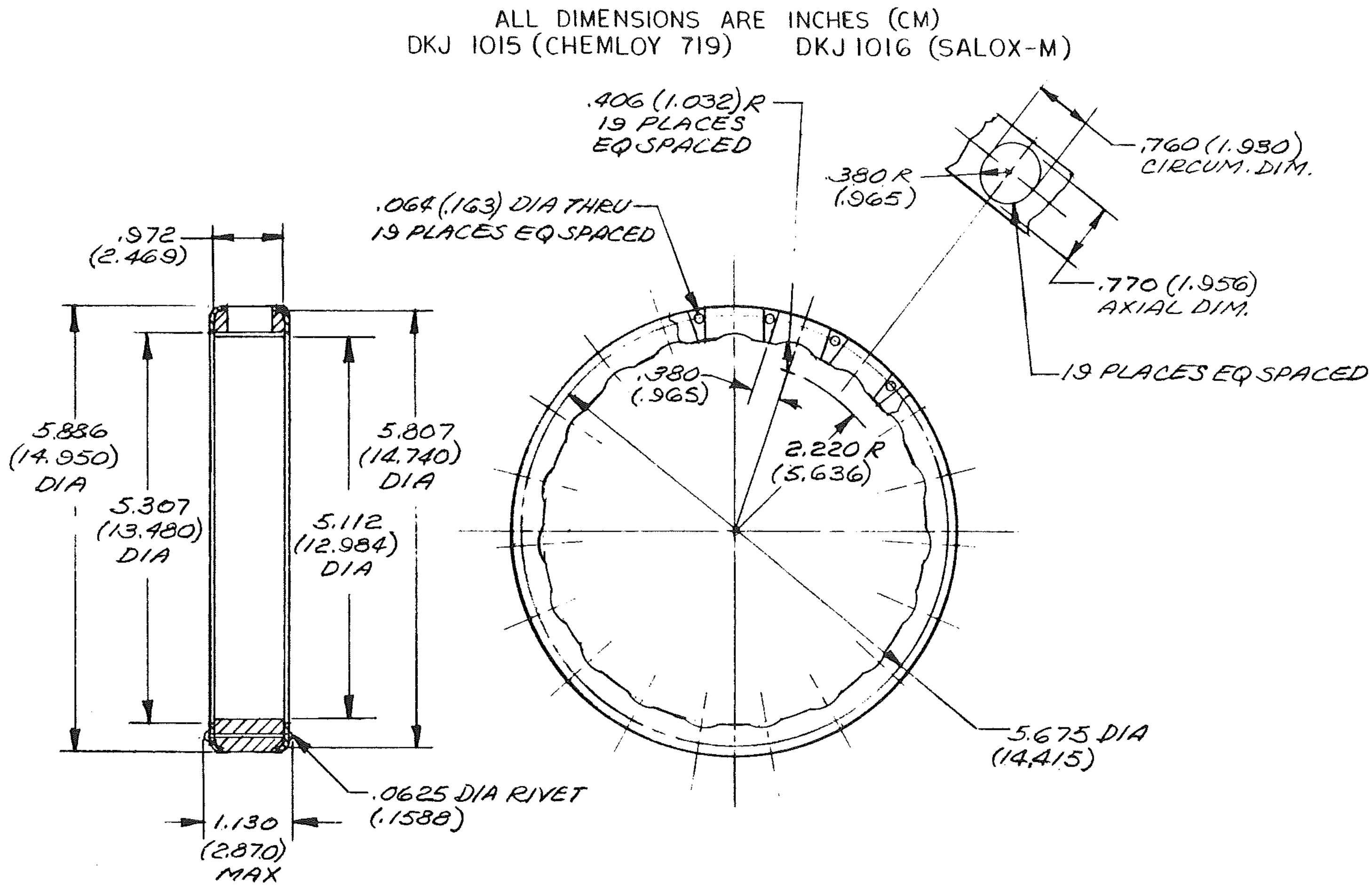

Figure 29. Original 19-Ball Cage Configuration

Visual inspection showed severe wear on the rear side of the cage pockets of the rear bearing (S/N 248). One pocket was worn through the lubricant to the rivet. Figure 30 shows the condition of the cage after testing.

P. TEST NO. 13A, BEARING SET NO. 3

This set of bearings, consisting of AISI 440C balls and races and the 19-ball Chemloy 719 cages, was tested in a further attempt to establish conditions for the 3-hr tests.

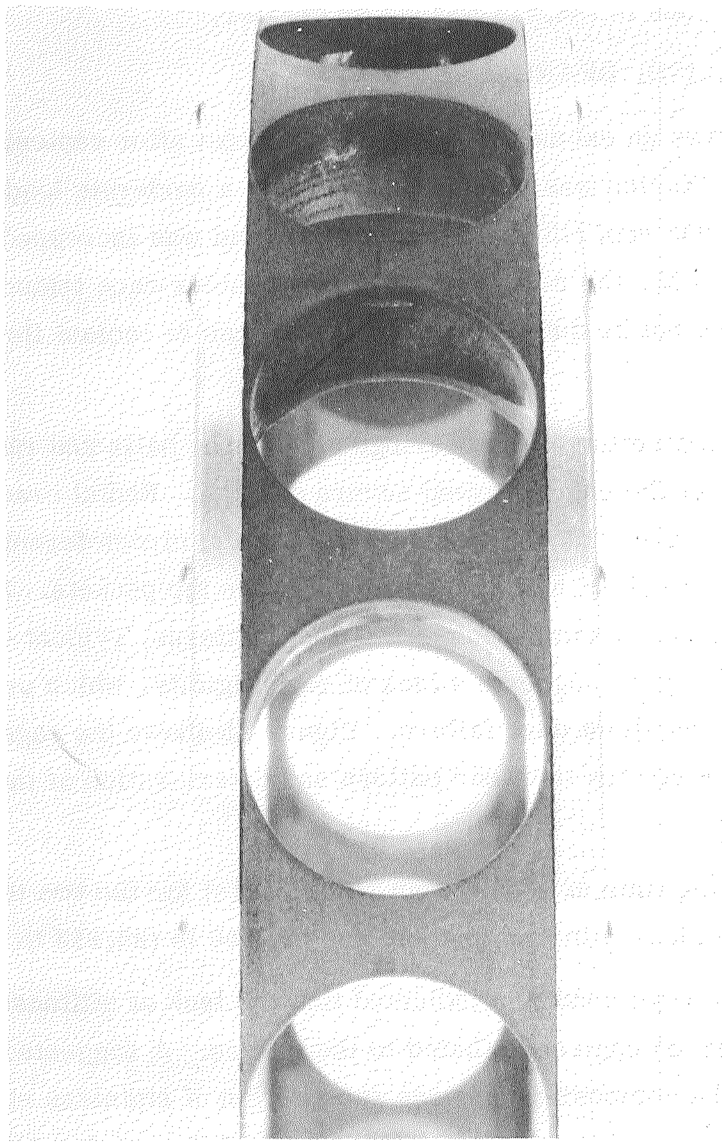

FE 95528

Figure 30. Bearing Cage S/N 248 Showing Wear Scar Depth to the Rivet FD 49340

Testing started with accelerations to 13,000 rpm (1361 rad/s) at an axial load of 2700 lb (12,010 N). The load was then increased to 4400 lb (19,572 N) and maintained for a 5-min stabilizing period, followed by 5-min at 6500 lb (28,913 N). Four minutes after establishing a load of 7200 lb (32,027 N) at 13,000 rpm (1361 rad/s), the hydrogen coolant supply was exhausted, so testing was stopped.

A total of 26 min at 13,000 rpm (1361 rad/s) were accumulated, of which 8.5 min were at 6500 lb (28,913 N) load or greater.

Q. TEST NO. 13B, BEARING SET NO. 3

This test was an extension of the previous test after replenishment of the coolant supply. Startup was made as usual, with a moderate load applied while accelerating 13,000 rpm (1361 rad/s). As the load was increased to the level of 6500 lb (28,913 N), the rear bearing (S/N L6) outer race temperature increased and could not be stabilized with an increase in coolant flow, so testing was terminated.

Post-test inspection of the bearings showed the balls and races to be in good condition, but the cages showed severe damage. Radial cracks were evident in the Chemloy 719 in alternate ball pockets; circumferential cracks were also evident in about half of the webs between the pockets. Seven rivets had failed by fatigue. Examination of the wear patterns, evident on both the ID and OD of the cages, suggests a lack of cage rigidity, which promoted the rivet fatigue and resultant cage failure. Figure 31 shows the cage from bearing S/N L5, which illustrates the wear pattern and deterioration of the Chemloy 719.

Total running time at 13,000 rpm (1361 rad/s) for the two tests was 32 min 15 sec, with 14 min at a load of 6500 to 7500 lb (28,913 to 33,362 N).

Study of the cage condition indicated that the lack of stiffness of the aluminum-reinforced cage contributed to the failure. A suggested further modification to the composite cage was substitution of stainless steel for the aluminum side rails and increasing the diameter of the retaining rivets. The resulting increase of stiffness should be approximately 2.5 to 3 times that of the aluminum-reinforced cage, with only 0.006-in. (0.015-cm) apparent diametral growth due to the change of coefficient of expansion when cooled to liquid hydrogen temperature.

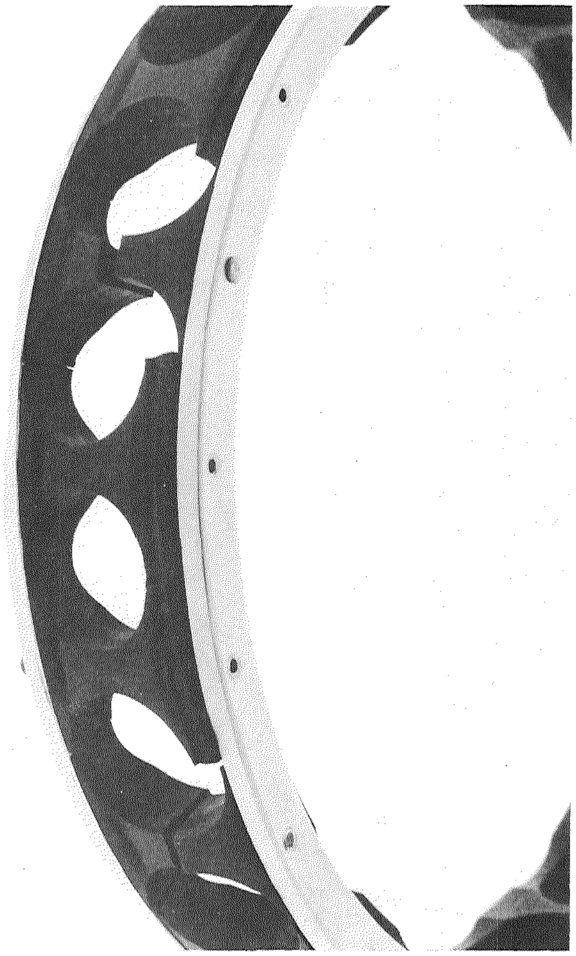

Figure 31. Cage From Bearing S/N L5 After Test No. 13 Showing Fractures to Chemloy 719 After Rivet Failures Due to Fatigue   FE 96145

With the concurrence of the NASA Program Manager, one pair of bearings was equipped with the steel-reinforced cages for testing of this modification. The cage modification is shown in figure 32.

R. TEST NO. 14A, BEARING SET NO. 6

This set of bearings (S/N L9 front and L10 rear), with AISI 440C races and Star J balls, was equipped with the steel-reinforced Salox-M cages. Testing was initiated at conditions of 4000 rpm (419 rad/s) and 2500 lb (11,120 N) load.

After stabilizing the test conditions, the speed was increased to 13,000 rpm (1361 rad/s) and 7200 lb (32,027 N) load. The test continued normally until fuel depletion caused the test to be stopped.

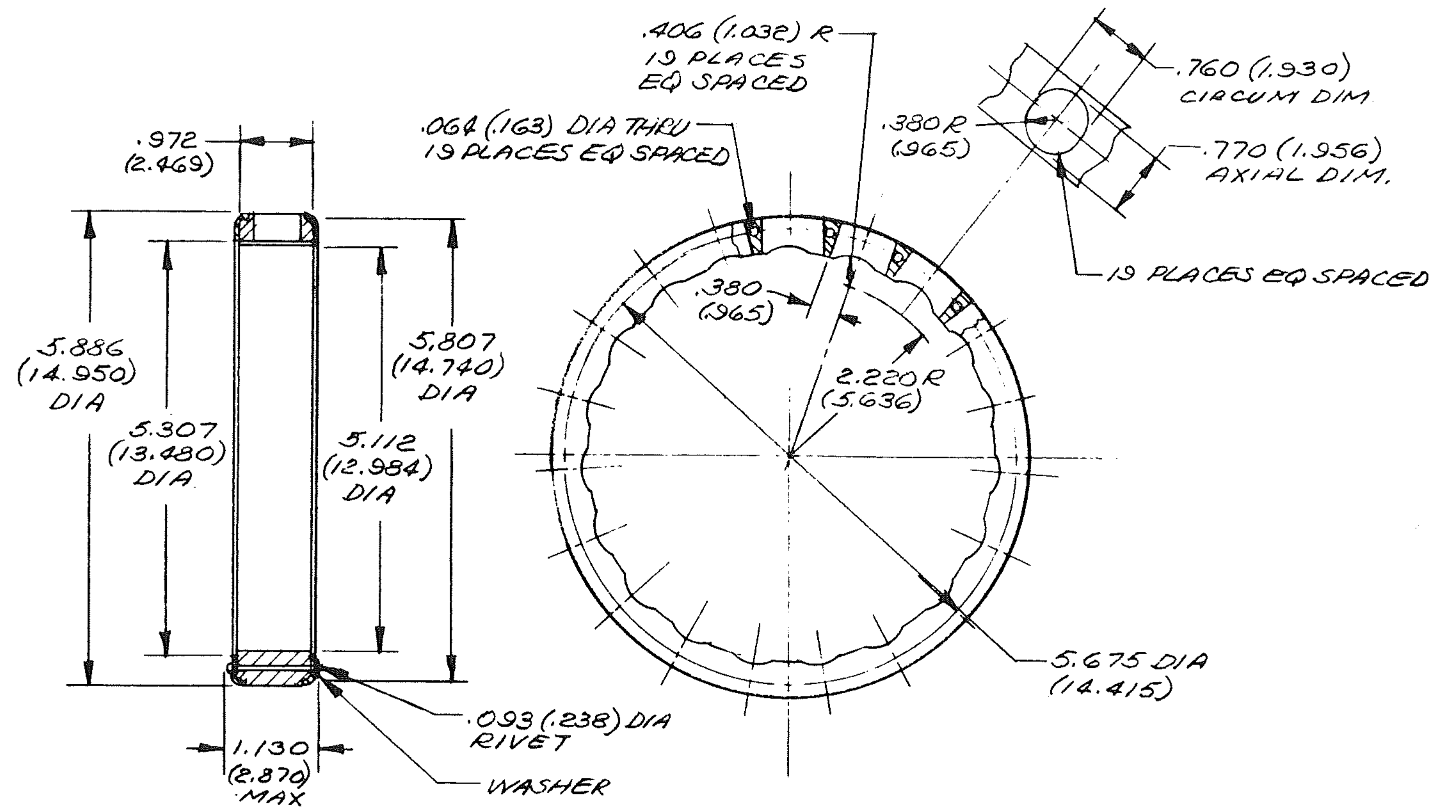

MODIFICATIONS:
1. AMS 4120 CAGE RAIL CHANGED TO 347 SS
2. RIVET DIAMETER

Figure 32. Nineteen-Ball Cage Modification

During this test, total running time of 41 min 6 sec was accumulated, with 23 min 40 sec at the 13,000 rpm (1361 rad/s) and 7200 lb (32,027 N) condition.

S. TEST NO. 14B, BEARING SET NO. 6

After replenishment of the fuel supply, testing was resumed at the same conditions as above. After the test conditions had stabilized, the coolant flowrate was reduced about 15% to conserve fuel. The bearings continued to run at constant temperature at this lower flowrate. Testing was terminated when a sudden increase in the rear bearing temperature could not be controlled by increased coolant flow.

Test time during this test portion was 25 min 41 sec, with 9 min 20 sec at 13,000 rpm (1361 rad/s) and 7200 lb (32,027 N) load. Total test time accumulated by this bearing set was 33 min at the maximum load/speed condition.

Post-test examination revealed one fractured ball in the rear bearing (S/N L10), as shown in figure 33. The failed ball and an intact ball from an adjacent ball pocket were subjected to laboratory analysis. No certain cause for the failure could be pinpointed, although slightly different structures appeared in the sectioned specimens (figure 34). Spectrographic examination did not show any material discrepancy in either ball. Hardness measurements were made and are presented in table III; these measurements show no significant material hardness difference between the intact and failed balls.

Since the new bearing cages (DKJ 6202) seemed to perform well in this test, the remaining bearings were similarly modified for the balance of the test program.

T. TEST NO. 15, BEARING SET NO. 7

Bearing set No. 7 (S/N 7 front and 8 rear), consisting of AISI 440C races, Star J balls and Salox-M cages with steel reinforcing rings, was used for test No. 15. This test was intended to run for 3 hr at 7200 lb (32,027 N) load at 13,000 rpm (1361 rad/s). The test started normally by acceleration to an indicated 13,000 rpm (1361 rad/s). At this condition, higher than normal vibration was encountered. The test was stopped to investigate the cause for this vibration. The investigation revealed that the digital counter being used for speed control had been improperly preset, causing the counter to indicate 13,000 rpm (1361 rad/s) when the rig was actually rotating at 17,000 rpm (1780 rad/s).

The operating conditions above 13,000 rpm (1361 rad/s) consisted of a transient lasting approximately 2 min as shown in figure 61.

Subsequent removal of the test rig and inspection of the bearings showed numerous radial and circumferential cracks in the Salox-M cage lubricant material. Figure 35 shows some of the cage fractures. The cage conditions warranted replacement prior to further testing, but this was not possible under the present program. The balls and races were undamaged.

A total running time of 8 min 4 sec was accumulated.

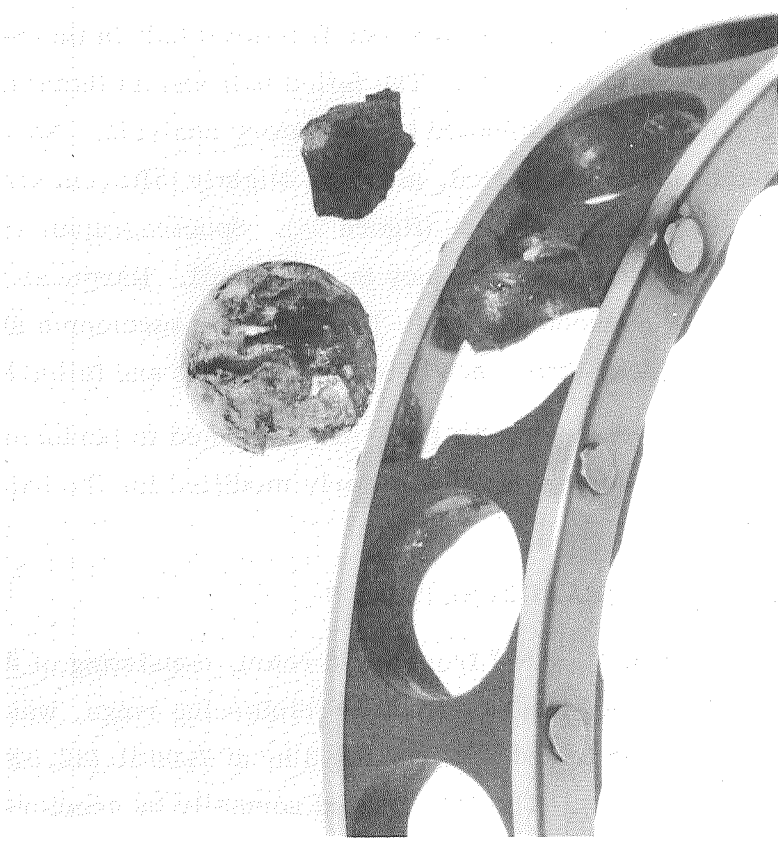

Figure 33. Test No. 14 Cage DKJ 6202, Bearings 2137774, S/N L10, With Fractured Star J Ball and Damage to Cage FE 97057

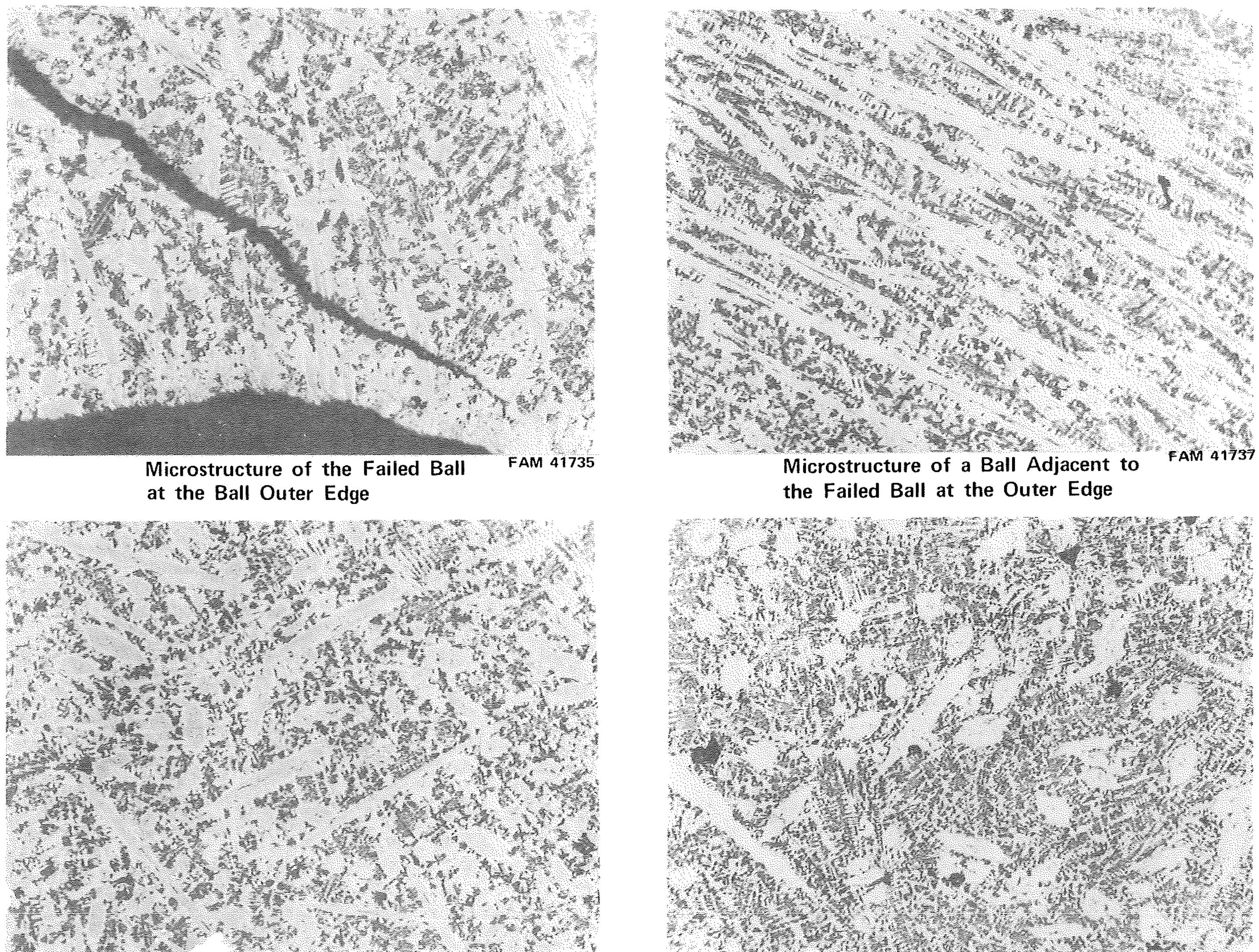

Microstructure of the Failed Ball at the Ball Outer Edge — FAM 41735

Microstructure of a Ball Adjacent to the Failed Ball at the Outer Edge — FAM 41737

Microstructure of the Failed Ball at the Ball Center — FAM 41736

Microstructure of a Ball Adjacent to the Failed Ball Center — FAM 41738

Figure 34. Microstructure of the Failed Ball and an Adjacent Ball Following Test No. 14B (100X)

FD 37642

Table III. Hardness Comparison of the Failed Ball and the Adjacent Ball Following Test 14B

Location	Rockwell C Hardness
Failed Ball Outer Edge	60±1
Failed Ball Center	56±2
Adjacent Ball Outer Edge	62±1
Adjacent Ball Center	59±1

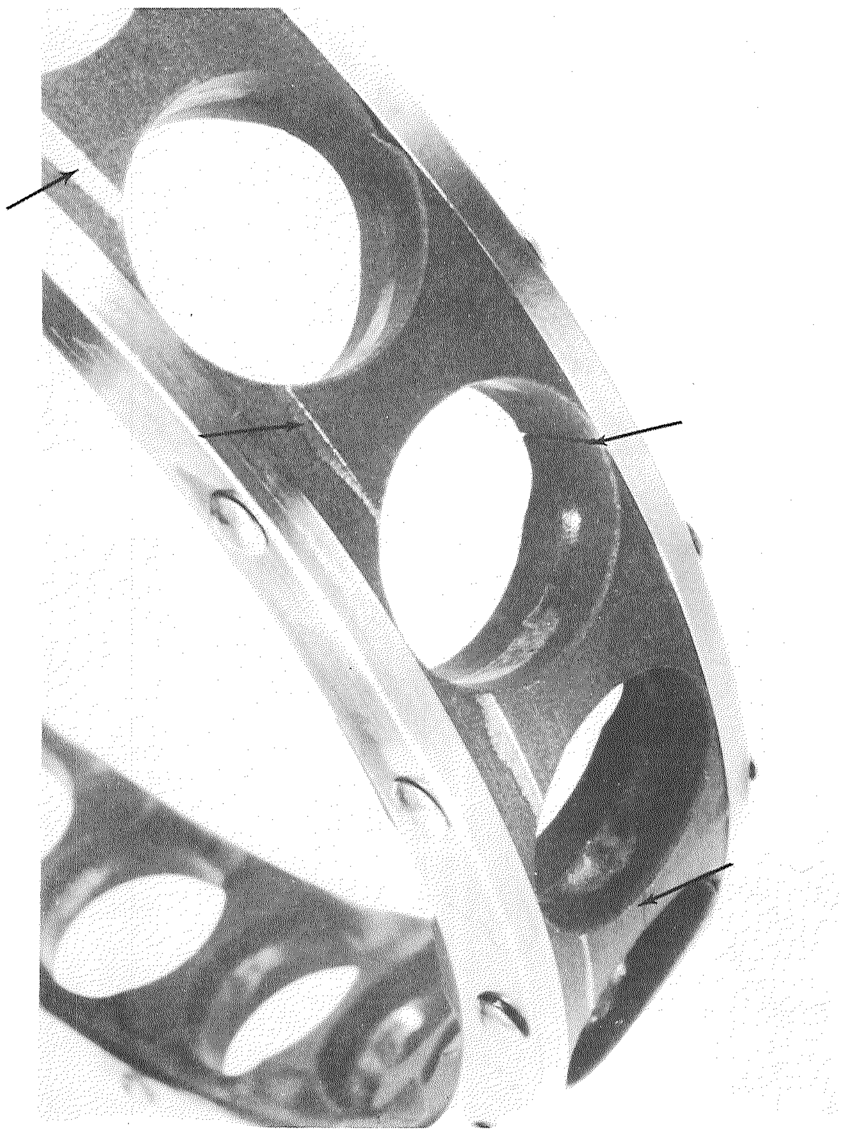

FE 98102

Figure 35. Cage L7, Fractures and Outer Race Rub, Test No. 15 FD 49343

U. TEST NO. 16A, BEARING SET NO. 8

Bearing set No. 8 (S/N L2 front and L6 rear) was modified at the request of the NASA Program Manager to include AISI 440C races and a Salox-M cage, with AISI 440C balls substituted for the Star J balls that were scheduled to be tested.

The test ran without incident at 13,000 rpm (1361 rad/s) and a 7200 lb (32,027 N) thrust load until the fuel supply was exhausted. This test completed 43 min 37 sec of running, of which 32 min were at the established test conditions.

V. TEST NO 16B, BEARING SET NO. 8

This test was a continuation of the previous test. Before test conditions were reached, the front bearing overheated and the test was terminated. Running time accumulated was 10 min 13 sec.

Post-test inspection showed the rear bearing (S/N L6) to be in excellent condition, except for two cage pocket fractures, (figure 36). The front bearing (S/N L2) showed severe wear and fracture to two cage pockets 180 deg apart. (See figure 37.)

Total time accumulated on this set of bearings was 53 min 50 sec, with 32 min at 13,000 rpm (1361 rad/s) and 7200 lb (32,027 N) axial load. Balls and races for both bearings were undamaged.

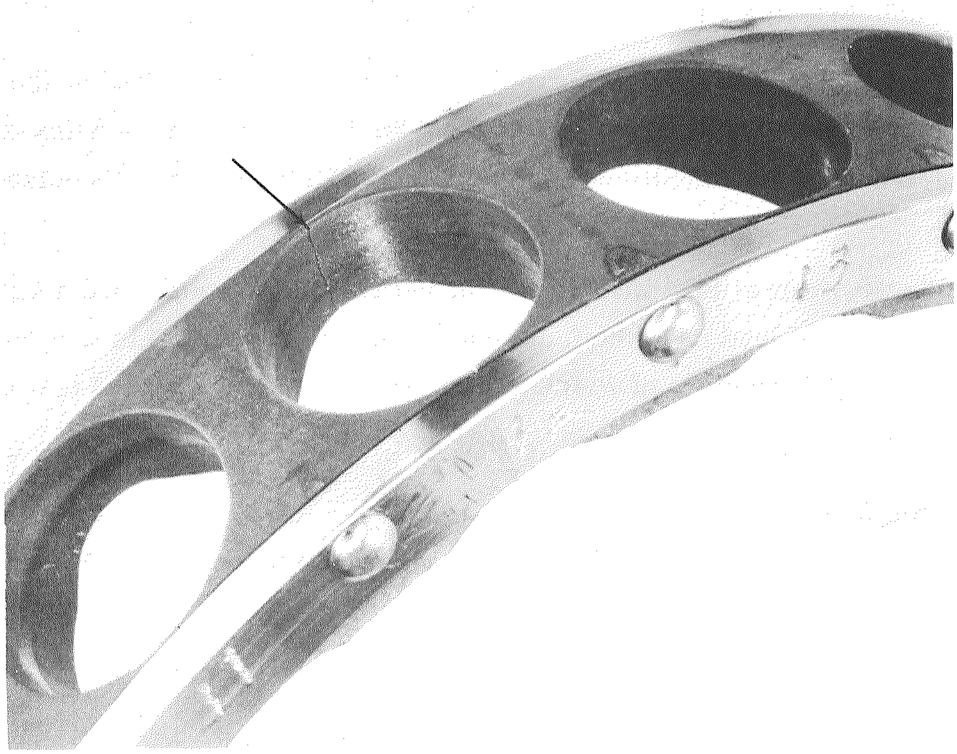

FE 98101

Figure 36. Cage L6, Wear and Typical Radial Crack Test No. 16A and 16B FD 49344

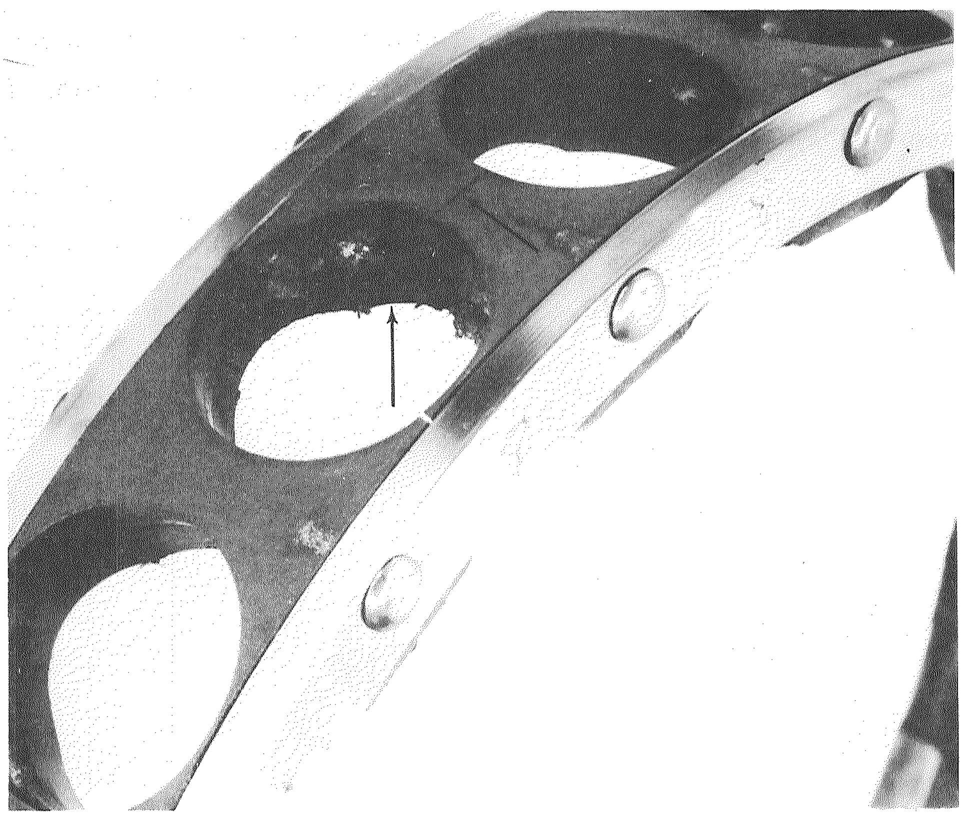

FE 98100

Figure 37. Cage L2 Pocket Wear and Fracture, Ball No. 7, Test No. 16A and 16B FD 49345

SECTION V
TEST RESULTS

A. INTRODUCTION

A series of 20 tests with eight bearing sets was conducted as described in Section IV. Basic information concerning test conditions and test results in summarized in table II, P. 28.

The test program served to answer some questions and pinpoint some problem areas. The load/speed capability of the AISI 440C-Chemloy 719 bearing was demonstrated to be at least 9000 lb (40,034 N) and 12,000 rpm (1256 rad/s). This limit is intuitively a function of time, so due to the limited test matrix, no absolute limit can be given.

The Stellite Star J balls - Salox-M combination was subject to ball failure due to the nonhomogeneity of the ball castings. However, one Star J bearing test (test No. 14A and B) ran longer than any of the AISI 440C-Chemloy 719 bearings. The Star J bearing also was the only bearing that was successfully restarted following a shutdown from a test in which there was no distress indicated.

A definite conclusion of the test program is that once a bearing has indicated distress in the form of an outer race overheat, the bearing cannot be operated in the same maximum load/speed regime as a new bearing.

A discussion of the results of the test program is presented below. The test program is broken down into a discussion of new bearing tests and previously tested bearing tests. The new bearing tests are subdivided into tests in which no distress was evident and tests in which distress was evident.

The previously tested bearing tests are subdivided into tests of bearings that had no previous distress during testing and bearings that had been subject to distress during previous testing.

Graphs of recorded data for all tests, except the shakedown tests with the NASA furnished Armalon cage bearings and Test No. 1 which did not rotate due to thermal contraction problems, are presented in Appendix A. Vibration data were recorded on tape and displayed on a meter for all tests. Following each test, the tapes were checked to verify the meter. No excessive vibration was noted on the meter or on the tape until test 15 (figure 61). While compiling the data in curve form, following test 10B, it was determined that the vibration tapes for the first 10 tests had been inadvertantly erased and no permanent record could be made.

The coolant flow rates established in the shakedown tests were such as to make the coolant inlet and discharge pressure and temperature insensitive to speed and thrust load changes during the shakedown tests. A shortage of recording instrumentation at that time would have delayed the testing so a decision was made to record the coolant inlet and discharge pressures and temperature manually when steady state values were reached. This procedure was used through test No. 9 after which instrumentation became available and was used for the remainder of the tests. Steady state data were reached and recorded during tests No. 2 and 4 but steady state conditions were not reached during tests 3 and 5 through 9. The coolant inlet and discharge pressure and temperature are missing for test No. 10 due to a recorder malfunction.

Bearing physical characteristics, such as dimensional data, surface finish and weights are presented in Appendix B. These data were taken after each test unless the bearing was destroyed or the test rig was not disassembled prior to the subsequent test. In one instance, following test No. 12, three measurements were not recorded on the inspection sheet and the oversight was not discovered prior to the release of the bearings to NASA at the end of the test program.

B. TESTS

Three of the eight new bearing sets tested (No. 2, 6, and 8) reached and maintained prescribed values of load and speed and did not show any sign of distress during their initial test. These were tests No. 2, 14A and 16A. Bearing distress is defined here as an increase in race temperature that could not be controlled by increasing the coolant flow (the condition referred to as overheating), or an increase in rig vibration. The remaining five sets of bearings overheated before reaching the desired load and speed conditions during their initial test. Of these, set No. 1 failed because of interference between the balls and the cage, set No. 3 had a coolant shortage, set No. 4 had mismatched balls, and sets No. 5 and 7 were subject to ball failure and overspeed respectively.

With the possible exception of set No. 5 in test No. 6, the inability of five of the eight sets of bearings to operate in the load/speed regime typically prescribed in the test program (7000 to 12,000 lb (31,138 to 53,379 N) axial load and 12,000 to 13,500 rpm (1256 to 1413 rad/s)) cannot be attributed solely to the prescribed load/speed condition, but was influenced by other factors such as ball material and dimensional quality control, and rig malfunctions. These five bearing sets (sets No. 1, 3, 4, 5, and 7) are discussed in the following paragraphs.

Bearing set No. 1 (test No. 1) suffered severe skidding because the unpredictable dimensional effects caused by the interaction of the various cage material thermal coefficients resulted in the cage interferring with rotation of the balls at liquid hydrogen temperatures.

Bearing set No. 3 (test No. 4) operated for 2.4 min at 12,000 lb (53,379 N) load and 12,000 rpm (1256 rad/s) before overheating. Post-test inspection disclosed no mechanical problem. Analysis of the coolant flowpath indicated the possibility of unequal coolant distribution, which could occur if the resistance to flow through one bearing was higher than through the other. There was no means of controlling flow through the individual bearing in the original test setup, in which the flow entered the rig between the two bearings, flowed outward through the bearings and discharged into a common manifold. This arrangement did not provide flow control to each bearing, but only total flow control by means of the rig discharge contol valve. Modifications to this system were made for better coolant control during later testing by supplying separate flow control to each bearing. These modifications are discussed in section IV.

An additional benefit of the modification was derived from the reversal of the flowpath through the bearing. This benefit came from utilizing the pumping action of the bearing to assist the coolant flow. Reference 1 describes test made with oil-lubricated bearings in support of this theory. The pumping action of the bearing was evident, for after the change of flow direction, subsequent tests showed a pressure drop across the bearings of approximately 1 psi (0.69 N/cm^2).

Bearing set No. 4 (test No. 5) was the first bearing with Stellite Star J balls that was tested. The rear bearing overheated while operating at 12,000 rpm (1256 rad/s) before the scheduled load of 9000 lb (40,034 N) was reached.

Post-test examination of the overheated bearing disclosed severe wear on the rear face of three of the ball pockets. The wear coincided with the locations of the three largest balls in the bearing. A check of pretest measurements disclosed a maximum ball diameter variation of 0.000160 in. (0.000406 cm). The larger balls had operated at a lower contact angle and the resulting lower relative speed had acted as a brake on cage rotation.

Bearing set No. 5 (test No. 6) experienced extensive failure of the Stellite Star J balls at approximately 5500 lb (24,465 N) while the load was being adjusted at a speed of 12,000 rpm (1256 rad/s). Four balls failed in the front bearing and one ball failed in the rear bearing.

Bearing set No. 7 (test No. 15) was inadvertently operated through a transient up to 17,000 rpm (1780 rad/s) because of an incorrect preset in the digital counter used for speed control in the test stand. The transient at conditions above the preset values lasted for approximately two minutes.

Twelve tests were made with bearing sets that had been tested previously. Three of the twelve tests were made with bearings that had not overheated during their previous test. These tests were No. 3, 14B and 16B and the bearings used were sets No. 2, 6, and 8 respectively. Set No. 2 was visually inspected prior to test No. 3 and the cages were not changed because only light wear was evident. Test No. 3 operated at 9000 lb (40,034 N) load and 12,000 rpm (1256 rad/s) for 1.25 min, but the race temperature would not stabilize, so the test was stopped. Prior to tests No. 14B and 16B the bearings were not inspected because there were no indications of distress from the monitoring instrumentation during preceding tests No. 14 and 16. The test rig was down just long enough to replenish the hydrogen supply. In test No. 14B the bearings operated at 7200 lb (32,027 N) load and 13,000 rpm (1361 rad/s) for 9.33 min before overheating. In test No. 16B the bearings operated at 2900 lb (12,900 N) load and 13,000 rpm (1361 rad/s) for 3.1 min, but when the load was increased the race temperature would not stabilize, so the test was stopped.

Nine of these twelve tests with used bearings were made with bearing sets of which one or both bearings had overheated during their previous testing. These were tests No. 7, 8, 9, 10A, 10B, 11, 12, 13A and 13B. The balls and races were visually inspected and approved before each of the above tests, and new cages were installed in each case except tests No. 10B, 12 and 13B, as explained in section IV. Six of the nine tests were scheduled for loads of from 9000 to 12,000 lb (40,034 to 53,379 N) at speeds of 12,000 to 13,500 rpm (1256 to 1413 rad/s). Overheating occurred in each case before the desired load/speed condition was reached. In one case (test No. 9), failure was due to the load bellows rupturing. The other three tests were scheduled to operate at lower load/speed conditions. The bearings in test No. 10B would not operate for more than 1.5 min at 2900 lb (12,900 N) load without overheating, and the result was a severely worn cage that was removed from the bearing after test No. 10B. Tests No. 11, 12, 13A and 13B were made to establish maximum values of load and speed for the endurance testing of the three remaining sets of new bearings. All bearings had been equipped with the 19-ball, split rail cages (DKJ 1015) just prior to test No. 11. The NASA LeRC Project Manager requested that bearing set two be tested for 5 min each at successively higher values of load and speed until distress was evident, after which the highest values of load and speed that the bearing negotiated successfully for 5 min would be chosen. Tests No. 11 and 12, using bearing set two, were an attempt to operate initially at a load and speed of 9000 lb (40,034 N) and 12,000 rpm (1256 rad/s). Both tests were stopped by bearings overheating at 7000 lb (31,138 N) load or less. Tests No. 13A and 13B were then conducted with bearing set three to accomplish the objective of tests No. 11 and 12. These tests resulted in the selection of 13,000 rpm (1361 rad/s) and 7200 lb (32,027 N) loads as the test conditions for the subsequent endurance tests.

The net result of the nine tests with bearings that had previously overheated was that only one bearing set operated with a stabilized race temperature at a load value of 7200 lb (32,027 N) or greater. This test (No. 13A) ran for 4 min at this condition and then would not repeat in test No. 13B when coolant supply depletion caused test No. 13A to be stopped.

C. PROBLEM AREAS

Each bearing that experienced distress during testing reflected that distress in the post-test cage condition. Bearing overheat always caused, or was the effect of, severe cage wear, as seen typically in figures 21, 24, 25, 27, 29, and 36. Excessive vibration was always exhibited as cracks in the side and pocket separating webs. These cracks can be seen in figures 32 and 36.

Two different cage designs, with two modifications to the first and one to the second, were used during this test program (figures 16, 19, 26, 28, and 31) in an attempt to minimize any cage dynamic problems. However, it was not possible to determine whether the cage problems were cause or effect, due to the limited test matrix of this program.

All bearings that had overheated during test had badly worn cage pockets. The only time that a cage was inspected between a successful and an unsuccessful test was following run No. 2. The cage was in good condition, exhibiting only slight rubbing. When the cage was removed following overheating after 1.25 min at the same operating conditions in test No. 3 as in test No. 2, severe pocket wear had occurred. The sequence of events cannot be established with the available instrumentation; therefore, this problem area cannot be defined as other than a change in the dynamics of the bearing components.

The original 19-ball cage shown in figure 29 was severely damaged in a fatigue mode in test No. 13B, although the indicated vibratory acceleration was no more severe than in the two previous tests with this cage design. The cage was strengthened as shown in figure 31, and only moderate damage occurred in later tests, even though the indicated vibratory accelerations were much more severe. Whether these vibrations are inherent in the cage design, or caused by something external to the cage, such as race waviness, cannot be determined within the scope of this program.

Four sets of Stellite Star J balls were tested during this program; these were in tests No. 5, 6, 14A, 14B and 15. Ball fractures occurred in tests No. 6 and 14B at 5800 lb (25,800 N) and 7200 lb (32,027 N) respectively. The highest load that the Stellite Star J ball was subjected to was 7500 lb (33,362 N) during test No. 14A. The failed balls and adjacent balls were sectioned and compared on the basis of: (1) photomicrographs showing typical voids; (2) spectrographic examination, which did not disclose any material discrepancy; and (3) hardness tests, which did not disclose any significant differences between balls. Some of the failed balls were returned to the vendor for failure analysis; the findings were that the balls failed due to internal voids formed during the casting process. Photomicrographs (figures 23a, 23b, and 34) showing the voids in the castings and a hardness comparison (table I) are presented in Section IV.

In four instances a restart was attempted when no distress was exhibited during a bearing test. The restarts, tests No. 3, 13B, 14B and 16B, were reported in Section IV. The bearings used were sets No. 2, 3, 6, and 8. Set No. 3 had previously overheated, but the remainder had not. Two of the sets (No. 3 and 8) would not accept the axial load used in their previously successful tests without the outer race temperatures rising sharply. The other two sets (No. 2 and 6) achieved the load/speed condition used in their previously successful tests and maintained a steady outer race temperature for 1.25 and 9.33 min respectively. Due to the limited number of available samples, it is not known if the two unsuccessful attempts and one partially successful attempt to restart and reach previously achieved values of load and speed are indicative of of a problem area associated with thermal coupling of the bearings and rig.

Allowable ball diameter deviations were specified by P&WA as ±0.000025 in. (0.000064 cm). Bearing set No. 4 was delivered with a variation of ±0.000080 in. (0.000203 cm) in the rear bearing and 0.000065 in. (0.000165 cm) in the front bearing. When set No. 4 was tested, (test No. 5), damage occurred in the rear bearing in the three pockets coinciding with the largest balls, as explained in Section IV, but not in the front bearing that also had a poorly matched set of balls.

Bearing set No. 5, with the rear bearing containing a matched set of balls and the front bearing mismatched similar to the bearings in set No. 4, was used in test No. 6. Both bearings overheated and experienced ball failures within 0.5 min at test conditions. Insufficient pocket wear was evident to provide additional data necessary to explain the cause for bearing overheating, and the effect of variations in ball diameters on cage wear remains undefined.

Another parameter that may have affected the testing results was the surface finish of the balls and races. The P&WA specification was for a No. 4 rms finish on both balls and races. (See figure 15.) Appendix B contains a listing of the dimensions, fits, clearances, surface finishes and the weights of the bearing components, both before the test and after, except when bearing failure occurred.

The bearings as received from the vendor were all within specification on surface finish and most were roughened two to three points during a test, regardless of whether overheating occurred. Therefore, it is concluded that this type of surface measurement is not sufficient to predict the operating capability of the bearing.

Just prior to the last series of tests (tests No. 11 through 16B), the NASA Project Manager requested that a new set of bearings with Stellite Star J balls and a new set bearings with AISI 440C balls be submitted to NASA for pretest and post-test profilometer traces of the bearing races. Bearing set No. 6 with Stellite Star J balls, was sent to NASA LeRC to be traced, but a new set of bearings with AISI 440C balls was not available, as all of them had been tested. Bearing set No. 3 was selected, based on a visual examination, as the best remaining set and was subsequently sent.

The profilometer tracings were made at NASA LeRC using methods described in NASA TN-D 3730. The pretest and post-test tracings have been arranged in pairs for ease of comparison and are presented as figures 38 through 44.

Comparisons of the race profiles from the Star J ball bearing (S/N L9) of set No. 6 shows an insignificant change to the inner or outer races after the 33 min of running at 13,000 rpm (1361 rad/s) and 7200 lb (32,027 N) load. During this test, bearing S/N L10 overheated and forced the termination of the test. The effect of overheating is clearly shown on the post-test tracing of the inner race (figure 40). Unfortunately, the outer race could not be traced after testing because of damage from a fractured ball, so the continuity of the comparison is not complete.

The other pair of bearings compared by profilometer traces was set No. 3, (bearing S/N L5 and L6) selected on the basis of visual examination as being in the best condition. These bearings had accumulated 19.5 min of rotation (mostly at low speed) and 2.4 min at 12,000 rpm (1256 rad/s) and 12,000 lb (53,379 N) load.

The pretest profilometer traces show wear paths that are quite deep (up to 375 millionths) as results of the previous tests. These tests (No. 4, 8 and 10) all had been terminated because of overheating of one bearing (front bearing (S/N L5) on test No. 4, rear bearing (S/N L6) on test No. 8, and front bearing (S/N L5) on test No. 10); therefore, both bearings had been subjected to overheating as well as to the high axial load.

The post-test profilometer traces were made after an additional 51 min of rotation, of which 4.0 min were at 13,000 rpm (1361 rad/s) and 7200 lb (32,027 N) load. Examination of these traces shows little additional wear due to the additional rotation and load test conditions.

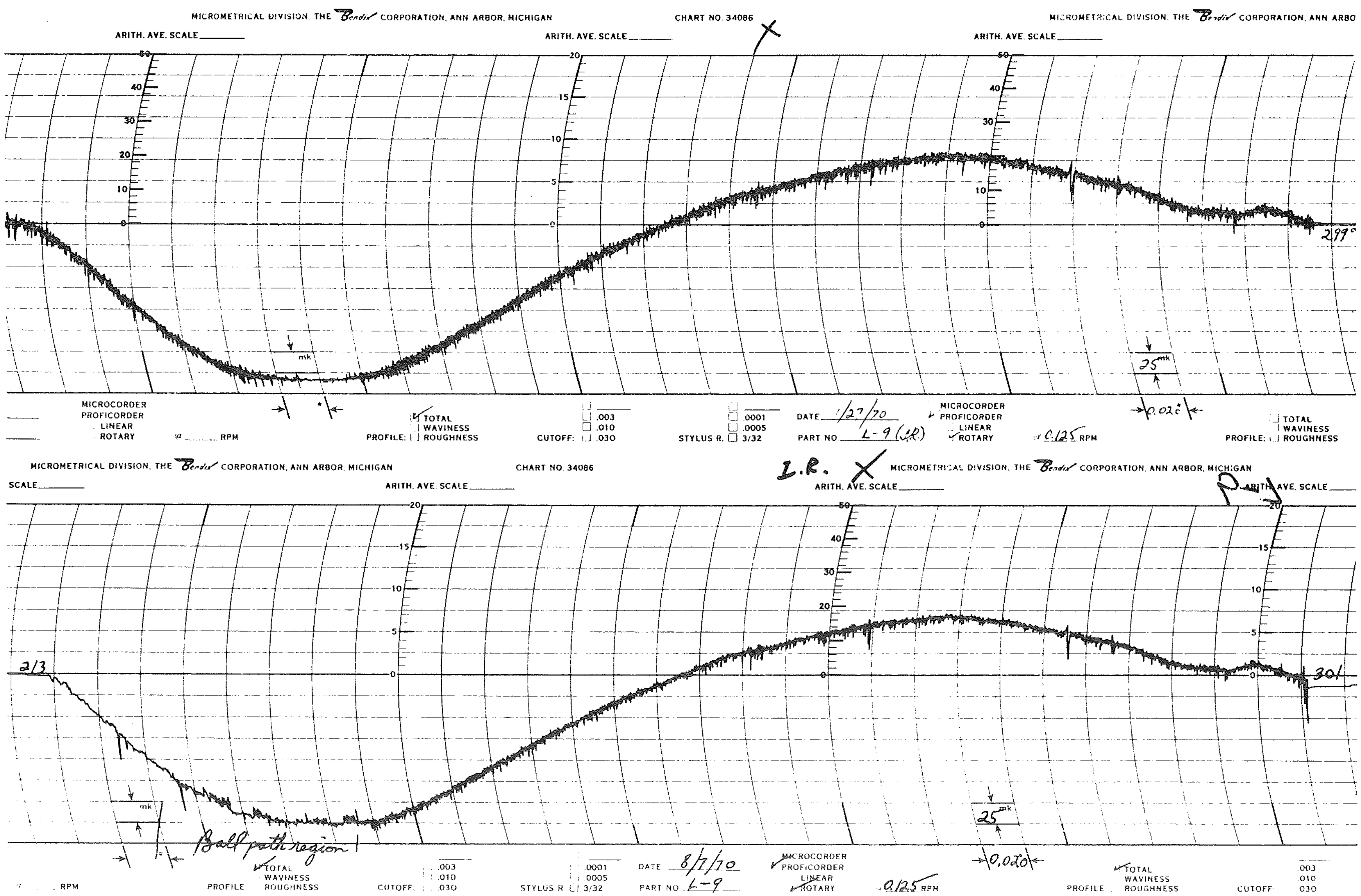

Figure 38. Comparative Profilometer Traces From AISI 440C Inner Race Run With Star J Balls and Salox-M Cage Lubricant (L9) FD 43458

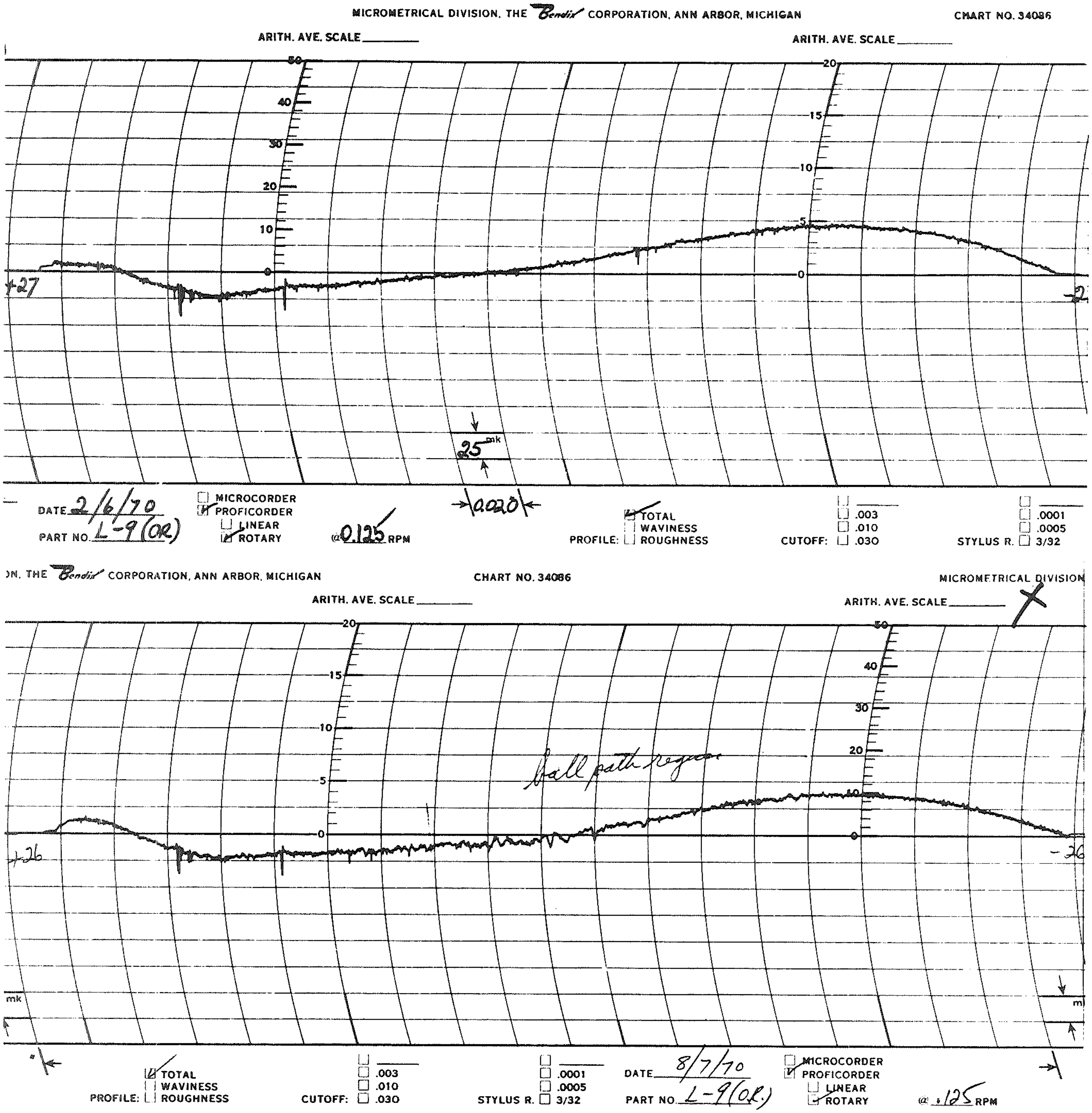

Figure 39. Comparative Profilometer Traces From AISI 440C Outer Race Run With Star J Balls and Salox-M Lubricant (L9)

FD 43459

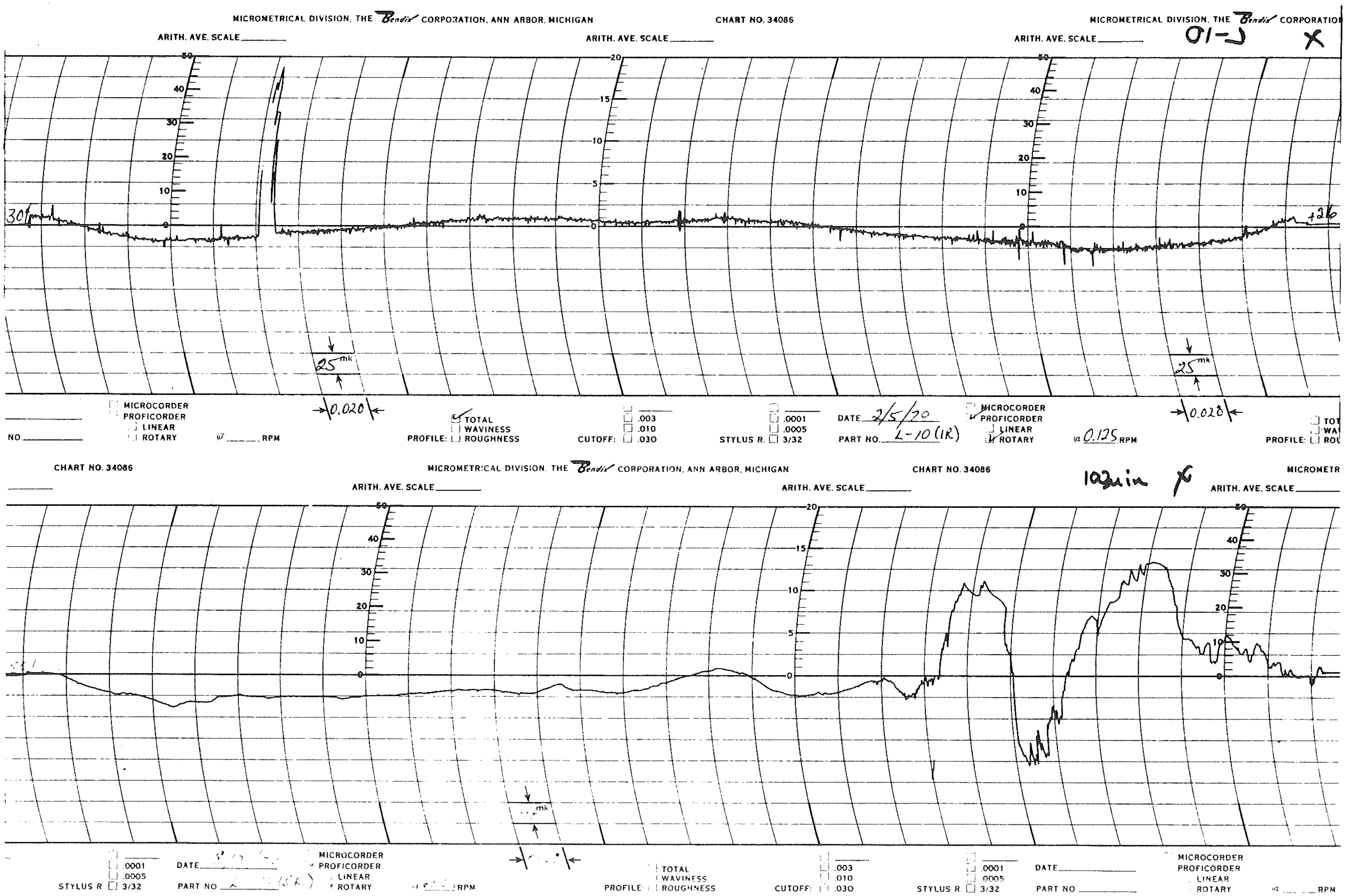

Figure 40. Comparative Profilometer Traces of AISI 440C Inner Race Run With Star J Balls and Salox-M Lubricant (L10)

FD 43460

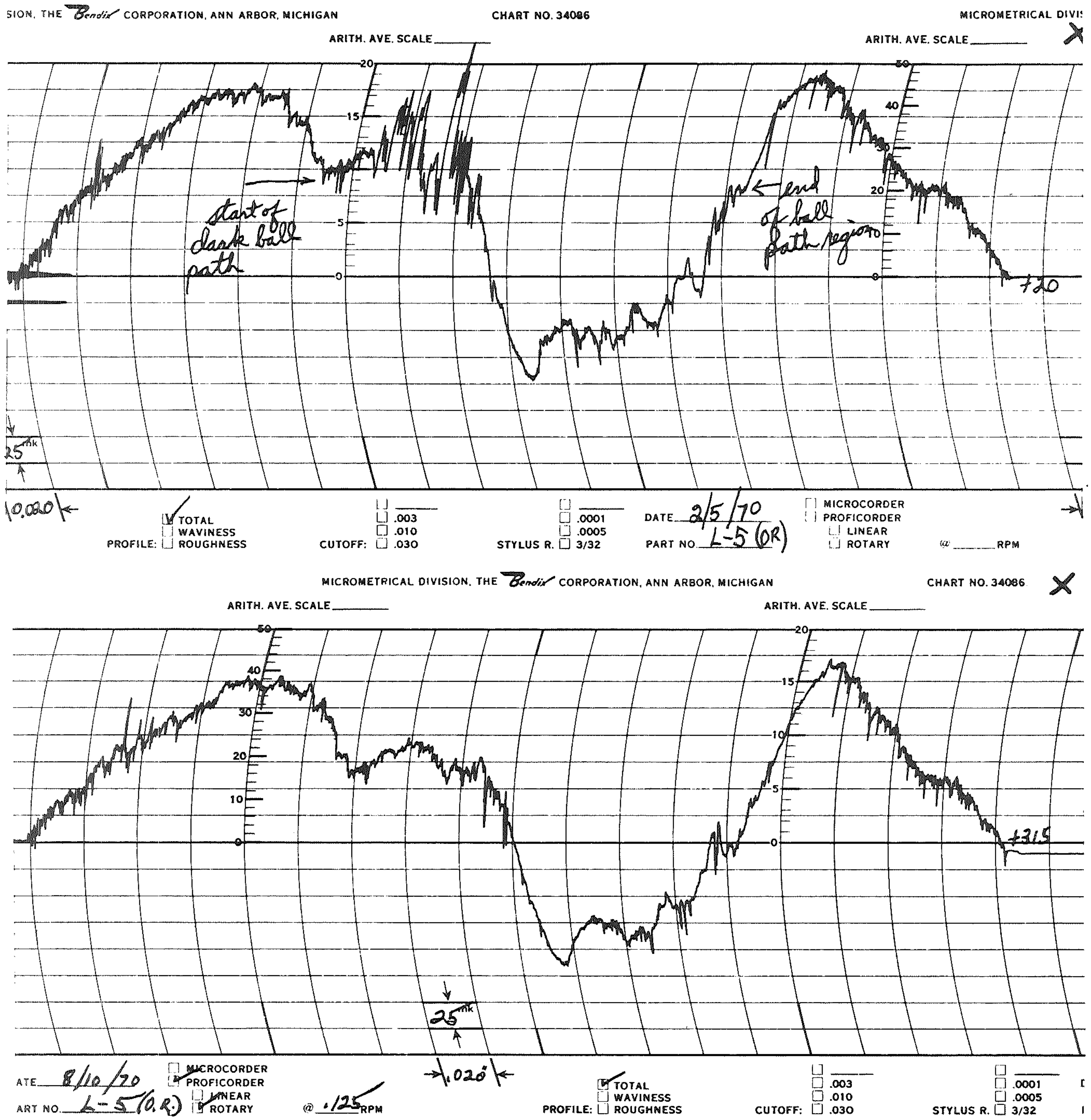

Figure 41. Comparative Profilometer Traces From AISI 440C Outer Race Run With AISI 440C Balls and Chemloy 719 Lubricant (L5) FD 43461

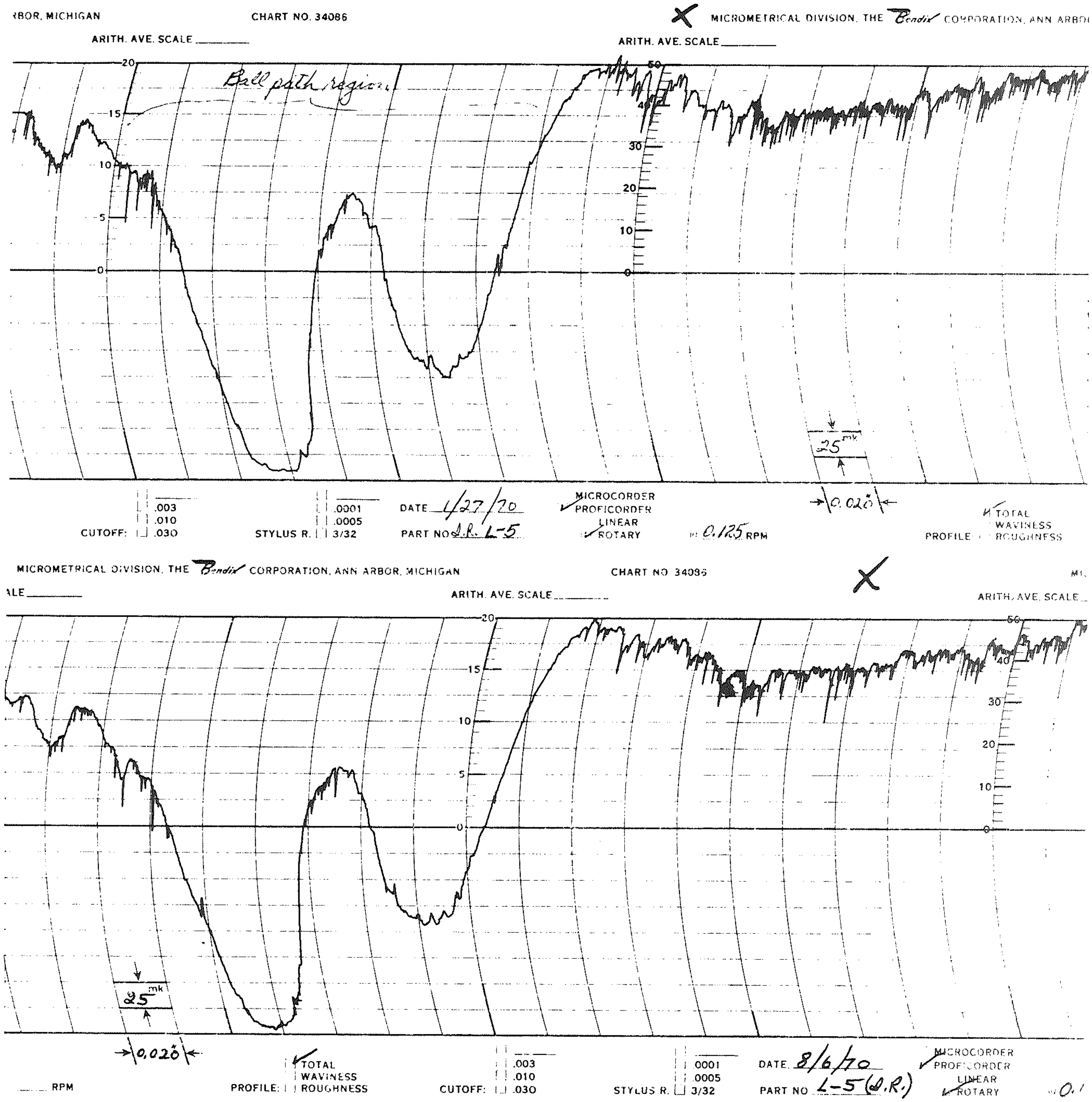

Figure 42. Comparative Profilometer Traces From AISI 440C Inner Race Run With AISI Balls and Chemloy 719 Lubricant (L5) FD 43455

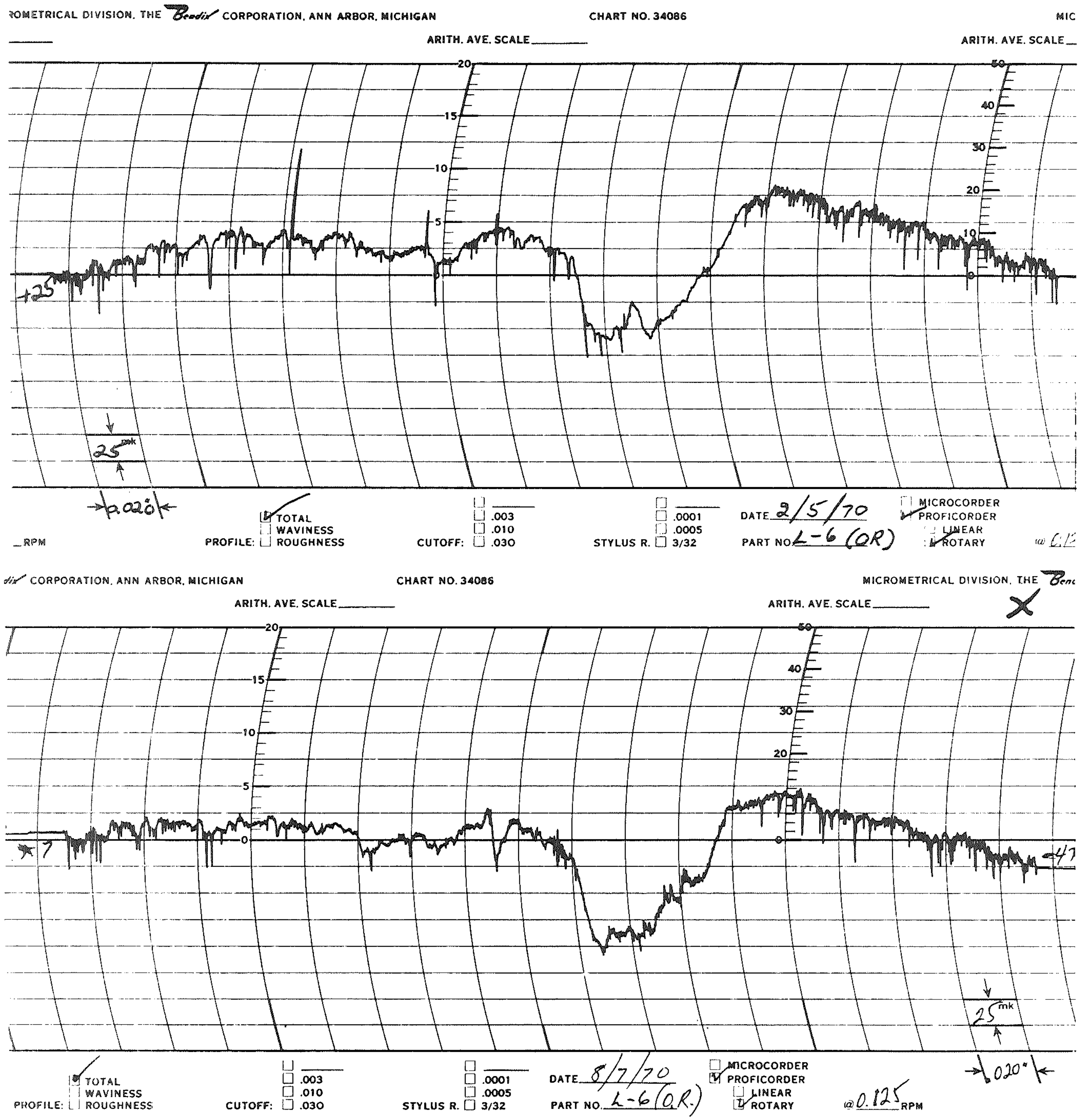

Figure 43. Comparative Profilometer Traces From AISI 440C Outer Race Run With AISI 440C Balls and Chemloy 719 Lubricant (L6) FD 43457

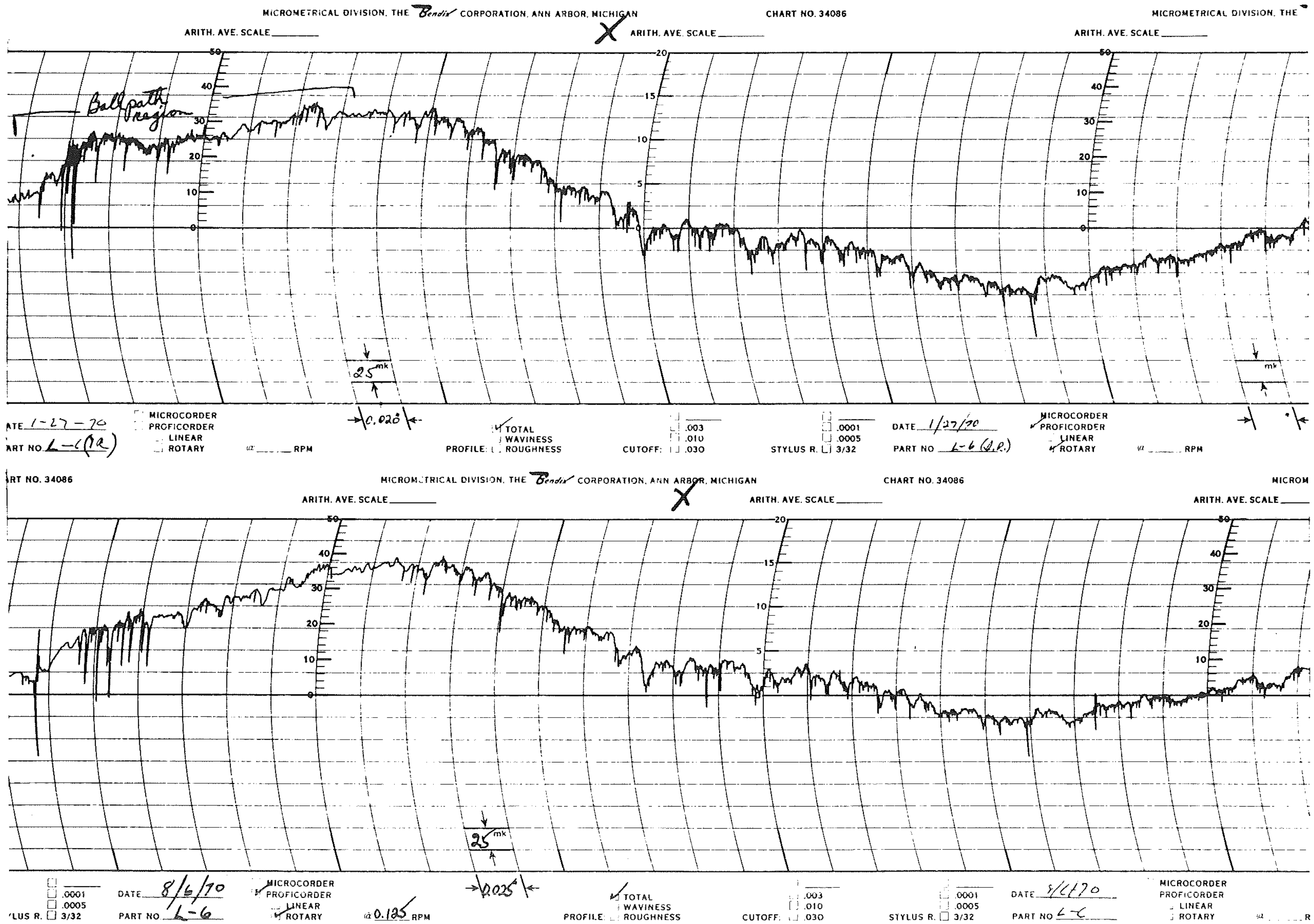

Figure 44. Comparative Profilometer Traces From AISI 440C Inner Race Run With AISI 440C Balls and Chemloy 719 Lubricant (L6)

FD 43456

Based on this small sample of profilometer traces, it is apparent that overheating the bearing races and balls has a definite deleterious effect on the bearing load/speed capability.

D. RECOMMENDATIONS

The decision to make profilometer tracings occurred too late to include before and after test tracings of any bearing sets except No. 3 and 6. The results, as discussed above, are definitive for the one test in which profiles were measured before and after the initial test. However, corroborative evidence is desirable because of the limited sampling.

While no pretest traces are available, sets No. 7 and 8 might provide insight into race wear problems if post-test tracings were made of the race profiles. Set No. 7 did not overheat but was subject to excessive vibration. It is desirable to determine if excessive vibration results in a wear track such as the track in the S/N L10 race (figure 40) that was attributed to bearing overheat.

Also, further evidence concerning the effect of race overheating is available in set No. 8. The races of bearing S/N L2 have been overheated while those of S/N L6 have not. Analysis of post-test profilometer tracings of bearing sets No. 7 and 8 was desireable, but tracings were not available.

Moderate to severe cage pocket wear and/or vibration cracks occurred in a majority of the tests in this program. Although frequency of wear failure was decreasing during the latter portion of the test program, cage web cracks due to vibratory acceleration were becoming more evident. A test program to determine the effect of cage dynamics on cage wear is recommended. Also, while the last modification to the cage appeared to enhance the capability of the cage to withstand vibration, some damage was still present. Therefore, a means of predicting, detecting and controlling destructive vibration levels is needed.

The previous ball failure discussion pointed out that a coarse grain structure including voids is a problem in Stellite Star J casting, and this was determined to be the cause of failure of the bearing that was submitted to the bearing vendor for ball failure analysis. It also prevented the fabrication and testing of Star J races. Because two of the three Star J bearings that reached prescribed load/speed conditions resulted in ball failures, it is not possible to evaluate this material properly until homogeneous fine grain castings are developed. Improvements in casting methods are also required to provide material for fabrication of Star J races. In addition, machining techniques must be developed to produce Star J races with the proper surface and waviness control. Current literature indicates the possibility that close control of surface finish, race roundness, and ball diameter and sphericity variations is necessary in the relatively pure thrust load regimes such as those required in this program. These effects and limits have not been determined quantitatively at this time.

A problem area that was not within the scope of this program, but one that needs to be investigated to enable bearing design advancements of the state-of-the-art of cryogenic bearings operating in a reducing atmosphere, is the determination of the proper applications of coolants and an understanding of the heat transfer characteristics of cryogenically cooled bearings. In this area of interest, the Bearing Branch of the NASA Lewis Research Center's Chemical Rocket Division developed a pilot cooling program for hydrogen cooled bearings based upon a simplified heat transfer analysis. Results are given in NASA TN's D-4616 and D-5607.

APPENDIX A

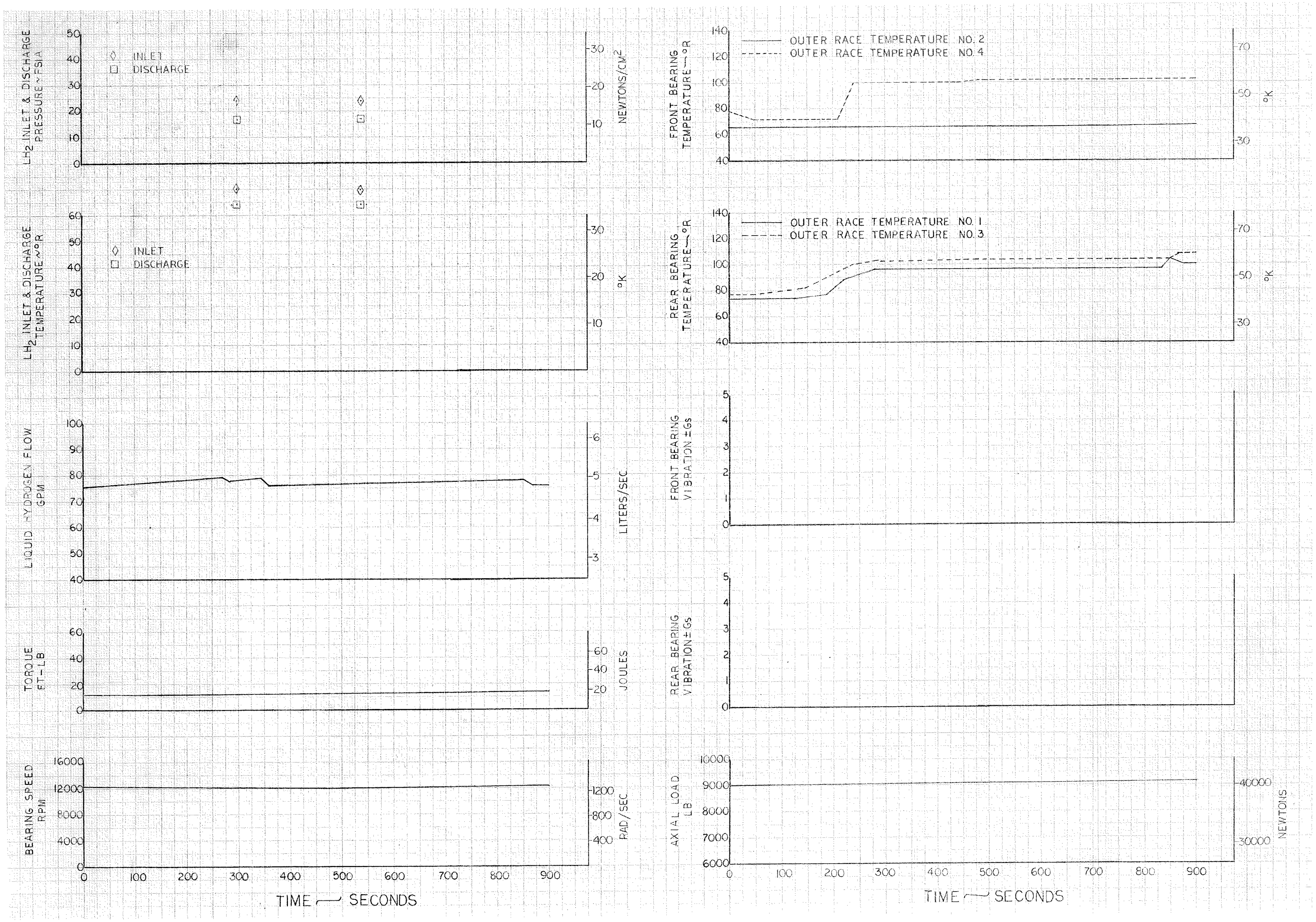

Figure 45. Test No. 2

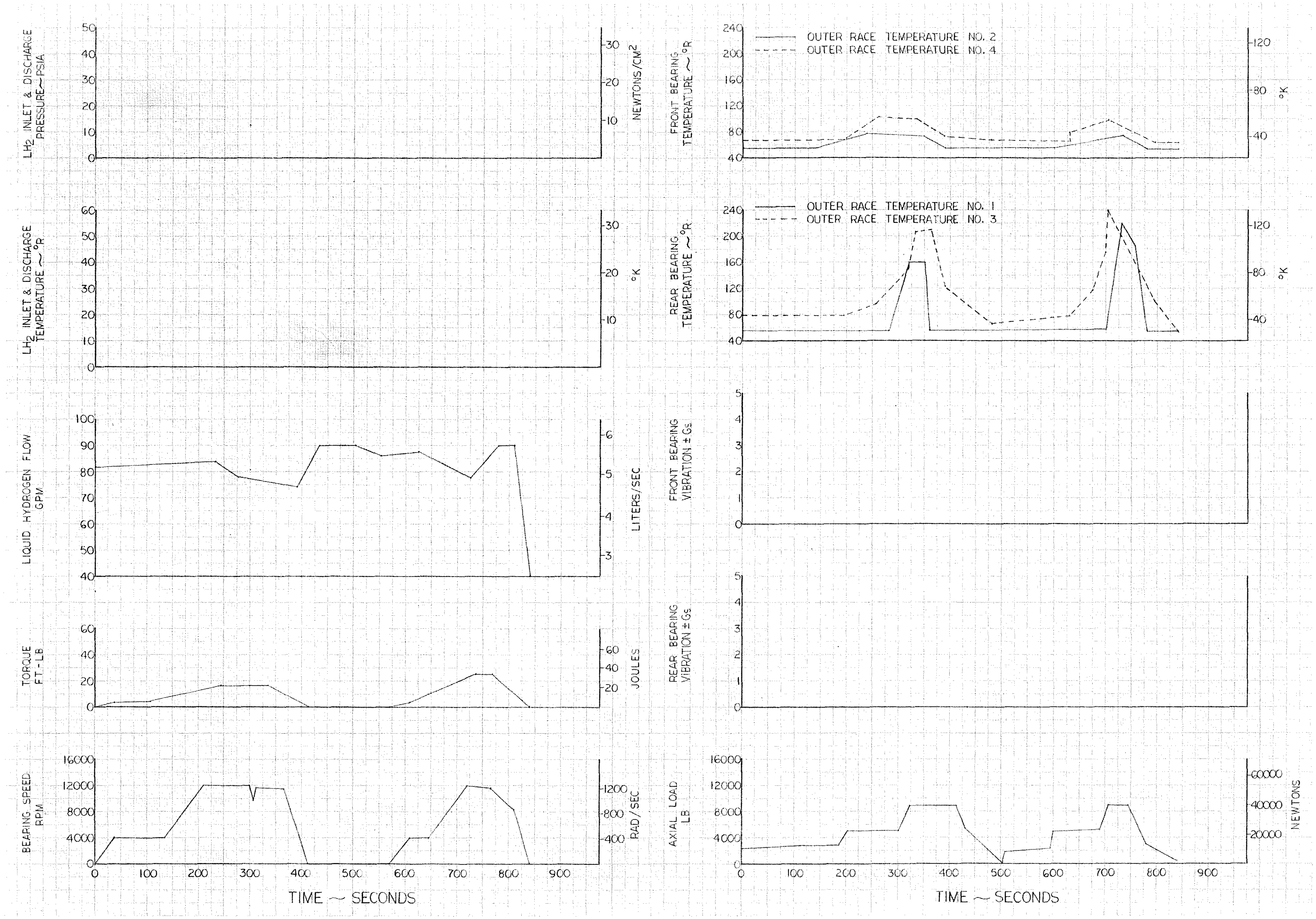

Figure 46. Test No. 3

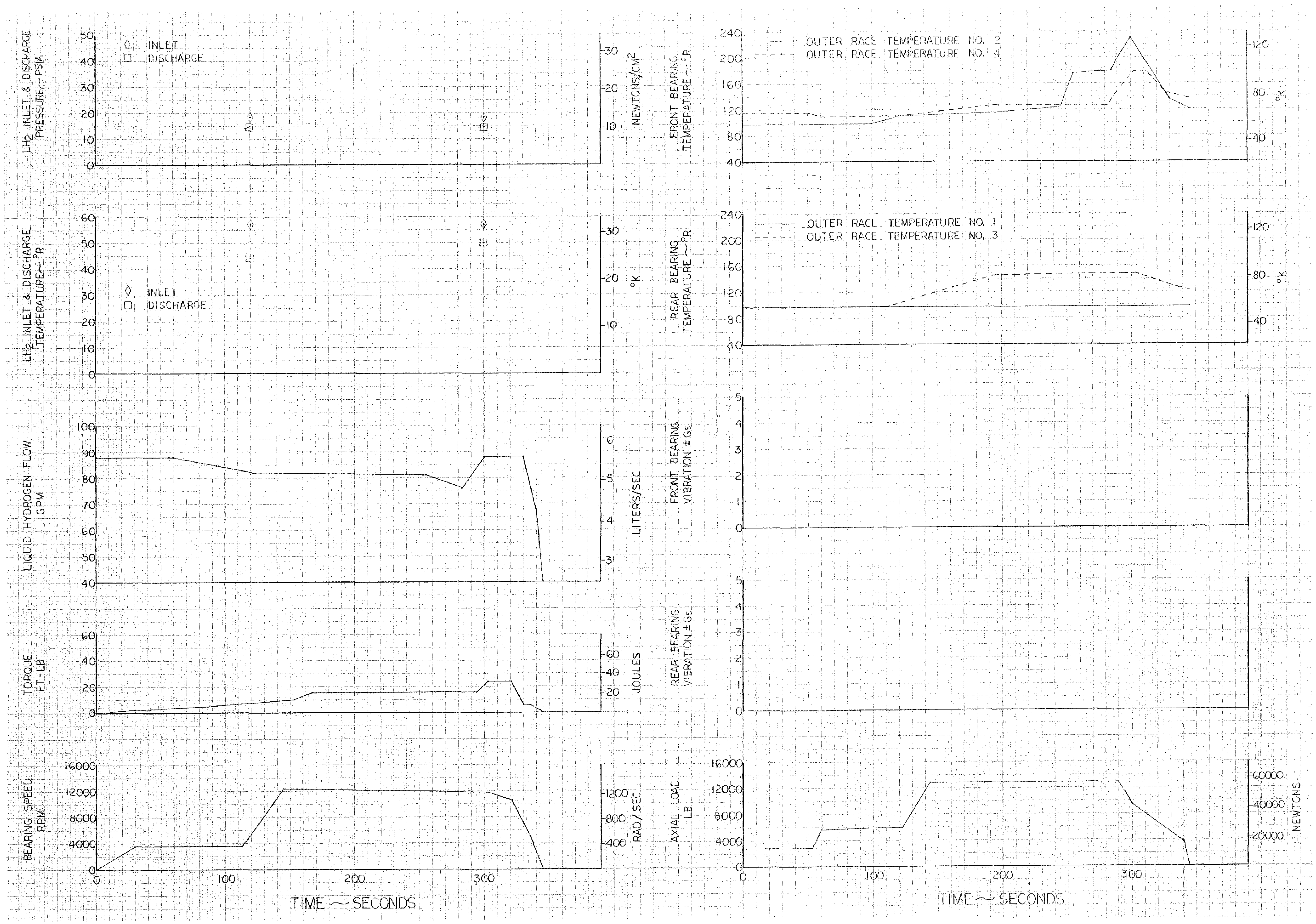

Figure 47. Test No. 4

DF 81505

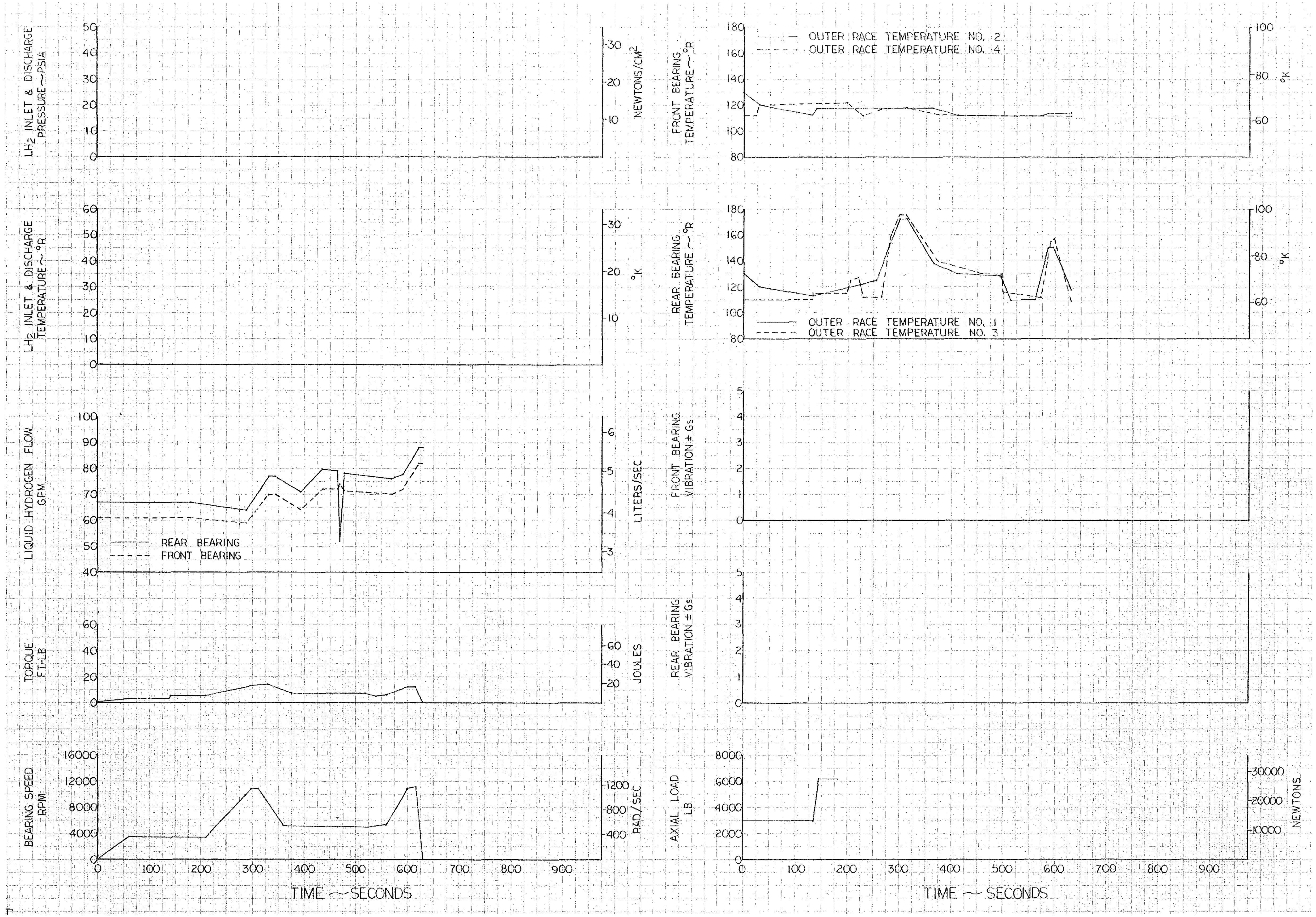

Figure 48. Test No. 5

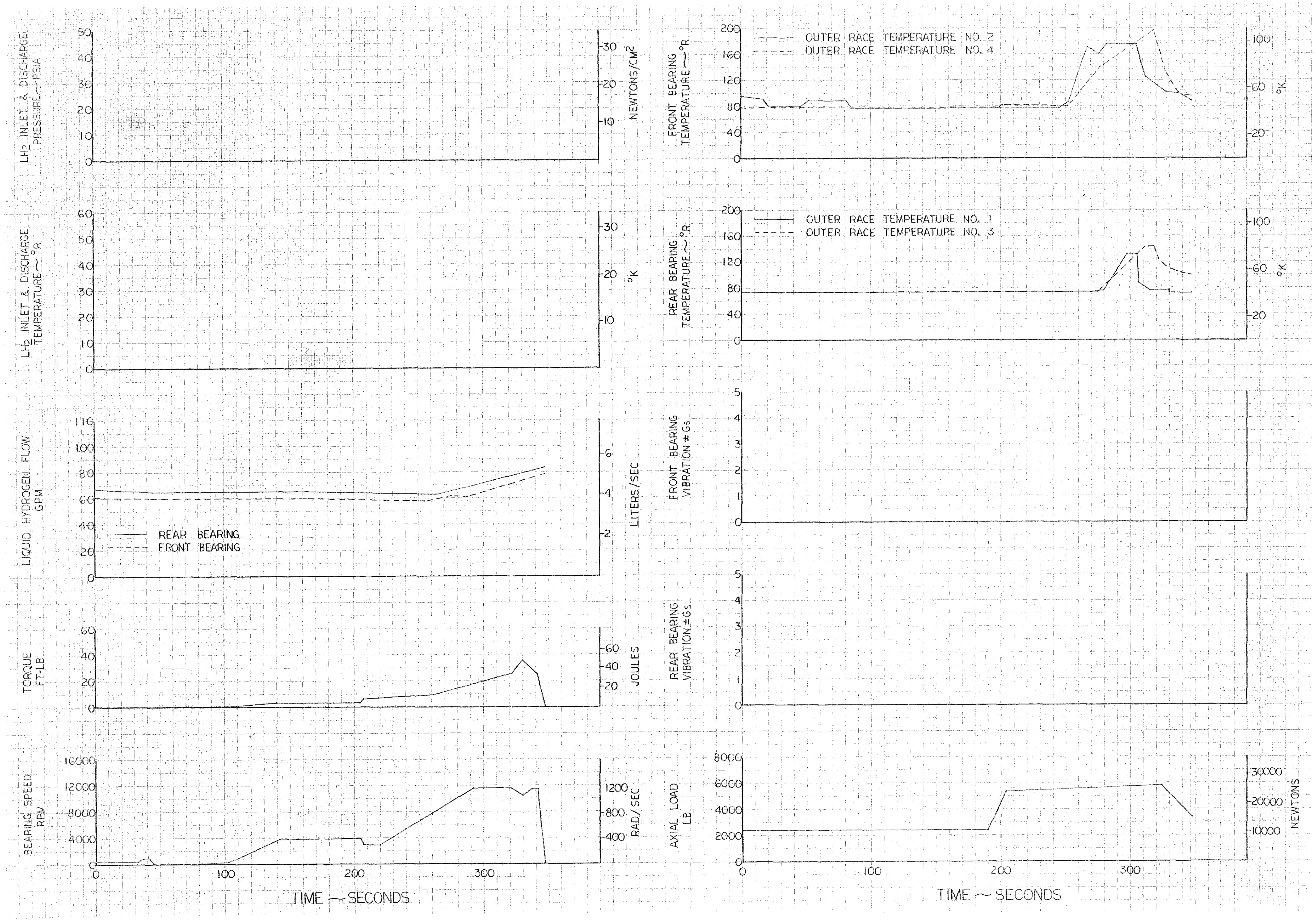

Figure 49. Test No. 6

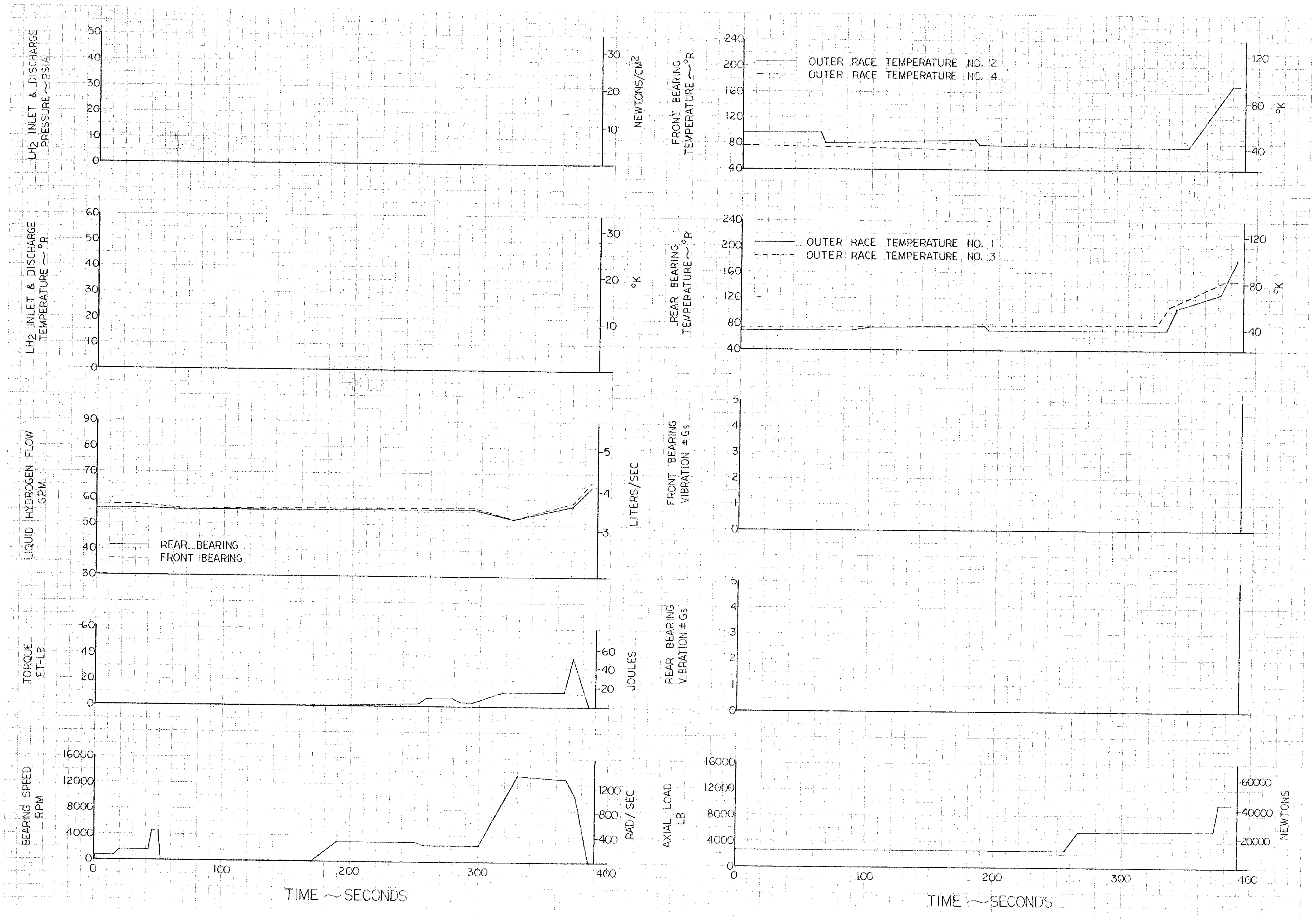

Figure 50. Test No. 7

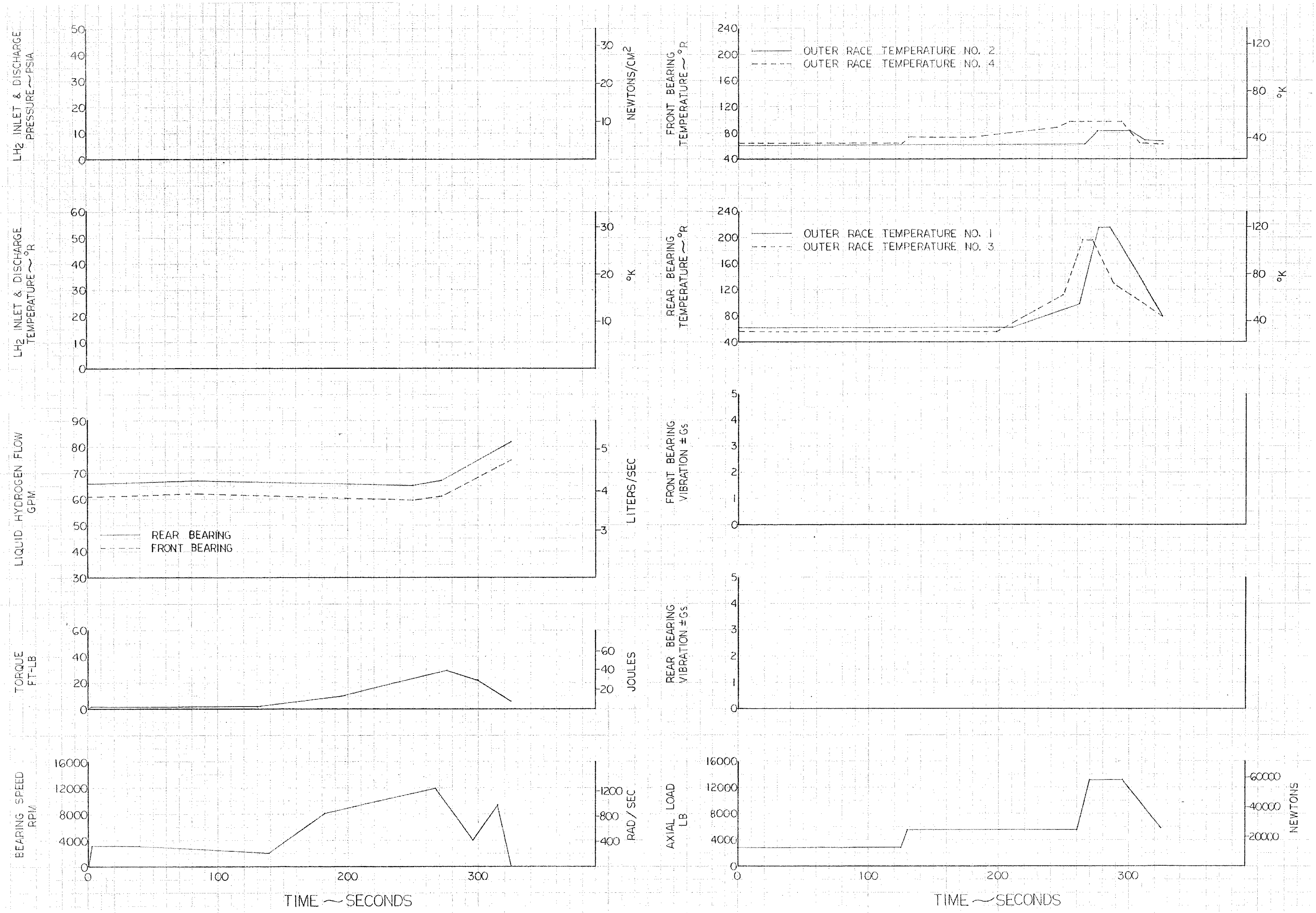

Figure 51. Test No. 8

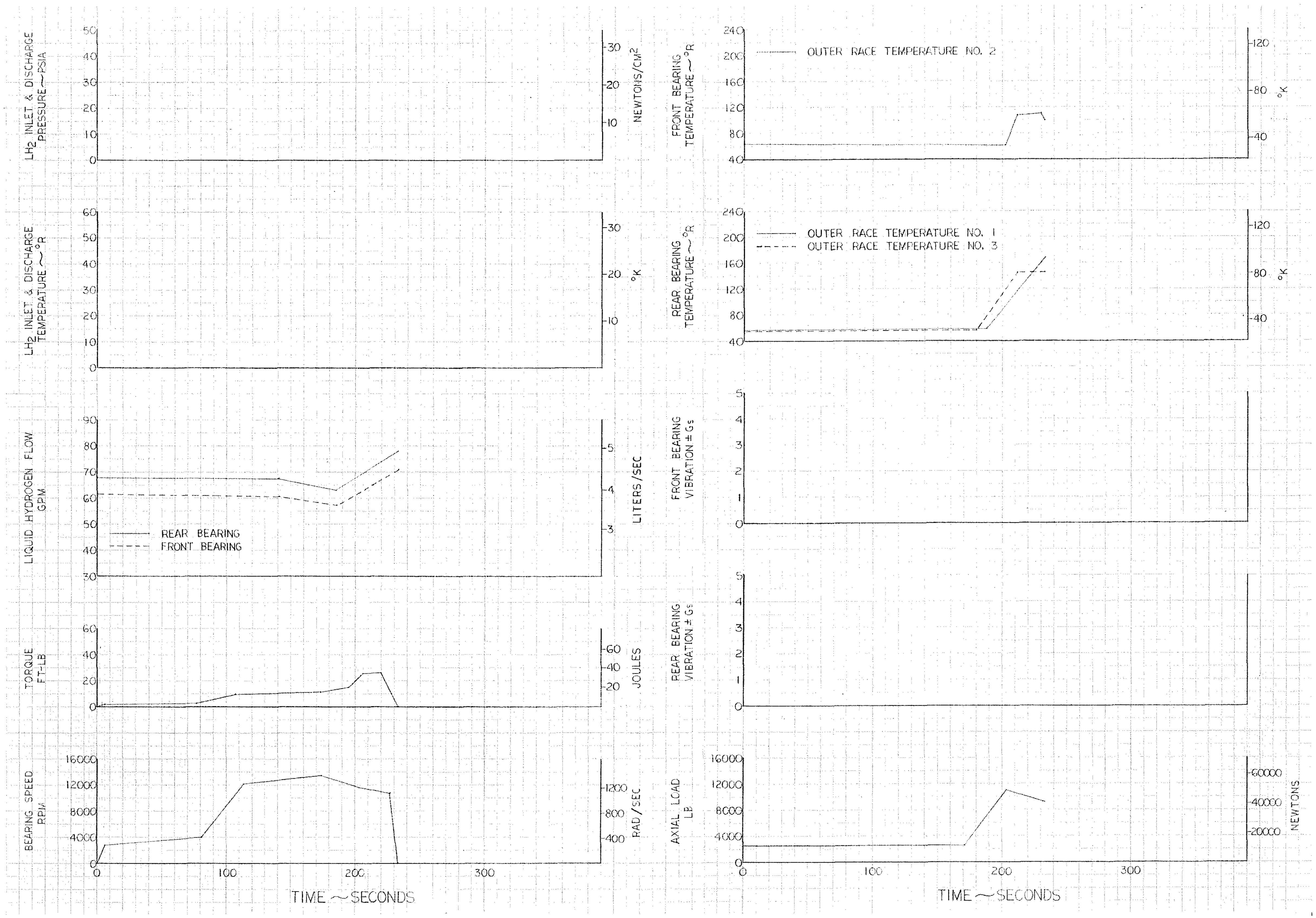

Figure 52. Test No. 9

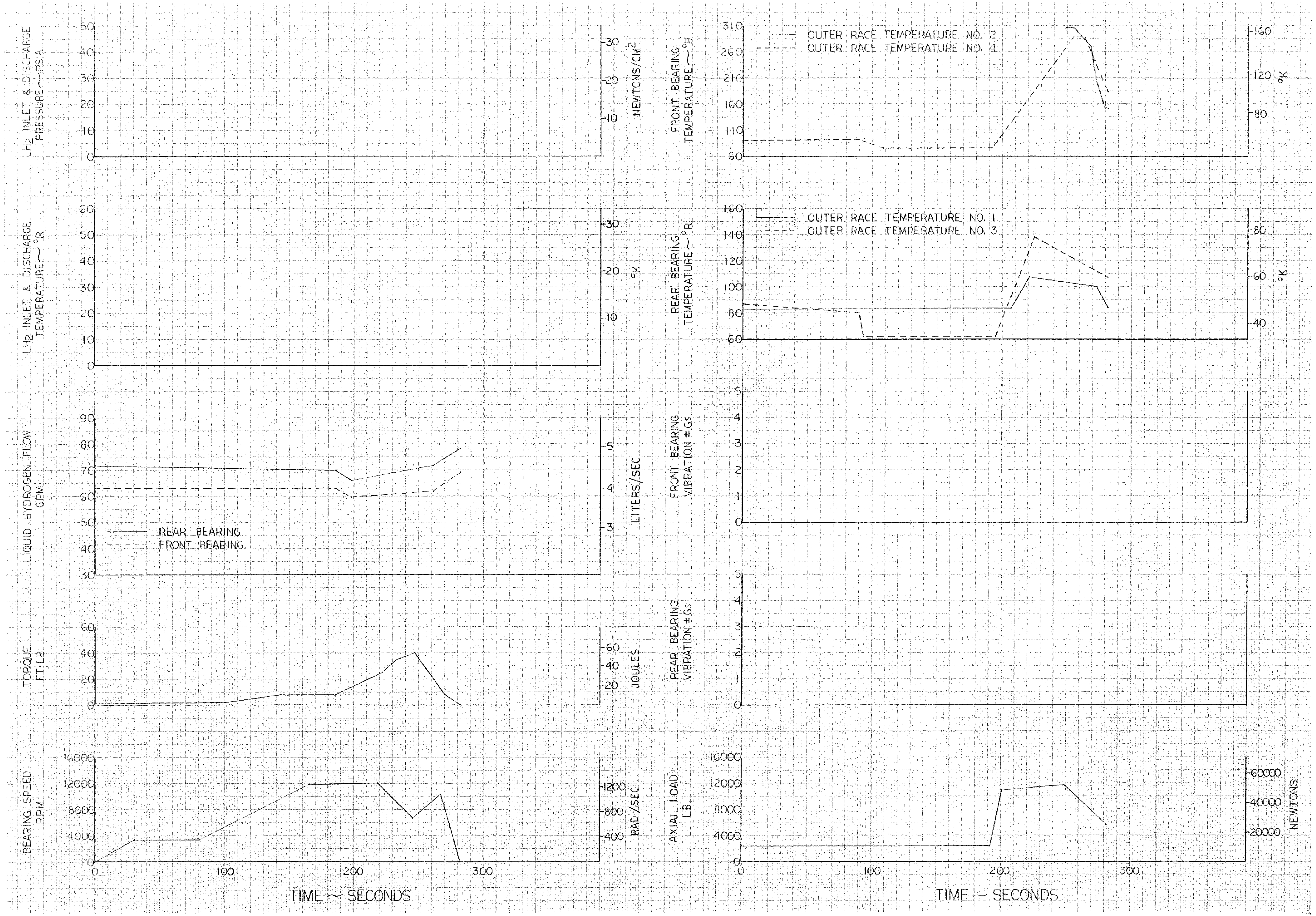

Figure 53. Test No. 10A

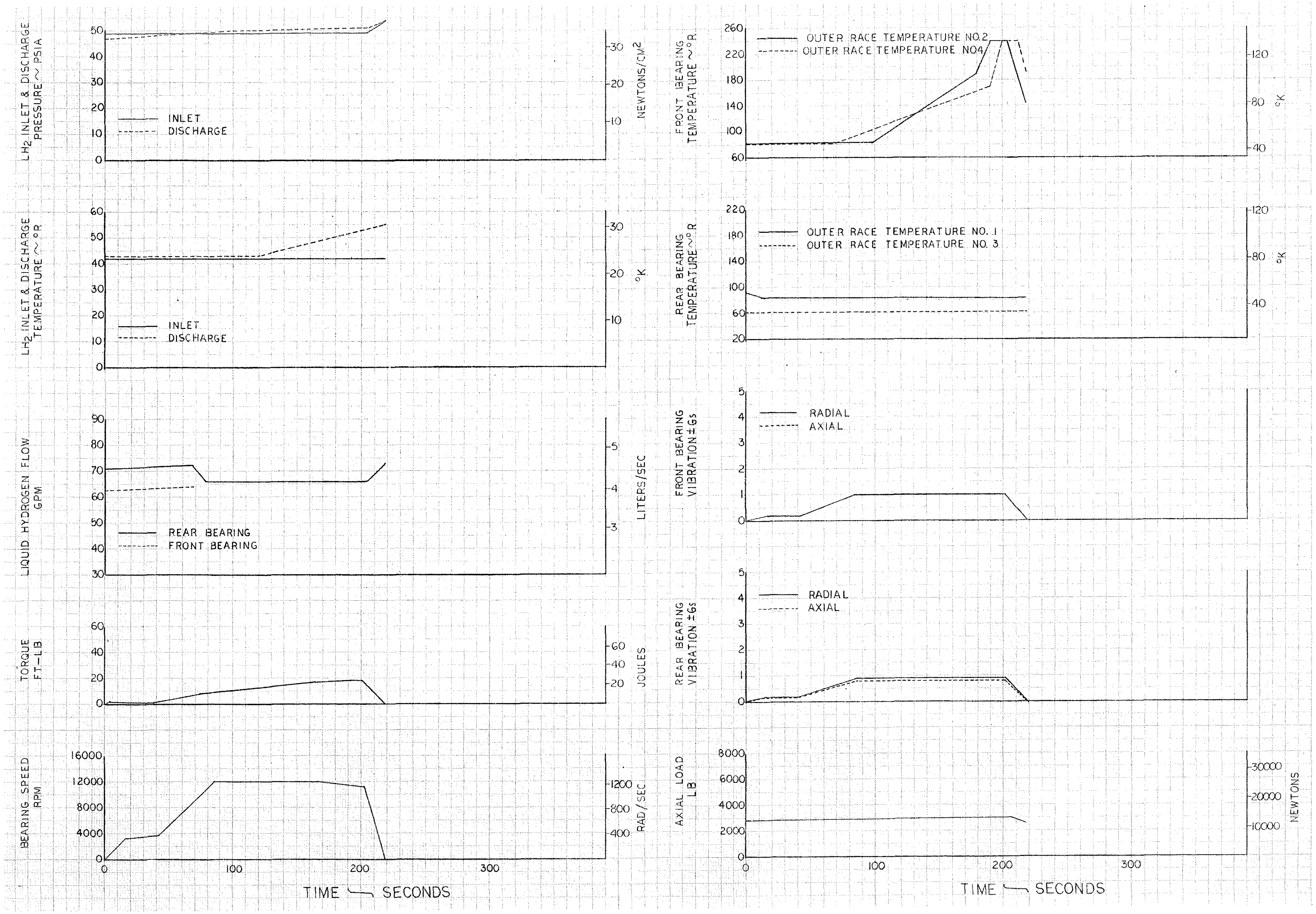

Figure 54. Test No. 10B

DF 81498

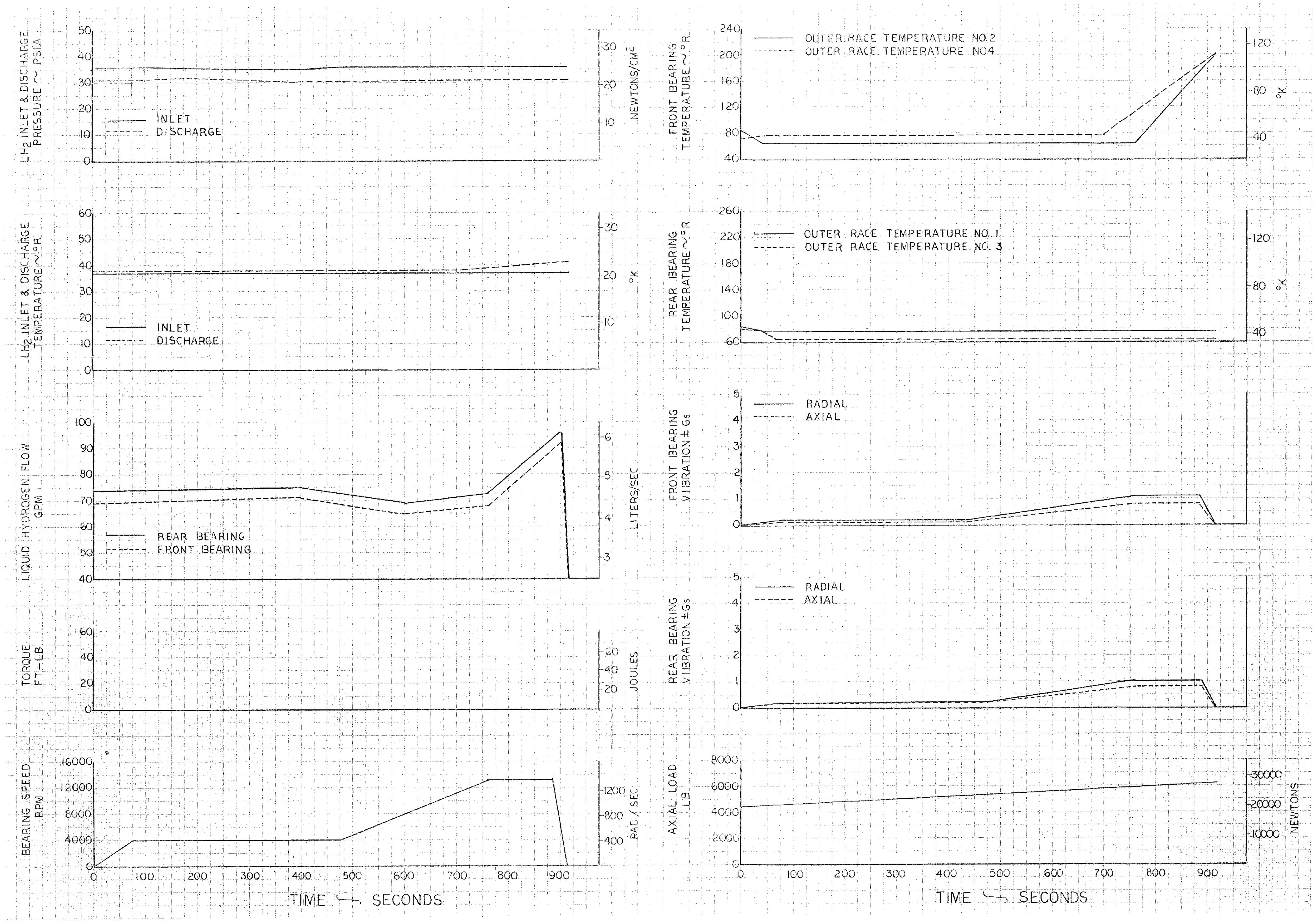

Figure 55. Test No. 11

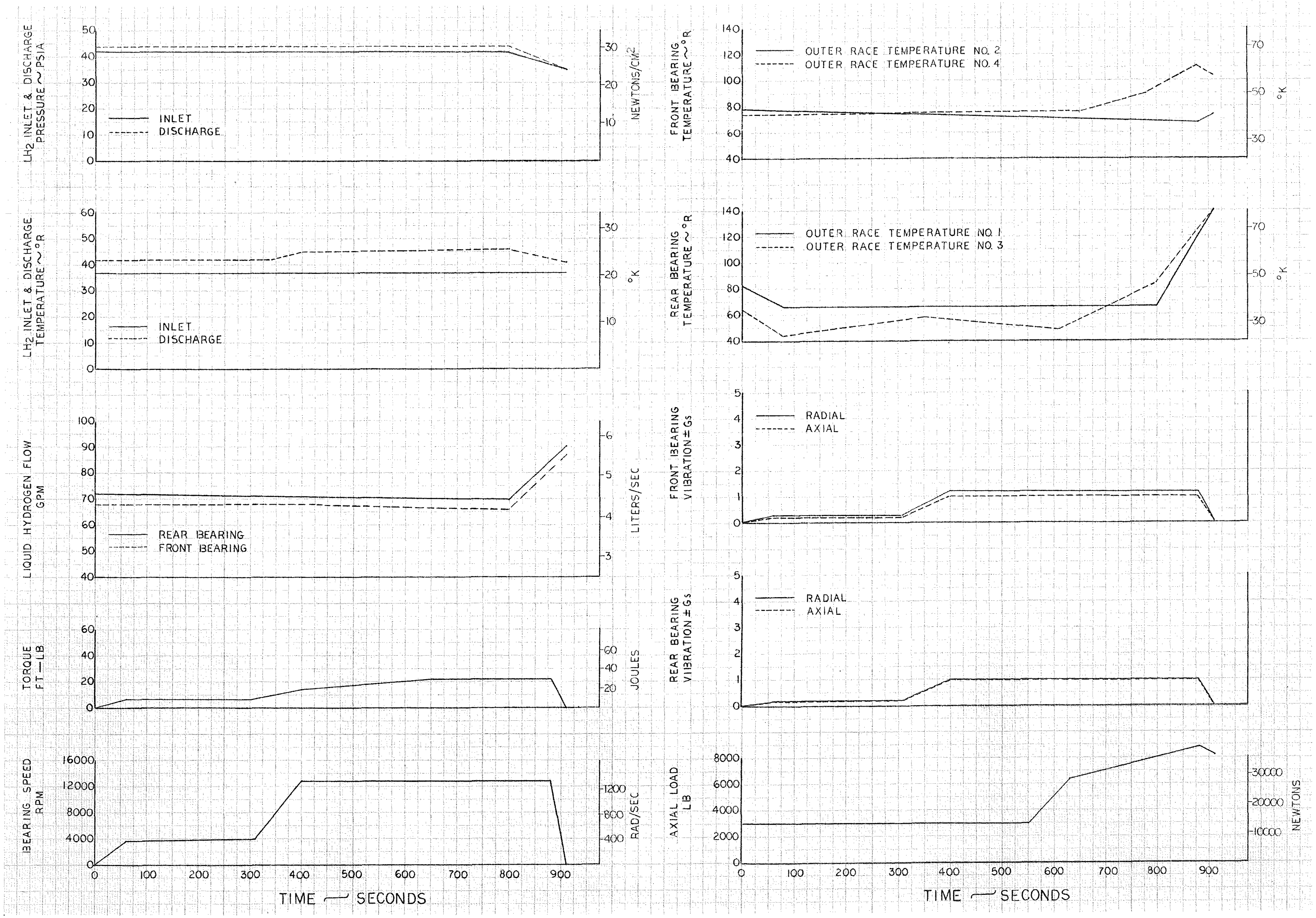

Figure 56. Test No. 12

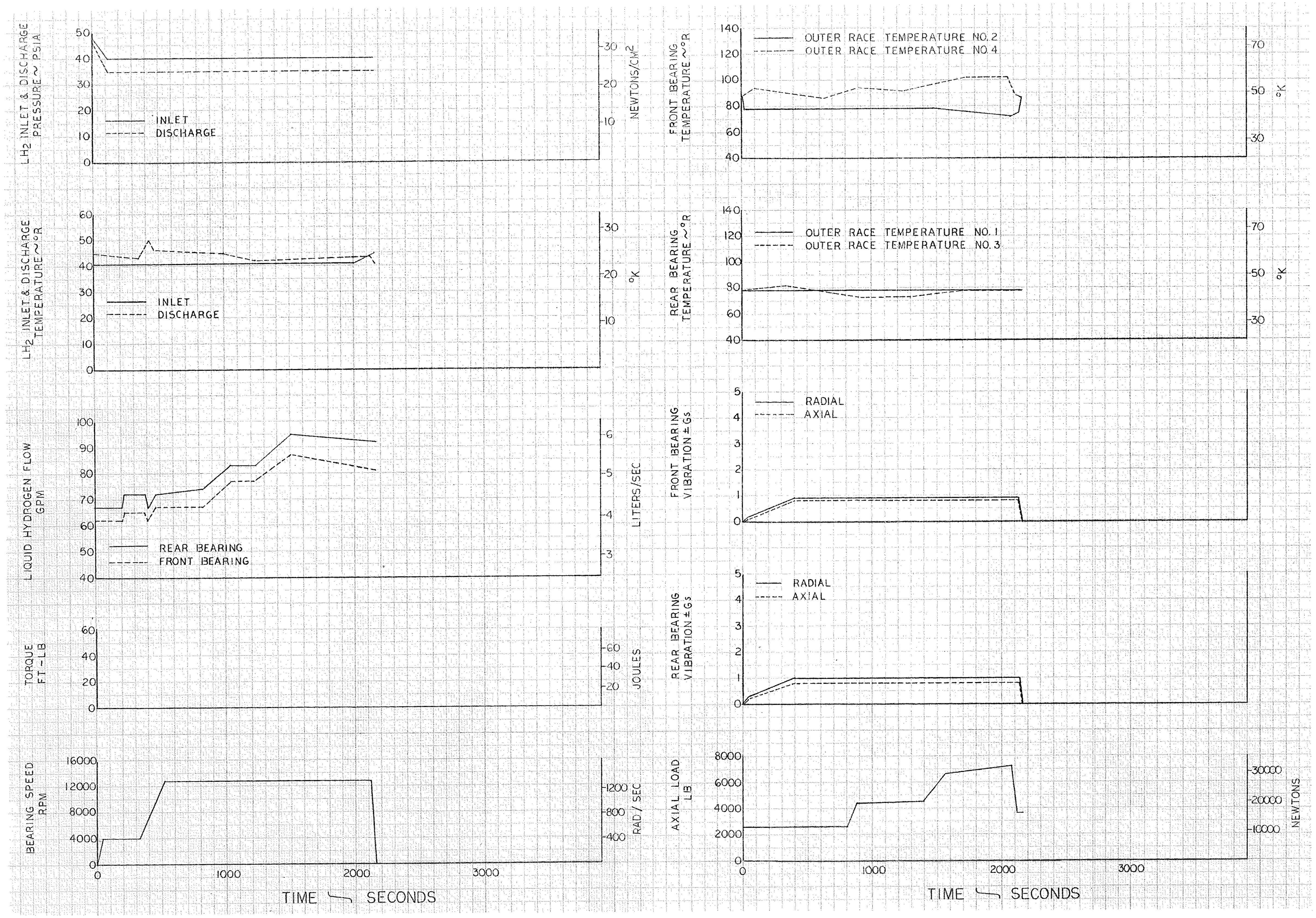

Figure 57. Test No. 13A

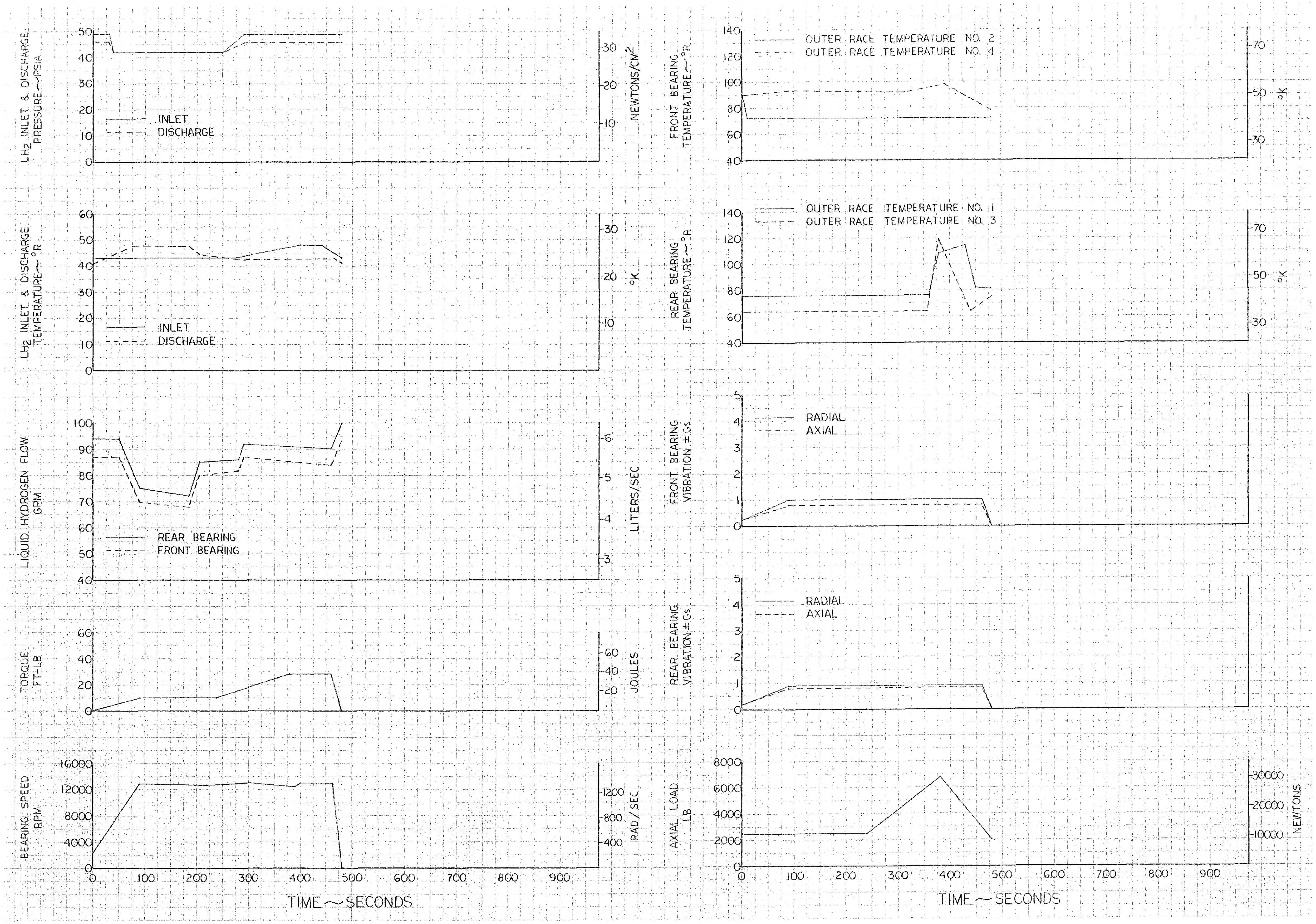

Figure 58. Test No. 13B

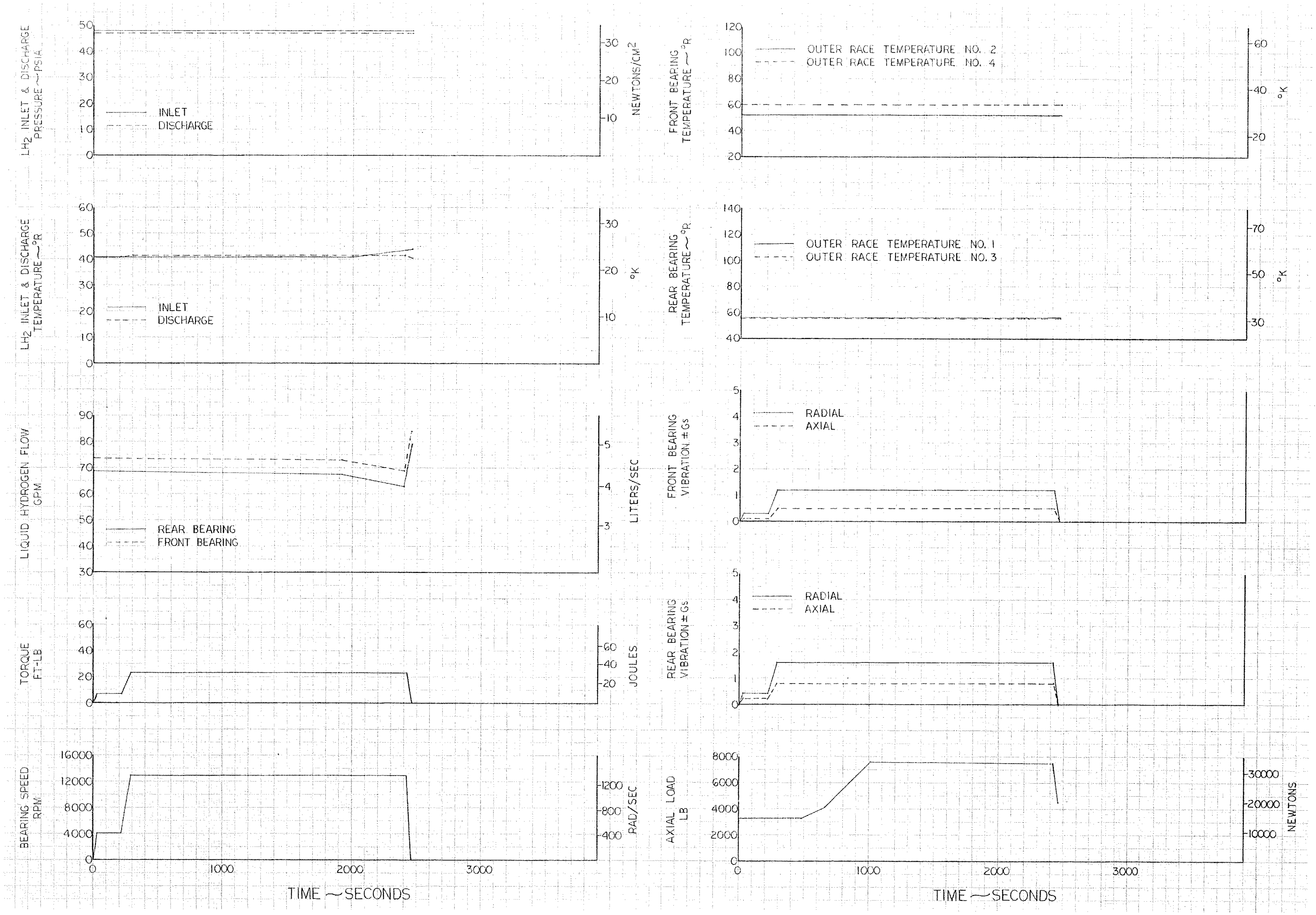

Figure 59. Test No. 14A

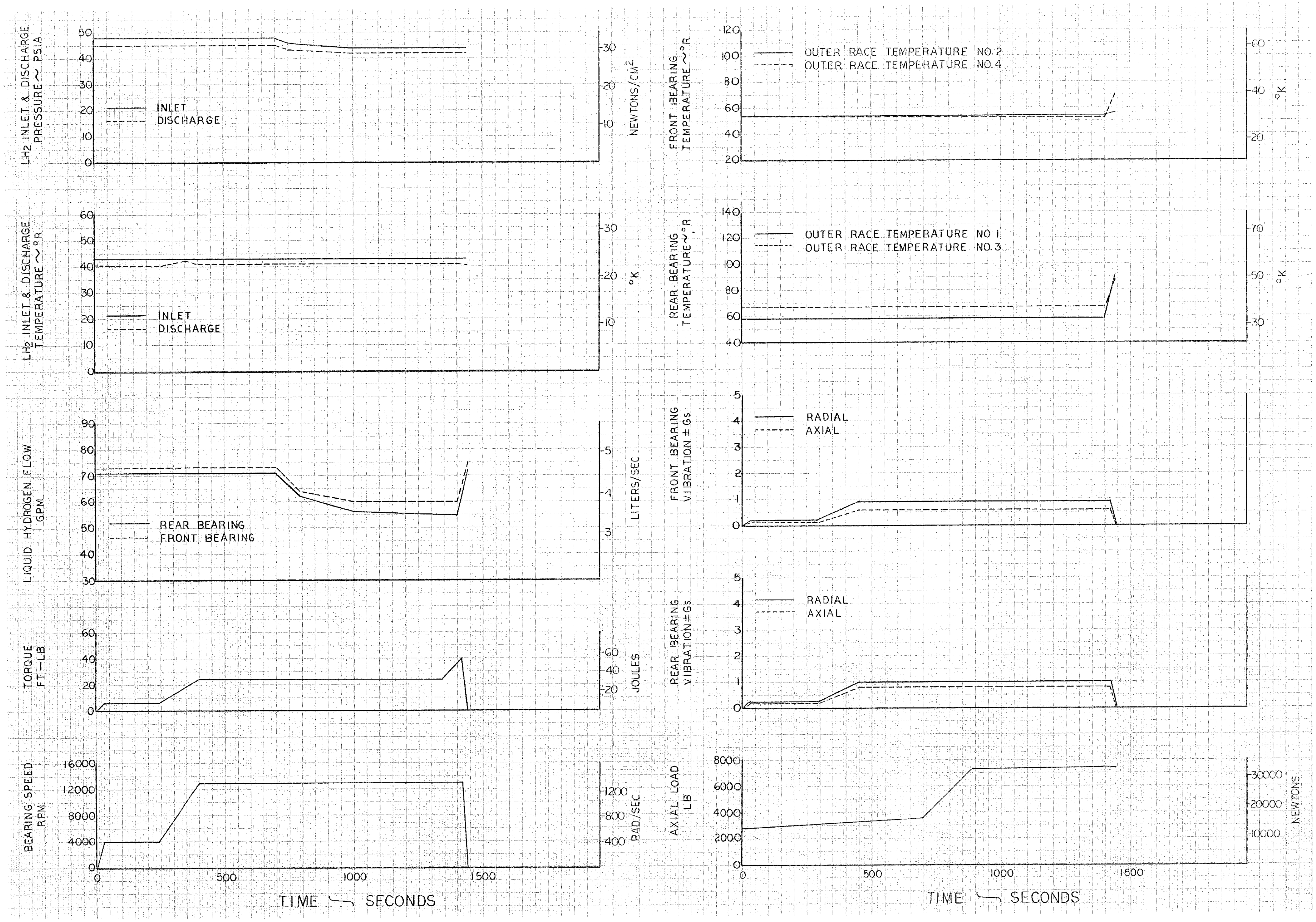

Figure 60. Test No. 14B

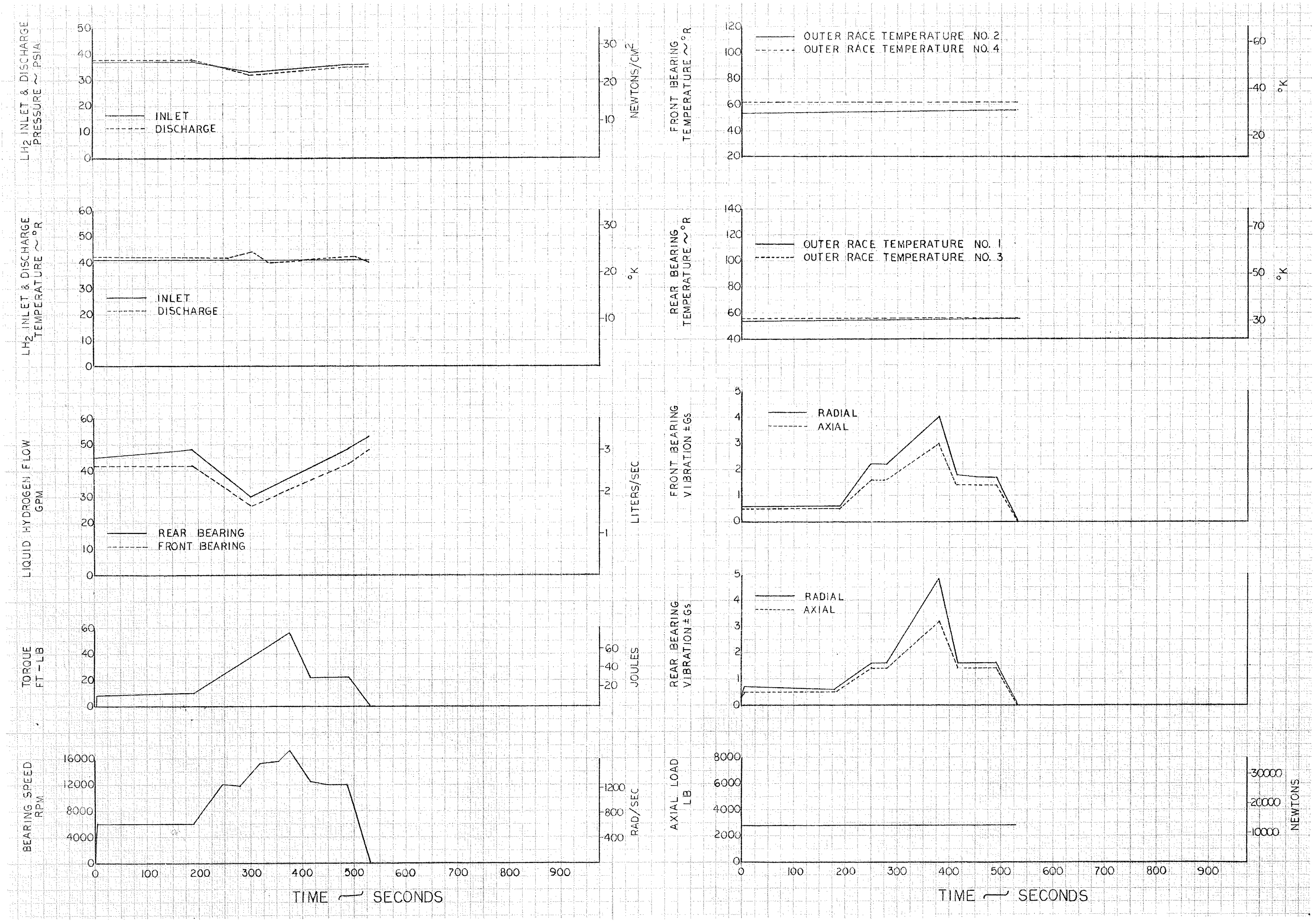

Figure 61. Test No. 15

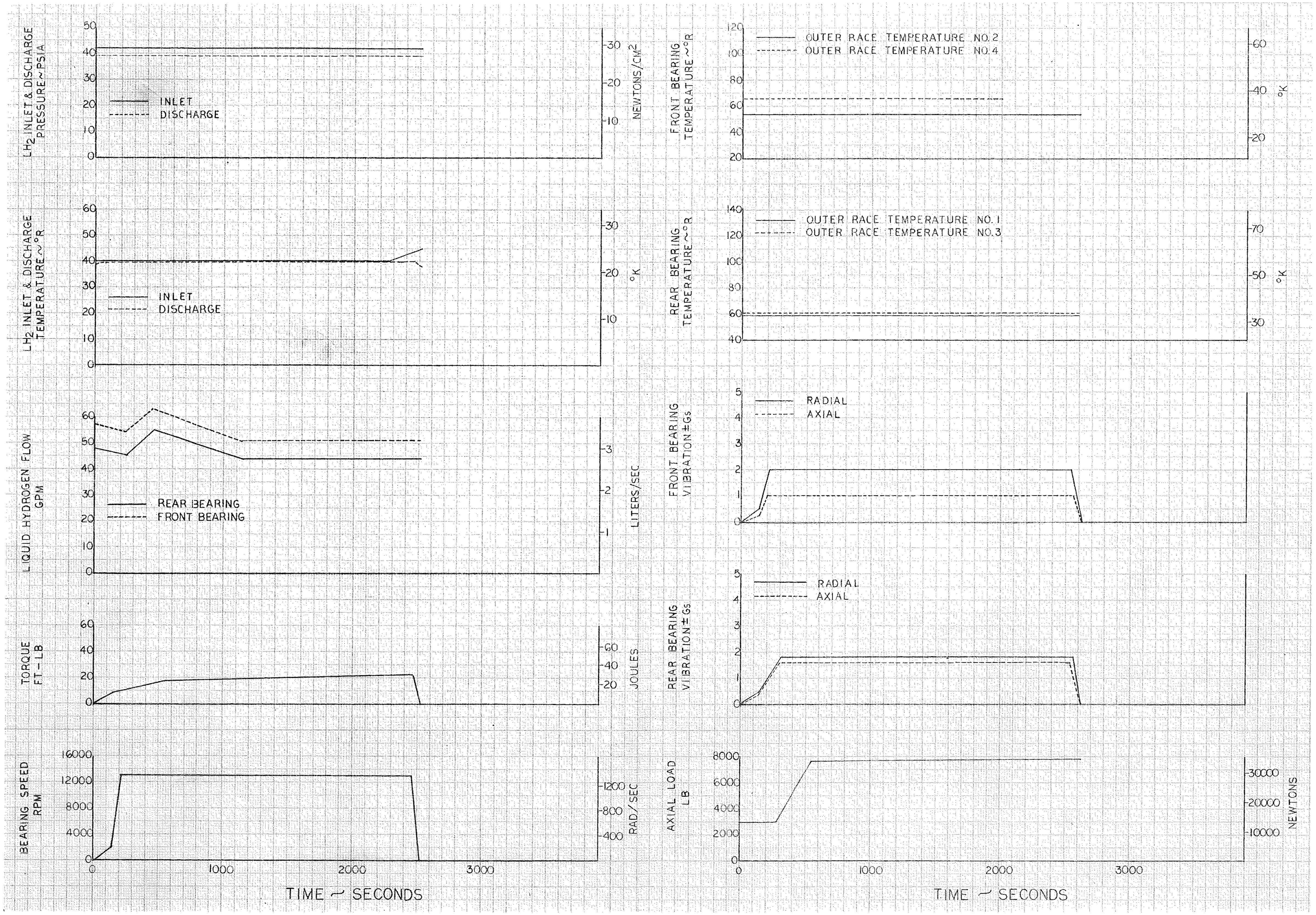

Figure 62. Test No. 16A

DF 81490

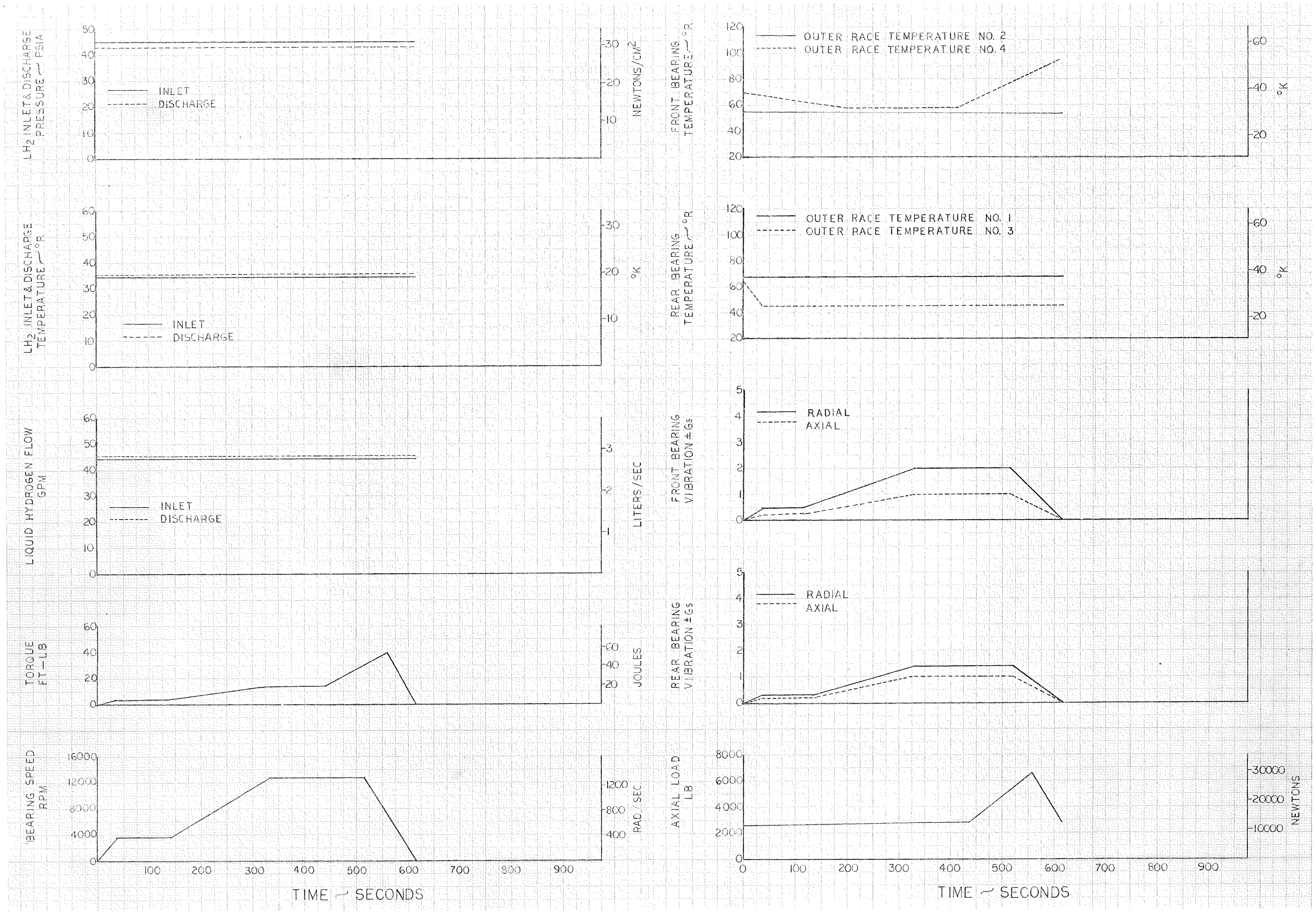

Figure 63. Test No. 16B

APPENDIX B

TEST RUN NO.: 1
BEARING SET NO.: 1
BEARING PART NO.: 2132197
DATE: 11-29-67

Front Bearing S/N 225 Rear Bearing S/N 226

Cage Config.: Original Cage: Chemloy 719 Balls: AISI 440C

	Pretest		Post Test		Parameter Change	
	S/N 225	S/N 226	S/N 225	S/N 226	S/N 225	S/N 226
Shaft Fit, tight (in.)	.0018	.0018				
(cm.)	.0046	.0046				
Housing Fit, loose						
(in.)	.0050	.0050				
(cm.)	.0127	.0127				
Total Ball Size Var.						
(μ in.)	50	20				
(μ m.)	1.27	.51				
Theor. Int. Clearance						
(in.)	.0079	.0081				
(cm.)	.0201	.0206				
Ball Parameters						
Average Weight (gm.)	24.3424	24.3272				
Average Surface Finish						
(μ in., rms)	2 - 4	2 - 3				
(μ m, rms)	.0508-.1016	.0508-.0762				
Average Diameter						
(in.)	0.71889	0.71874				
(cm.)	1.82598	1.8256				
Cage Parameters			Bearing Failure	Bearing Failure		
Weight (gm.)	147.84	148.94				
Average Pocket Dia.						
(in.) Axial	0.7312	0.7329				
(cm.) Axial	1.8572	1.8616				
(in.) Circumferential	0.7271	0.7258				
(cm.) Circumferential	1.8468	1.8435				
Inside Diameter						
(in.)	5.100	5.100				
(cm.)	12.954	12.954				
Inner Race Parameters						
Weight (gm.)	621.62	621.70				
Surface Finish						
(μ in., rms)	2 - 4	2 - 4				
(μ m, rms)	.0508-.1016	.0508-.1016				
Outer Race Parameters						
Weight (gm.)	749.23	749.78				
Surface Finish						
(μ in., rms)	2 - 4	2 - 4				
(μ m, rms)	.0508-.1016	.0508-.1016				

TEST RUN NO.: 2
BEARING SET NO.: 2
BEARING PART NO.: 2132197
DATE: 12-26-67

Front Bearing S/N 248 — Rear Bearing S/N 249

Cage Config.: CKJ 7153 — Cage: Chemloy 719 — Balls: AISI 440C

	Pretest		Post Test		Parameter Change	
	S/N 248	S/N 249	S/N 248	S/N 249	S/N 248	S/N 249
Shaft Fit, tight (in.)	.0020	.0020	.0020	.0018	0	-.0002
(cm.)	.0051	.0051	.0051	.0045	0	-.0005
Housing Fit, loose						
(in.)	.0050	.0050	.0050	.0050	0	0
(cm.)	.0127	.0127	.0127	.0127	0	0
Total Ball Size Var.						
(μ in.)	40	60	60	200	+20	+140
(μ m.)	1.016	1.524	1.524	5.08	+.508	+3.556
Theor. Int. Clearance						
(in.)	.008	.009	.0083	.009	+.0003	0
(cm.)	.0203	.0229	.0211	.0229	+.0008	0
Ball Parameters						
Average Weight (gm.)	24.3307	24.3166	24.3309	24.3165	+0.0002	-0.0001
Average Surface Finish						
(μ in., rms)	2 - 3	2 - 3	*	*		
(μ m, rms)	.0508-.0762	.0508-.0762				
Average Diameter						
(in.)	0.71855	0.71840	0.71877	0.71863	+0.00022	+0.00023
(cm.)	1.82512	1.82474	1.82568	1.82532	+0.00056	+0.00058
Cage Parameters						
Weight (gm.)	141.97	142.60	140.44	141.89	-1.53	-0.71
Average Pocket Dia.						
(in.) Axial	0.7559	0.7553	0.7513	0.7513	-0.0046	-0.0040
(cm.) Axial	1.9200	1.9185	1.9083	1.9083	-0.0117	-0.0102
(in.) Circumferential	0.7531	0.7524	0.7526	0.7576	-0.0005	+0.0052
(cm.) Circumferential	1.9129	1.9111	1.9116	1.9243	-0.0013	+0.0132
Inside Diameter						
(in.)	5.107	5.110	5.117	5.115	+0.010	+0.005
(cm.)	12.972	12.979	12.997	12.992	+0.025	+0.013
Inner Race Parameters						
Weight (gm.)	622.42	621.80	622.42	621.79	0.00	-0.01
Surface Finish						
(μ in., rms)	4 - 5	4	*	*		
(μ m, rms)	.1016-.127	.1016				
Outer Race Parameters						
Weight (gm.)	750.00	749.91	750.02	749.90	+0.02	-0.01
Surface Finish						
(μ in., rms)	5 - 8	7 - 9	*	*		
(μ m, rms)	.127-.2032	.1778-.2286				

* Not measured, cage material deposits left in place for next test.

TEST RUN NO.: 3
BEARING SET NO.: 2
BEARING PART NO.: 2132197
DATE: 4-16-68

Front Bearing S/N 248 Rear Bearing S/N 249

Cage Config.: CKJ 7153 Cage: Chemloy 719 Balls: AISI 440C

	Pretest		Post Test		Parameter Change	
	S/N 248	S/N 249	S/N 248	S/N 249	S/N 248	S/N 249
Shaft Fit, tight (in.)	.0020	.0018	.0019	.0018	-.0001	0
(cm.)	.0051	.0046	.0048	.0046	-.0003	0
Housing Fit, loose						
(in.)	.0050	.0050	.0050	.0050	0	0
(cm.)	.0127	.0127	.0127	.0127	0	0
Total Ball Size Var.						
(μin.)	60	300	50	480	-10	+180
(μm.)	1.524	7.620	1.27	12.192	-.254	+4.572
Theor. Int. Clearance						
(in.)	.0083	.009	.0086	.0084	+.0003	-0.006
(cm.)	.0211	.0229	.0218	.0213	+.0007	-0.0016
Ball Parameters						
Average Weight (gm.)	24.3309	24.3165	24.3307	24.3104	-0.0002	-0.0061
Average Surface Finish						
(μin., rms)	*	*	3 - 4	5 - 7		
(μm, rms)			.0762-.1016	.1270-.1778		
Average Diameter						
(in.)	0.71877	0.71863	0.71873	0.71856	-0.00004	-0.00007
(cm.)	1.82568	1.82532	1.82557	1.82514	-0.00011	-0.00018
Cage Parameters						
Weight (gm.)	140.44	141.89	140.46	140.60	+0.02	-1.29
Average Pocket Dia.						
(in.) Axial	0.7513	0.7513	0.7509	0.7497	-0.0004	-0.0016
(cm.) Axial	1.9083	1.9083	1.9073	1.9042	-0.0010	-0.0041
(in.) Circumferential	0.7526	0.7526	0.7533	0.7707	+0.0007	+0.0181
(cm.) Circumferential	1.9116	1.9116	1.9134	1.9576	+0.0018	+0.0460
Inside Diameter						
(in.)	5.117	5.115	5.112	5.113	-0.005	-0.002
(cm.)	12.997	12.992	12.984	12.987	-0.013	-0.005
Inner Race Parameters						
Weight (gm.)	622.42	621.79	622.43	621.72	+0.01	-0.07
Surface Finish						
(μin., rms)	*	*	4 - 5	5 - 6		
(μm, rms)			.1016-.1270	.1270-.1524		
Outer Race Parameters						
Weight (gm.)	750.00	749.91	749.98	749.81	-0.02	-0.10
Surface Finish						
(μin., rms)	*	*	5 - 6	6 - 7		
(μm, rms)			.1270-.1524	.1524-.1778		

* Not measured, cage material deposits left in place for this test.

TEST RUN NO.: 4
BEARING SET NO.: 3
BEARING PART NO.: 2132197
DATE: 4-18-68

Front Bearing S/N L-5 Rear Bearing S/N L-6

Cage Config.: CKJ 7153 Cage: Chemloy 719 Balls: AISI 440C

	Pretest		Post Test		Parameter Change	
	S/N L-5	S/N L-6	S/N L-5	S/N L-6	S/N L-5	S/N L-6
Shaft Fit, tight (in.)	.0018	.0018	.0018	.0019	0	+.0001
(cm.)	.0046	.0046	.0046	.0048	0	+.0002
Housing Fit, loose						
(in.)	.0050	.0050	.0050	.0050	0	0
(cm.)	.0127	.0127	.0127	.0127	0	0
Total Ball Size Var.						
(μ in.)	20	0	150	30	+130	+30
(μ m.)	.508	0	3.81	.762	+3.302	+.762
Theor. Int. Clearance						
(in.)	.0081	.0083	.0080	.0084	-0.0001	+.0001
(cm.)	.0206	.0211	.0203	.0213	-0.0003	+.0002
Ball Parameters						
Average Weight (gm.)	24.3585	24.3566	24.3582	24.3568	-0.0003	+0.0002
Average Surface Finish						
(μ in., rms)	3 - 4	3 - 4	3 - 4	3 - 4	0	0
(μ m, rms)	.0762-.1016	.0762-.1016	.0762-.1016	.0762-.1016	0	0
Average Diameter						
(in.)	0.71878	0.71875	0.71881	0.71883	+0.00003	+0.00008
(cm.)	1.82570	1.82563	1.82578	1.82583	+0.00008	+0.00020
Cage Parameters						
Weight (gm.)	139.69	139.65	138.92	139.61	-0.77	-0.04
Average Pocket Dia.						
(in.) Axial	0.7549	0.7556	0.7449	0.7502	-0.0100	-0.0054
(cm.) Axial	1.9174	1.9192	1.8920	1.9055	-0.0254	-0.0137
(in.) Circumferential	0.7531	0.7536	0.7542	0.7538	+0.0011	+0.0002
(cm.) Circumferential	1.9129	1.9141	1.9157	1.9147	+0.0028	+0.0006
Inside Diameter						
(in.)	5.117	5.117	5.115	5.116	-0.002	-0.001
(cm.)	12.997	12.997	12.992	12.995	-0.005	-0.002
Inner Race Parameters						
Weight (gm.)	622.68	621.08	622.63	621.03	-0.05	-0.05
Surface Finish						
(μ in., rms)	4 - 6	4 - 5	4 - 6	4 -5	0	0
(μ m, rms)	.1016-.1524	.1016-.127	.1016-.1524	.1016-.1270	0	0
Outer Race Parameters						
Weight (gm.)	747.18	747.21	747.14	747.03	-0.04	-0.18
Surface Finish						
(μ in., rms)	5 - 7	5 - 8	5 - 7	5 - 8	0	0
(μ m, rms)	.1270-.1778	.127-.2032	.1270-.1778	.1270-.2032	0	0

TEST RUN NO.: 5
BEARING SET NO.: 4
BEARING PART NO.: 2137774
DATE: 5-15-68

Front Bearing S/N L-4 | Rear Bearing S/N L-5

Cage Config.: CKJ 8836 | Cage: Salox-M | Balls: Star-J

	Pretest		Post Test		Parameter Change	
	S/N L-4	S/N L-5	S/N L-4	S/N L-5	S/N L-4	S/N L-5
Shaft Fit, tight (in.)	.0019	.0019	.0019	.0018	0	-.0001
(cm.)	.0048	.0048	.0048	.0046	0	-.0002
Housing Fit, loose						
(in.)	.0050	.0050	.0050	.0050	0	0
(cm.)	.0127	.0127	.0127	.0127	0	0
Total Ball Size Var.						
(μ in.)	130	160	100	220	-30	+60
(μ m.)	3.302	4.064	2.54	5.588	.762	+1.524
Theor. Int. Clearance						
(in.)	.0080	.0080	.0076	.0078	-.0004	-.0002
(cm.)	.0203	.0203	.0193	.0198	-.001	-.0005
Ball Parameters						
Average Weight (gm.)	27.9412	27.9638	27.9384	27.9716	-0.0028	+0.0078
Average Surface Finish						
(μ in., rms)	2 - 3	2 - 3	3 - 4	3 - 4	1	1
(μ m, rms)	.0508-.0762	.0508-.0762	.0762-.1016	.0762-.1016	.0254	.0254
Average Diameter						
(in.)	0.71868	0.71868	0.71869	0.71872	+0.00001	+0.00004
(cm.)	1.82545	1.82545	1.82547	1.82555	+0.00002	+0.00010
Cage Parameters						
Weight (gm.)	174.80	175.16	174.37	174.51	-0.43	-0.65
Average Pocket Dia.						
(in.) Axial	0.7657	0.7647	0.7765	0.7742	+0.0108	+0.0095
(cm.) Axial	1.9449	1.9423	1.9723	1.9665	+0.0274	+0.0242
(in.) Circumferential	0.7598	0.7617	0.7636	0.7601	+0.0038	-0.0016
(cm.) Circumferential	1.9299	1.9347	1.9395	1.9307	+0.0096	-0.0040
Inside Diameter						
(in.)	5.124	5.122	5.133	5.124	+0.009	+0.002
(cm.)	13.015	13.010	13.038	13.015	+0.023	+0.005
Inner Race Parameters						
Weight (gm.)	625.23	625.33	621.6	625.1	-3.63	-0.23
Surface Finish						
(μ in., rms)	6 - 10	4 - 6	100-200	16 - 24	94 - 190	12 - 18
(μ m, rms)	.1524-.254	.1016-.1524	2.54-5.08	.4064-.6096	2.3876-4.826	.3048-.4572
Outer Race Parameters						
Weight (gm.)	750.00	750.53	746.9	750.1	-3.1	-0.43
Surface Finish						
(μ in., rms)	3 - 4	5 - 8	40 - 45	15 - 20	37 - 41	10 - 12
(μ m, rms)	.0762-.1016	.127-.2032	1.016-1.143	.381-.508	.9398-1.0416	.254-.3048

TEST RUN NO.: 6
BEARING SET NO.: 5
BEARING PART NO.: 2137774
DATE: 5-22-68

Front Bearing S/N L-1 — Rear Bearing S/N L-3

Cage Config.: CKJ 8836 — Cage: Salox-M — Balls: Star-J

	Pretest		Post Test		Parameter Change	
	S/N L-1	S/N L-3	S/N L-1	S/N L-3	S/N L-1	S/N L-3
Shaft Fit, tight (in.)	0.0017	0.0019				
(cm.)	0.0043	0.0048				
Housing Fit, loose						
(in.)	0.0053	0.0053				
(cm.)	0.0135	0.0135				
Total Ball Size Var.						
(μ in.)	160	20				
(μ m.)	4.064	0.508				
Theor. Int. Clearance						
(in.)	0.008	0.0082				
(cm.)	.0203	0.0254				
Ball Parameters						
Average Weight (gm.)	27.9489	27.9621				
Average Surface Finish						
(μ in., rms)	3 - 4	2 - 3				
(μ m, rms)	.0762-.1016	.0508-.0762				
Average Diameter						
(in.)	0.71869	0.71865				
(cm.)	1.82547	1.82537	Bearing	Bearing		
Cage Parameters			Failure	Failure		
Weight (gm.)	174.62	172.21				
Average Pocket Dia.						
(in.) Axial	0.7607	0.7602				
(cm.) Axial	1.9322	1.9309				
(in.) Circumferential	07588	0.7595				
(cm.) Circumferential	1.9274	1.9291				
Inside Diameter						
(in.)	5.120	5.123				
(cm.)	13.005	13.012				
Inner Race Parameters						
Weight (gm.)	625.25	628.40				
Surface Finish						
(μ in., rms)	3 - 5	2 - 4				
(μ m, rms)	.0762-.127	.0508-.1016				
Outer Race Parameters						
Weight (gm.)	750.50	747.68				
Surface Finish						
(μ in., rms)	4 - 6	5 - 10				
(μ m, rms)	.1016-.1524	.127-.254				

TEST RUN NO.: 7
BEARING SET NO.: 2
BEARING PART NO.: 2132197
DATE: 5-13-68

Front Bearing S/N 248 | Rear Bearing S/N 249

Cage Config.: CKJ 7153 | Cage: Chemloy 719 | Balls: AISI 440C

	Pretest		Post Test		Parameter Change	
	S/N 248	S/N 249	S/N 248	S/N 249	S/N 248	S/N 249
Shaft Fit, tight (in.)	.0019	.0018	0.0018	0.0018	−0.0001	0
(cm.)	.0048	.0046	0.0046	0.0046	−0.002	0
Housing Fit, loose						
(in.)	.0050	.0050	0.0050	0.0050	0	0
(cm.)	.0127	.0127	0.0127	0.0127	0	0
Total Ball Size Var.						
(μin.)	50	480	100	120	+50	−360
(μm.)	1.27	12.192	2.54	3.048	−1.27	−9.144
Theor. Int. Clearance						
(in.)	.0086	.0084	0.0083	0.0086	−0.0003	+0.0002
(cm.)	.0218	.0213	0.0211	0.0218	−0.0007	+0.0005
Ball Parameters						
Average Weight (gm.)	24.3307	24.3085	24.3310	24.3081	+0.0003	−0.0004
Average Surface Finish						
(μin., rms)	3 − 4	5 − 7	5 − 7	6 − 8	2 − 3	1
(μm, rms)	.0762−.1016	.1270−.1778	.127−.1778	.1524−.2032	.0508−.1016	.0254
Average Diameter						
(in.)	0.71873	0.71856	0.71870	0.71852	−0.00003	−0.00004
(cm.)	1.82557	1.82514	1.82550	1.82504	−0.00007	−0.00010
Cage Parameters						
Weight (gm.)	140.46	140.00	139.95	138.73	−0.51	−1.27
Average Pocket Dia.						
(in.) Axial	0.7509	0.7557	0.7485	0.7469	−0.0024	−0.0088
(cm.) Axial	1.9073	1.9195	1.9012	1.8971	−0.0061	−0.0224
(in.) Circumferential	0.7533	0.7534	0.7547	0.7631	+0.0014	+0.0097
(cm.) Circumferential	1.9134	1.9136	1.9169	1.9383	+0.0035	+0.0247
Inside Diameter						
(in.)	5.112	5.119	5.112	5.116	0	−0.003
(cm.)	12.984	13.002	12.984	12.995	0	−0.007
Inner Race Parameters						
Weight (gm.)	622.42	621.72	622.40	621.70	−0.02	−0.02
Surface Finish						
(μin., rms)	4 − 5	5 − 6	5 − 7	5 − 7	1 − 2	0 − 1
(μm, rms)	.1016−.1270	.127−.1524	.127−.1778	.127−.1778	.0254−.0508	0−.0254
Outer Race Parameters						
Weight (gm.)	749.98	749.81	749.90	749.80	−0.08	−0.01
Surface Finish						
(μin., rms)	5 −6	6 − 7	5 − 7	6 − 8	0 − 1	0 − 1
(μm, rms)	.127−.1524	.1524−.1778	.127−.1778	.1524−.2032	0 −.0254	0−.0254

TEST RUN NO.: 8
BEARING SET NO.: 3
BEARING PART NO.: 2132197
DATE: 6-4-68

Front Bearing S/N L-5 | Rear Bearing S/N L-6

Cage Config.: CKJ 7153 | Cage: Chemloy 719 | Balls: AISI 440C

	Pretest		Post Test		Parameter Change	
	S/N L-5	S/N L-6	S/N L-5	S/N L-6	S/N L-5	S/N L-6
Shaft Fit, tight (in.)	.0018	.0019	.0019	0.0018	+.0001	-0.0001
(cm.)	.0046	.0048	.0048	0.0046	+.0002	-0.0002
Housing Fit, loose						
(in.)	.0050	.0050	.0051	0.0053	+.0001	+0.0003
(cm.)	.0127	.0127	.01295	0.0135	+.00025	+0.0008
Total Ball Size Var.						
(μ in.)	0	30	10	20	+10	-10
(μ m.)	0	.762	.254	0.508	+.254	-.254
Theor. Int. Clearance						
(in.)	.008	.0084	.0082	0.0088	+0.0002	+0.0004
(cm.)	.0203	.0213	.0208	0.0224	+0.0005	+0.0011
Ball Parameters						
Average Weight (gm.)	24.3582	24.3568	24.3581	24.3560	-0.0001	-0.0008
Average Surface Finish						
(μ in., rms)	3 - 4	3 - 4	4 - 6	5 - 9	1 - 2	2 - 5
(μ m, rms)	.0762-.1016	.0762-.1016	.1016-.1524	.127-.2286	.0254-.0508	.0508-.127
Average Diameter						
(in.)	0.71881	0.71883	0.71880	0.71884	-0.00001	+0.00001
(cm.)	1.82578	1.82583	1.82575	1.82585	-0.00003	+0.00002
Cage Parameters						
Weight (gm.)	138.92	139.61	134.64	139.48	-4.28	-0.13
Average Pocket Dia.						
(in.) Axial	0.7450	0.7502	0.7611	0.7497	+0.0161	-0.0005
(cm.) Axial	1.8923	1.9055	1.9332	1.9042	+0.0409	-0.0013
(in.) Circumferential	0.7543	0.7538	0.7628	0.7559	+0.0085	+0.0021
(cm.) Circumferential	1.9159	1.9147	1.9375	1.9200	+0.0216	+0.0053
Inside Diameter						
(in.)	5.116	5.115	5.116	5.114	0	-0.001
(cm.)	12.995	12.992	12.995	12.990	0	-0.002
Inner Race Parameters						
Weight (gm.)	622.63	621.03	622.61	621.00	-0.02	-0.03
Surface Finish						
(μ in., rms)	4 - 6	4 - 5	4 - 6	5 - 7	0	1 - 2
(μ m, rms)	.1016-.1524	.1016-.127	.1016-.1524	.127-.1778	0	.0254-.0508
Outer Race Parameters						
Weight (gm.)	747.14	747.03	747.10	747.05	-0.04	+0.02
Surface Finish						
(μ in., rms)	5 - 7	5 - 8	5 - 9	7 - 10	0 - 2	2
(μ m, rms)	.127-.1778	.127-.2032	.127-.2286	.1778-.254	0-.0508	.0508

TEST RUN NO.: 9
BEARING SET NO.: 2
BEARING PART NO.: 2132197
DATE: 7-1-68

Front Bearing S/N 248 Rear Bearing S/N 249

Cage Config.: CKJ 7256 Cage: Chemloy 719 Balls: AISI 440C

	Pretest		Post Test		Parameter Change	
	S/N 248	S/N 249	S/N 248	S/N 249	S/N 248	S/N 249
Shaft Fit, tight (in.)	0.0018	0.0018	0.0018	0.0018	0	0
(cm.)	0.0046	0.0046	0.0046	0.0046	0	0
Housing Fit, loose						
(in.)	0.0050	0.0050	0.0050	0.0050	0	0
(cm.)	0.0127	0.0127	0.0127	0.0127	0	0
Total Ball Size Var.						
(μ in.)	100	120	170	20	+70	-100
(μ m.)	2.54	3.048	4.318	.508	+1.778	-2.54
Theor. Int. Clearance						
(in.)	0.0083	0.0086	0.0083	0.0088	0	+0.0002
(cm.)	0.0211	0.0218	0.0211	0.0224	0	+0.0006
Ball Parameters						
Average Weight (gm.)	24.3299	24.3077	24.3306	24.3079	+0.0007	+0.0002
Average Surface Finish						
(μ in., rms)	5 - 7	6 - 8	5 - 7	7 - 9	0	1
(μ m, rms)	.1270-.1778	1524-.2032	.127-.1778	.1778-.2286	0	.0254
Average Diameter						
(in.)	0.71878	0.71860	0.71880	0.71857	+0.00002	-0.00003
(cm.)	1.82570	1.82524	1.82575	1.82517	+0.00005	-0.00007
Cage Parameters						
Weight (gm.)	132.87	135.78	132.20	133.31	-0.67	-2.47
Average Pocket Dia.						
(in.) Axial	0.7742	0.7744	0.7751	0.7746	+0.0009	+0.0002
(cm.) Axial	1.9665	1.9670	1.9688	1.9675	+0.0023	+0.0005
(in.) Circumferential	0.7635	0.7638	0.7671	0.7692	+0.0036	+0.0054
(cm.) Circumferential	1.9393	1.9401	1.9484	1.9538	+0.0091	+0.0137
Inside Diameter						
(in.)	5.122	5.122	5.122	5.124	0	+0.002
(cm.)	13.010	13.010	13.010	13.015	0	+0.005
Inner Race Parameters						
Weight (gm.)	622.40	621.70	622.42	621.70	+0.02	0
Surface Finish						
(μ in., rms)	5 - 7	5 - 7	5 - 7	6 - 8	0	1
(μ m, rms)	.127-.1778	.127-.1778	.127-.1778	.1524-.2032	0	.0254
Outer Race Parameters						
Weight (gm.)	750.00	749.80	750.00	749.83	0	+0.03
Surface Finish						
(μ in., rms)	5 - 7	6 - 8	6 - 10	8 - 10	1 - 3	2
(μ m, rms)	.127-.1778	1524-.2032	.1524-.254	.2032-.2540	.0254-.0762	.0508

TEST RUN NO.: 10A & 10B
BEARING SET NO.: 3
BEARING PART NO.: 2132197
DATE: 7-9-68

Front Bearing S/N L-5 Rear Bearing S/N L-6

Cage Config.: CKJ 9256 Cage: Chemloy 719 Balls: AISI 440C

	Pretest		Post Test		Parameter Change	
	S/N L-5	S/N L-6	S/N L-5	S/N L-6	S/N L-5	S/N L-6
Shaft Fit, tight (in.)	.0019	.0018	.0018	.0018	-.0001	0
(cm.)	.0048	.0046	.0046	.0046	-.0002	0
Housing Fit, loose						
(in.)	.0051	.0053	.0050	.0050	-.0001	-0.0003
(cm.)	.01295	.0135	.0127	.0127	-.00025	-0.0008
Total Ball Size Var.						
(μ in.)	10	20	10	40	0	+20
(μ m.)	0.254	0.508	.254	1.016	0	+.508
Theor. Int. Clearance						
(in.)	.0082	.0088	.0082	.0072	0	-0.0016
(cm.)	.0208	.0224	.0208	.0183	0	-0.0041
Ball Parameters						
Average Weight (gm.)	24.3581	24.3560	24.3543	24.3359	-0.0038	-0.0201
Average Surface Finish						
(μ in., rms)	4 - 6	5 - 9	5 - 9	6 - 10	1 - 3	1
(μ m, rms)	.1016-.1524	.1270-.2286	.127-.2286	.1524-.254	.0254-.0762	.0254
Average Diameter						
(in.)	0.71860	0.71883	0.71866	0.71867	+0.00006	-0.00016
(cm.)	1.82524	1.82583	1.82540	1.82542	+0.00016	-0.00041
Cage Parameters						
Weight (gm.)	133.31	133.60	130.08	133.58	-3.23	-0.02
Average Pocket Dia.						
(in.) Axial	0.7767	0.7765	0.7747	0.7774	=0.0020	+0.0009
(cm.) Axial	1.9728	1.9723	1.9677	1.9746	-0.0051	+0.0023
(in.) Circumferential	0.7634	0.7629	0.7664	0.7733	+0.0030	+0.0104
(cm.) Circumferential	1.9390	1.9378	1.9467	1.9642	+0.0077	+0.0264
Inside Diameter						
(in.)	5.124	5.119	5.123	5.120	-0.001	+0.001
(cm.)	13.015	13.002	13.012	13.005	-0.003	+0.003
Inner Race Parameters						
Weight (gm.)	622.60	621.11	622.50	621.20	-0.10	+0.09
Surface Finish						
(μ in., rms)	4 - 6	5 - 7	6 - 12	7 - 15	2 - 6	2 - 8
(μ m, rms)	.1016-.1524	.127-.1778	.1524-.3048	.1778-.381	.0508-.1524	.0508-.2032
Outer Race Parameters						
Weight (gm.)	747.11	747.11	747.10	747.10	=0.01	-0.01
Surface Finish						
(μ in., rms)	5 - 9	7 - 10	7 - 10	9 - 15	2 - 1	2 - 5
(μ m, rms)	.127-.2286	.1778-.2540	.1778-.254	.2286-.381	.0508-.0254	.0508-.1270

TEST RUN NO.: 11 & 12*
BEARING SET NO.: 2
BEARING PART NO.: 2132197
DATE: 1-21 & 28-70

Front Bearing S/N* Rear Bearing S/N*

Cage Config.: DKJ 1015 Cage: Chemloy 719 Balls: AISI 440C

	Pretest		Post Test		Parameter Change	
	S/N 248	S/N 249	S/N 248	S/N 249	S/N 248	S/N 249
Shaft Fit, tight (in.)	.0018	.0018	N.A.	N.A.		
(cm.)	.0046	.0046	N.A.	N.A.		
Housing Fit, loose						
(in.)	.0050	.0050	N.A.	N.A.		
(cm.)	.0127	.0127	N.A.	N.A.		
Total Ball Size Var.						
(μ in.)	170	20	50	220	-120	+200
(μ m.)	4.318	.508	1.27	5.588	-3.048	+5.08
Theor. Int. Clearance						
(in.)	.0083	.0088	N.A.	N.A.		
(cm.)	.0211	.0224	N.A.	N.A.		
Ball Parameters						
Average Weight (gm.)	24.3299	24.3573	24.3299	24.3507	0	-0.0066
Average Surface Finish						
(μ in., rms)	5 - 7	7 - 9	10 - 12	8 - 10	5	1
(μ m, rms)	.1270-.1778	.1778-.2286	.2540-.3048	.2032-.2540	.1270	.0254
Average Diameter						
(in.)	0.71874	0.71877	0.71879	0.71875	+0.00005	-0.00002
(cm.)	1.82560	1.82568	1.82573	1.82563	+0.00013	-0.00005
Cage Parameters						
Weight (gm.)	135.20	135.00	135.00	134.80	-0.20	-0.20
Average Pocket Dia.						
(in.) Axial	0.7708	0.7727	0.7712	0.7742	+0.0004	+0.0015
(cm.) Axial	1.9578	1.9627	1.9588	1.9665	+0.0010	+0.0038
(in.) Circumferential	0.7600	0.7610	0.7683	0.7700	+0.0083	+0.0090
(cm.) Circumferential	1.9304	1.9329	1.9515	1.9558	+0.0211	+0.0229
Inside Diameter						
(in.)	5.110	5.110	5.120	5.118	+0.010	+0.008
(cm.)	12.979	12.979	13.005	13.000	+0.026	+0.021
Inner Race Parameters						
Weight (gm.)	622.20	621.50	622.10	621.60	-0.10	+0.10
Surface Finish						
(μ in., rms)	5 - 7	6 - 8	8 - 11	10 - 14	3 - 4	4 - 6
(μ m, rms)	.1270-.1778	.1524-.2032	.2032-.2794	.254-.3556	.0762-.1016	.1016-.1524
Outer Race Parameters						
Weight (gm.)	749.70	749.80	749.70	749.60	0	-0.20
Surface Finish						
(μ in., rms)	6 - 10	8 - 10	8 - 14	10 - 13	2 - 4	2 - 3
(μ m, rms)	.1524-.2540	.2032-.2540	.2032-.3556	.254-.3302	.0508-.1016	.0508-.0762

* The test bearings were not inspected after Test No. 11.
The bearing location on the shaft was changed for Test No. 12.

N.A. - Not available

TEST RUN NO.: 13A & 13B
BEARING SET NO.: 3
BEARING PART NO.: 2132197
DATE: 2-19 & 20-70

Front Bearing S/N L-5 Rear Bearing S/N L-6

Cage Config.: DKJ 1015 Cage: Chemloy 719 Balls: AISI 440C

	Pretest		Post Test		Parameter Change	
	S/N L-5	S/N L-6	S/N L-5	S/N L-6	S/N L-5	S/N L-6
Shaft Fit, tight (in.)	.0018	.0018	.0018	.0018	0	0
(cm.)	.0046	.0046	.0046	.0046	0	0
Housing Fit, loose						
(in.)	.0050	.0050	.0050	.0050	0	0
(cm.)	.0127	.0127	.0127	.0127	0	0
Total Ball Size Var.						
(μ in.)	10	40	40	30	+30	-10
(μ m.)	.254	1.016	1.016	.762	+.762	-.254
Theor. Int. Clearance						
(in.)	.0082	.0072	.0072	.0071	-.0010	-.0001
(cm.)	.0208	.0183	.0183	.0180	-.0025	-.0003
<u>Ball Parameters</u>						
Average Weight (gm.)	24.3582	24.3560	24.3576	24.3557	-0.0006	-0.0003
Average Surface Finish						
(μ in., rms)	5 - 9	6—10	5 - 9	6 - 10	0	0
(μ m, rms)	.125-.2286	.1524-.254	.1270-.2286	.1524-.2540	0	0
Average Diameter						
(in.)	0.71878	0.71867	0.71875	0.71874	-0.00003	+0.00007
(cm.)	1.82570	1.82542	1.82563	1.82560	-0.00007	+0.00018
<u>Cage Parameters</u>						
Weight (gm.)	135.20	135.00	134.60	129.70	-0.60	-5.3
Average Pocket Dia.						
(in.) Axial	0.7716	0.7717	0.7627	0.7724	-0.0089	+0.0007
(cm.) Axial	1.9599	1.9601	1.9373	1.9619	-0.0226	+0.0018
(in.) Circumferential	0.7633	0.7585	0.7661	0.7654	+0.0028	+0.0069
(cm.) Circumferential	1.9388	1.9266	1.9459	1.9441	+0.0071	+0.0175
Inside Diameter						
(in.)	5.116	5.111	5.115	5.110	-0.001	-0.001
(cm.)	12.995	12.982	12.992	12.979	-0.003	-0.003
<u>Inner Race Parameters</u>						
Weight (gm.)	622.50	621.20	622.40	621.00	-0.10	-0.20
Surface Finish						
(μ in., rms)	6 - 12	7 - 15	6 - 12	7 - 15	0	0
(μ m, rms)	.1524-.3048	.1778-.381	.1524-.3048	.1778-.3810	0	0
<u>Outer Race Parameters</u>						
Weight (gm.)	747.10	747.10	746.90	747.00	-0.20	-0.10
Surface Finish						
(μ in., rms)	7 - 10	9 - 15	7 - 10	9 - 15	0	0
(μ m, rms)	.1778-.254	.1016-.381	.1770-.2540	.2286-.3810	0	0

TEST RUN NO.: 14A & 14B
BEARING SET NO.: 6
BEARING PART NO.: 2137774
DATE: 3-19-70

Front Bearing S/N L-9 | Rear Bearing S/N L-10

Cage Config.: DKJ 6202 | Cage: Salox-M | Balls: Star J

	Pretest		Post Test		Parameter Change	
	S/N L-9	S/N 1 10	S/N L-9	S/N L-10	S/N L-9	S/N L-10
Shaft Fit, tight (in.)	.0019	.0019	.0018	.0025	-.0001	+.0006
(cm.)	.0048	.0048	.0046	.0064	-.0002	+.0016
Housing Fit, loose						
(in.)	.0050	.0051	.0050	.0050	0	-1
(cm.)	.0127	.01295	.0127	.0127	0	-0.00025
Total Ball Size Var.						
(μ in.)	190	40	100	30	-90	-10
(μ m.)	4.826	1.016	2.54	.762	-2.286	-.254
Theor. Int. Clearance						
(in.)		.0083	.0080	.0090		+.0007
(cm.)		.0211	.0203	.0229		+.0018
Ball Parameters						
Average Weight (gm.)	27.9662	27.9728	27.9764	27.9720	+0.0102	-.0008
Average Surface Finish						
(μ in., rms)	3 - 4	3 - 4	3 - 4	5 - 7	0	2 - 3
(μ m, rms)	.0762-.1016	.0762-.1016	.0762-.1016	.1270-.1778	0	.0508-.0762
Average Diameter						
(in.)	0.71870	0.71870	0.71879	0.71878	+0.00009	+0.00008
(cm.)	1.82550	1.82550	1.82573	1.82570	+0.00023	+0.00020
Cage Parameters						
Weight (gm.)	224.70	222.00	224.50	221.50	-0.20	-.50
Average Pocket Dia.						
(in.) Axial	0.7731	0.7711	0.7685	0.7690	-0.0046	-0.0021
(cm.) Axial	1.9637	1.9586	1.9520	1.9533	-0.0117	-0.0053
(in.) Circumferential	0.7597	0.7597	0.7620	0.7671	+0.0023	+0.0074
(cm.) Circumferential	1.9296	1.9296	1.9355	1.9484	+0.0059	+0.0188
Inside Diameter						
(in.)	5.111	5.113	5.111	5.113	0	0
(cm.)	12.982	12.987	12.982	12. 987	0	0
Inner Race Parameters						
Weight (gm.)	625.70	627.80	625.50	627.80	-0.20	0
Surface Finish						
(μ in., rms)	3 - 5	3 - 5	3 - 5	8 - 10	0	5
(μ m, rms)	.0762-.1270	.0762-.1270	.0762-.1270	.2032-.2540	0	.1270
Outer Race Parameters						
Weight (gm.)	747.70	747.00	747.10	746.90	-0.60	-0.10
Surface Finish						
(μ in., rms)	3 - 4	4 - 6	3 - 5	7 - 8	0 - 1	3 - 2
(μ m, rms)	.0762-.1016	.1016-.1524	.0762-.1270	.1778-.2032	0-.0254	.0762-.0508

TEST RUN NO.: 15
BEARING SET NO.: 7
BEARING PART NO.: 2137774
DATE: 3-19-70

Front Bearing S/N L-7 Rear Bearing S/N L-8

Cage Config.: DKJ 6202 Cage: Salox-M Balls: Star J

	Pretest		Post Test		Parameter Change	
	S/N L-7	S/N L-8	S/N L-7	S/N L-8	S/N L-7	S/N L-8
Shaft Fit, tight (in.)	.0018	.0018	.0017	.0018	-.0001	0
(cm.)	.0046	.0046	.0043	.0046	-.0003	0
Housing Fit, loose						
(in.)	.0051	.0050	.0050	.0050	-.0001	0
(cm.)	.01295	.0127	.0127	.0127	-.00025	0
Total Ball Size Var.						
(μ in.)	40	20	130	30	+90	+10
(μ m.)	1.016	.508	3.302	.762	+2.286	+.254
Theor. Int. Clearance						
(in.)	.0078	.0077	.0080	.0077	+.0002	0
(cm.)	.0198	.0196	.0203	.0196	+.0005	0
Ball Parameters						
Average Weight (gm.)	27.9940	27.9679	27.9535	27.9988	-0.0405	+0.0309
Average Surface Finish						
(μ in., rms)	2 - 3	2 - 3	3 - 4	3 - 4	1	1
(μ m, rms)	.0508-.0762	.0508-.0762	.0762-.1016	.0762-.1016	.0254	.0254
Average Diameter						
(in.)	0.71882	0.71873	0.71867	0.71877	-0.00015	+0.00004
(cm.)	1.82580	1.82557	1.82542	1.82568	-0.00038	+0.00011
Cage Parameters						
Weight (gm.)	224.80	225.20	224.00	224.50	-0.80	-0.70
Average Pocket Dia.						
(in.) Axial	0.7712	0.7716	0.7779	0.7714	+0.0067	-0.0002
(cm.) Axial	1.9588	1.9599	1.9759	1.9594	+0.0171	-0.0005
(in.) Circumferential	0.7594	0.7593	0.7653	0.7653	+0.0059	+0.0060
(cm.) Circumferential	1.9289	1.9286	1.9439	1.9439	+0.0150	+0.0153
Inside Diameter						
(in.)	5.108	5.112	5.125	5.113	+0.017	+0.001
(cm.)	12.974	12.984	13.018	12.987	+0.044	+0.003
Inner Race Parameters						
Weight (gm.)	624.5	627.3	627.4	624.5	+2.9	-2.8
Surface Finish						
(μ in., rms)	3 - 5	2 - 3	4 - 7	4 - 9	1 - 2	2 - 6
(μ m, rms)	.0762-.127	.0508-.0762	.1016-.1778	.1016-.2286	.0254-.0508	.0508-.1524
Outer Race Parameters						
Weight (gm.)	747.7	750.2	745.1	747.6	-2.6	-2.6
Surface Finish						
(μ in., rms)	2 - 3	2 - 3	3 - 4	3 - 20	1	1 - 17
(μ m, rms)	.0508-.0762	.0508-.0762	.0762-.1016	.0762-.508	.0254	.0254-.4318

TEST RUN NO.: 16A & 16B
BEARING SET NO.: 8
BEARING PART NO.: DKJ 7743
DATE: 4-27-70

Front Bearing S/N L-2 | Rear Bearing S/N L-6

Cage Config.: DKJ 6202 | Cage: Salox-M | Balls: AISI 440C

	Pretest		Post Test		Parameter Change	
	S/N L-2	S/N L-6	S/N L-2	S/N L-6	S/N L-2	S/N L-6
Shaft Fit, tight (in.)	.0018	.0018	.0014	.0014	-.0004	-.0004
(cm.)	.0046	.0046	.0036	.0036	-.0010	-.0010
Housing Fit, loose						
(in.)	.0052	.0051	.0051	.0050	-.0001	-.0001
(cm.)	.0132	.01295	.01295	.0127	-.00025	-.00025
Total Ball Size Var.						
(μ in.)	50	20	390	40	+340	+20
(μ m.)	1.27	.508	9.906	1.016	+8.636	+.508
Theor. Int. Clearance						
(in.)	.0080	.0082	.0080	.0083	0	+.0001
(cm.)	.0203	.0208	.0203	.0211	0	+.0003
Ball Parameters						
Average Weight (gm.)	24.3573	24.3507	24.3588	24.3577	+0.0015	+0.0070
Average Surface Finish						
(μ in., rms)	2 - 3	2 - 3	3 - 4	3 - 4	1	1
(μ m, rms)	.0508-.0762	.0508-.0762	.0762-.1016	.0762-.1016	.0254	.0254
Average Diameter						
(in.)	0.71877	0.71875	0.71867	0.71872	-0.00010	-0.00003
(cm.)	1.82568	1.82563	1.82542	1.82555	-0.00026	-0.00008
Cage Parameters						
Weight (gm.)	230.10	229.30	229.90	228.20	-0.20	-1.10
Average Pocket Dia.						
(in.) Axial	0.7743	0.7723	0.7688	0.7727	-0.0055	+0.0004
(cm.) Axial	1.9667	1.9616	1.9528	1.9627	-0.0139	+0.0011
(in.) Circumferential	0.7612	0.7583	0.7696	0.7587	+0.0084	+0.0004
(cm.) Circumferential	1.9334	1.9261	1.9548	1.9271	+0.0214	+0.0010
Inside Diameter						
(in.)	5.108	5.114	5.110	5.108	+0.002	-0.006
(cm.)	12.974	12.990	12.979	12.974	+0.005	-0.016
Inner Race Parameters						
Weight (gm.)	624.50	624.40	624.70	624.70	+0.20	+0.30
Surface Finish						
(μ in., rms)	3 - 5	3 - 5	4 - 5	5 - 9	1 - 0	2 - 4
(μ m, rms)	.0762-.127	.0162-.127	.1016-.127	.127-.2286	.0254-0	.0508-.1016
Outer Race Parameters						
Weight (gm.)	751.60	747.50	751.80	747.70	+0.20	+0.20
Surface Finish						
(μ in., rms)	4 - 6	5 - 8	5 - 15	5 - 15	1 - 9	0 - 7
(μ m, rms)	.1016-.1524	.127-.2032	.127-.381	.127-.381	.0254-.2286	0-.1778

Cage Pocket Wear Scar

Test No.	Minor Diameter of Largest Scar, in.	cm	Minor Diameter of Typical Scar, in.	cm
1	(a)			
2	(b)			
3	0.280	0.7112	0.060	0.1524
4	(c)			
5	0.190	0.4826	0.090	0.2286
6	0.340	0.8636	0.160	0.4064
7	0.340	0.8636	0.090	0.2286
8	0.160	0.4064	0.090	0.2286
9	0.160	0.4064	0.120	0.3048
10A	(d)			
10B	(e)		0.090	0.2286
11	(d)			
12	0.370	0.9398	0.160	0.4064
13A	(d)			
13B	0.340	0.8636	0.160	0.4064
14A	(d)			
14B	(e)		0.160	0.4064
15	0.160	0.4064	0.160	0.4064
16A	(e)			
16B	0.310	0.4874	0.160	0.4064

(a) Balls seized in cage and the only scar was at manufacturing split

(b) Was not measured due to negligiable wear

(c) Coolant flow split caused overheat with no damage to cage

(d) Rig was not disassembled before next test

(e) Minor axis greater than cage thickness.

DISTRIBUTION LIST*

Copies R	Copies D**	Recipient	Designee
		National Aeronautics and Space Administration Lewis Research Center 21000 Brookpark Road Cleveland, Ohio 44135	
1		Contracting Officer, MS 500-313	
5		Liquid Rocket Technology Branch, MS 500-209	
1		Technical Report Control Office, MS 5-5	
1		Technology Utilization Office, MS 3-16	
2		AFSC Liaison Office, 501-3	
2		Library	
1		Office of Reliability and Quality Assurance, MS 500-111	
1		D. L. Nored, Chief, LRTB, MS 500-209	
3		W. R. Britsch, Project Manager, MS 500-209	
1		E. W. Conrad, MS 500-204	
1		B. Lubarsky, MS 3-3	
1		A. Ginsburg, MS 5-3	
1		E. E. Bisson, MS 5-3	
1		R. L. Johnson, MS 23-2	
1		W. J. Anderson, MS 23-2	
1		H. Scibbe, MS 6-1	
1		H. Sliney, MS 23-2	
2		Chief, Liquid Experimental Engineering, RPX Office of Advanced Research and Technology NASA Headquarters Washington, D. C. 20546	
2		Chief, Liquid Propulsion Technology, RPL Office of Advanced Research and Technology NASA Headquarters Washington, D. C. 20546	
1		Director, Launch Vehicles and Propulsion, SV Office of Space Science and Applications NASA Headquarters Washington, D. C. 20546	
1		Chief, Environmental Factors and Aerodynamics Code RV-1 Office of Advanced Research and Technology NASA Headquarters Washington, D. C. 20546	

*The report is sent directly to the recipient noted on page 115 only. On the remaining pages, the report is sent to the technical librarian of the "recipient," with a copy of the letter of transmittal to the attention of the person named under the column "Designee."

**R - Recipient
D - Designee

Copies R	Copies D	Recipient	Designee
1		Chief, Space Vehicles Structures Office of Advanced Research and Technology NASA Headquarters Washington, D. C. 20546	
1		Director, Advanced Manned Missions, MT Office of Manned Space Flight NASA Headquarters Washington, D. C. 20546	
6		NASA Scientific and Technical Information Facility P. O. Box 33 College Park, Maryland 20740	G. Drobka
1		Director, Technology Utilization Division Office of Technology Utilization NASA Headquarters Washington, D. C. 20546	
1		National Aeronautics and Space Administration Ames Research Center Moffett Field, California 94035 Attn: Library	
1		National Aeronautics and Space Administration Flight Research Center P. O. Box 273 Edwards, California 93523 Attn: Library	
1		National Aeronautics and Space Administration Goddard Space Flight Center Greenbelt, Maryland 20771 Attn: Library	Merland L. Moseson, Code 620
1		National Aeronautics and Space Administration John F. Kennedy Space Center Cocoa Beach, Florida 32931 Attn: Library	Dr. Kurt H. Debus
1		National Aeronautics and Space Administration Langley Research Center Langley Station Hampton, Virginia 23365 Attn: Library	E. Cortwright Director

Copies R	Copies D	Recipient	Designee
1		National Aeronautics and Space Administration Manned Spacecraft Center Houston, Texas 77001 Attn: Library	J. G. Thibodaux, Jr. Chief, Propulsion and Power Division
1	1 1	National Aeronautics and Space Administration George C. Marshall Space Flight Center Huntsville, Alabama 35812 Attn: Library	Hans G. Paul Loren Gross
1	1	Jet Propulsion Laboratory 4800 Oak Grove Drive Pasadena, California 91103 Attn: Library	Henry Burlage, Jr. Duane Dipprey
1		Defense Documentation Center Cameron Station, Building 5 5010 Duke Street Alexandria, Virginia 22314 Attn: TISIA	
1		Office of the Director of Defense Research and Engineering Washington, D. C. 20301 Attn: Office of Asst. Dir. (Chem. Technology)	
1		RTD (RTNP) Bolling Air Force Base Washington, D. C. 20332	
1		Arnold Engineering Development Center Air Force Systems Command Tullahoma, Tennessee 37389 Attn: Library	Dr. H. K. Doetsch
1		Advanced Research Projects Agency Washington, D. C. 20525 Attn: Library	
1		Aeronautical Systems Division Air Force Systems Command Wright-Patterson Air Force Base, Dayton, Ohio Attn: Library	D. L. Schmidt Code ARSCNC-2
1		Air Force Missile Test Center Patrick Air Force Base, Florida Attn: Library	L. J. Ullian

Copies R	Copies D	Recipient	Designee
1		Air Force System Command Andrews Air Force Base Washington, D. C. 20332 Attn: Library	
1	1	Air Force Rocket Propulsion Laboratory (RPR) Edwards, California 93523 Attn: Library	Lester Tepe
1		Air Force Rocket Propulsion Laboratory (RPM) Edwards, California 93523 Attn: Library	
1		Air Force FTC (FTAT-2) Edwards Air Force Base, California 93523 Attn: Library	
1		Air Force Office of Scientific Research Washington, D. C. 20333 Attn: Library	SREP, Dr. J. F. Masi
1		Space and Missile Systems Organization Air Force Unit Post Office Los Angeles, California 90045 Attn: Technical Data Center	
1		Office of Research Analyses (OAR) Holloman Air Force Base, New Mexico 88330 Attn: Library	
1		Headquarters U. S. Air Force Washington, D. C. Attn: Library	Col. C. K. Stambaugh, Code AFRST
1		Commanding Officer U. S. Army Research Office (Durham) Box CM, Duke Station Durham, North Carolina 27706 Attn: Library	
1		U. S. Army Missile Command Redstone Scientific Information Center Redstone Arsenal, Alabama 35808 Attn: Document Section	Dr. W. Wharton

Copies R	Copies D	Recipient	Designee
		Bureau of Naval Weapons Department of the Navy Washington, D. C. Attn: Library	J. Kay, Code RTMS-41
1		Commander U. S. Navy Missile Center Point Mugu, California 93041 Attn: Technical Library	
1		Commander U. S. Naval Weapons Center China Lake, California 93557 Attn: Library	W. F. Thorm Code 4562
1		Commanding Officer Naval Research Branch Office 1030 E. Green Street Pasadena, California 91101 Attn: Library	
1		Director (Code 6180) U. S. Naval Research Laboratory Washington, D. C. 20390 Attn: Library	H. W. Carhart J. M. Krafft
1		Picatinny Arsenal Dover, New Jersey 07801 Attn: Library	
1		Air Force Aero Propulsion Laboratory Research and Technology Division Air Force Systems Command Wright-Patterson AFB, Ohio 45433 Attn: APRP (Library)	R. Quigley C. M. Donaldson
1	 1 1	Aerojet Liquid Rocket Company P. O. Box 13222 Sacramento, California 95813 Attn: Technical Library 2484-2015A	R. Stiff W. Campbell W. W. Heath F. Malaire J. B. Accinelli
1	 1 1	Aerospace Corporation 2400 E. El Segundo Blvd. Los Angeles, California 90045 Attn: Library-Documents	J. G. Wilder J. H. Todd F. Ghabremani

Copies R	Copies D	Recipient	Designee
		ARO, Incorporated Arnold Engineering Development Center Arnold AF Station, Tennessee 37389 Attn: Library	
1		Bell Aerosystems, Inc. Box 1 Buffalo, New York 14240 Attn: Library	Mario Messina
1		Boeing Company Space Division P. O. Box 868 Seattle, Washington 98124 Attn: Library	
1		Boeing Company 1625 K Street, N. W. Washington, D. C. 20006	
1		Chemical Propulsion Information Agency Applied Physics Laboratory 8621 Georgia Avenue Silver Spring, Maryland 20910	Tom Reedy
1		Chrysler Corporation Missile Division P. O. Box 2628 Detroit, Michigan Attn: Library	S. L. Terry
1		Curtiss-Wright Corporation Wright Aeronautical Division Woodridge, New Jersey Attn: Library	
1	1	General Electric Company Flight Propulsion Laboratory Department Cincinnati, Ohio Attn: Library	E. N. Bamberger C. C. Moore
1		IIT Research Institute Technology Center Chicago, Illinois 60616 Attn: Library	C. K. Hersh
1		Lockheed Missiles and Space Company P. O. Box 504 Sunnyvale, California 94087 Attn: Library	

Copies R	Copies D	Recipient	Designee
1		Lockheed Propulsion Company P. O. Box 111 Redlands, California 92374 Attn: Library, Thackwell	
1		Marquardt Corporation 16555 Saticoy Street Box 2013 - South Annex Van Nuys, California 91409	
1		McDonnell Douglas Aircraft Corporation P. O. Box 516 Lambert Field, Missouri 63166 Attn: Library	
1	1 1	Rocketdyne Division North American Rockwell Inc. 6633 Canoga Avenue Canoga Park, California 91304 Attn: Library, Department 596-306	R. J. Thompson S. F. Iacobellis G. S. Wong Myles Butner
1		Space and Information Systems Division North American Rockwell 12214 Lakewood Blvd. Downey, California Attn: Library	
1		Purdue University Lafayette, Indiana 47907 Attn: Library (Technical)	Dr. Bruce Reese
1		Stanford Research Institute 333 Ravenswood Avenue Menlo Park, California 94025 Attn: Library	Dr. Gerald Marksman
1		TRW Systems Inc. 1 Space Park Redondo Beach, California 90278 Attn: Tech. Lib. Doc. Acquisitions	D. H. Lee
1		TRW TAPCO Division 23555 Euclid Avenue Cleveland, Ohio 44117	P. T. Angell
1		United Aircraft Corporation Pratt & Whitney Division Florida Research and Development Center P. O. Box 2691 West Palm Beach, Florida 33402 Attn: Library	R. J. Coar

Copies R	Copies D	Recipient	Designee
1		Garrett Corporation Airesearch Division Phoenix, Arizona, 85036 Attn: Library	R. Bullock Lyle Six
1		Garrett Corporation Airesearch Division Los Angeles, California Attn: Library	
1		Brown University Providence, R. I. Attn: Technical Library	
1		Pennsylvania State University State College, Pennsylvania Attn: Library	Dr. M. Seoik Dr. H. W. Hall Dr. B. Lakshminarayan
1	1	Iowa State University Ames, Iowa Attn: Library	Dr. George Serovy
1	1	California Institute of Technology Pasadena, California Attn: Library (Technical)	Dr. A. Acosta
1		Massachusetts Institute of Technology Cambridge, Mass. Attn: Library	
1		Hydronautics Incorporated Pindell School Road Laurel, Maryland	
1		Ford Motor Company American Road Dearborn, Michigan	M. Ference, Jr.
1		Worthington Corporation Advanced Products Division 401 Worthington Avenue Harrison, New Jersey	Allan Budris W. K. Jekat
	1	Atomic Energy Commission Division fo Reactor Development and Technology Washington, D. C. 20767	N. Grossman

Copies R	Copies D	Recipient	Designee
1		Naval Ship Research and Development Center Annapolis Division Annapolis, Maryland, 21402	W. V. Smith
1		Naval Ship Systems Command Washington, D. C. 20360	J. E. Dray (SNHIP 6148)
	1	U. S. Army Engineering R&D Labs Gas Turbine Test Facility Fort Belvoir, Virginia 22060	W. Crim
	1	U. S. Army Aviation Materials Laboratory Ft. Eustis, Virginia 23604	J. N. Danials SAVFE-AS
1	1	Battlelle Memorial Institute Columbus Laboratories 505 King Avenue Columbus, Ohio 43201 Attn: Library	C. M. Allen
1	1	Fafnir Bearing Company 37 Booth Street New Britain, Conn. 06050 Attn: Library	R. J. Matt
1	1	Franklin Institute Research Labs Benjamin Franklin Parkway Philadelphia, Pa. 19103 Attn: Library	J. Rumbarger
1		Mechanical Technology Incorporated 968 Albany-Shaker Blvd. Latham, New York 12110 Attn: Library	
	1	Inductrial Tectonic, Inc. 18301 Santa Fe Avenue Compton, California 90024	H. Hanau
1		National Science Foundation Engineering Division 1800 G. Street, N. W. Washington, D. C. 20540 Attn: Library	
	1	Office of Naval Research Washington, D. C. 20360	S. W. Doroff ONR/463

Copies R	Copies D	Recipient	Designee
	1	SKF Industries, Inc.	T. Tallian
	1	Engineering and Research Center	L. Sibley
		1100 First Avenue	
		King of Prussia, Pennsylvania 19406	
1		Sunstrand Denver	
		2480 West 70 Avenue	
		Denver, Colorado 80221	
		Attn: Library	
	1	TRW Marlin Rockwell Division	A. S. Irwin
		402 Chandler Street	
		Jamestown, New York 14701	
	1	NASA/Marshall Space Flight Center	
		NASA RL-10 Project Manager 1-E-R	
		Huntsville, Alabama 35812	
1		Naval Ship Research and Development Center	Dr. W. B. Morgan
		Code 526	
		Washington, D. C. 20007	
1	1	AEC-NASA	F. C. Schwenk
		Space Nuclear Propulsion Office, NPO	N. J. Gerstein
		NASA Headquarters	
		Germantown, Maryland	